Investigation of the role of CCR2 and activin A in fibrosis development during experimental autoimmune orchitis

Inaugural Dissertation

submitted to the

Faculty of Medicine

in partial fulfillment of requirements

for the PhD-Degree

of the Faculty of Medicine

of the Justus Liebig University of Giessen

by

Wei Peng

from

Hunan, China

Giessen 2023

From the Department of Anatomy and Cell Biology

Director/Chairman: Prof. Dr. Andreas Meinhardt

Faculty of Medicine

Justus Liebig University of Giessen, Germany

First Supervisor and Committee Member: Prof. Dr. Andreas Meinhardt/ Dr. Monika Fijak

Second Supervisor and Committee Member: Prof. Dr. Gerhard Schuler

Committee Members: Prof. Dr. Martin Diener/ Prof. Dr. Sandra Goericke-Pesch

Date of Doctoral Defense: 30th January, 2023

TABLE OF CONTENTS

1. INTRODUCTION

1.1. Male infertility

Infertility has become an important issue affecting men's health. It is estimated that around 15 % of couples worldwide suffer from infertility, with the male factor accounting for 50% (Choy and Eisenberg, 2018). A large variety of causes and risk factors contribute to male infertility, including congenital factors (genetic mutation, cryptorchidism or Y chromosome microdeletions), acquired factors (varicocele, urogenital infections, post-inflammatory conditions or autoimmune diseases) and idiopathic risk factors (smoking, alcohol abuse or obesity) (Agarwal et al., 2021). Inflammation of the male genital tract caused by pathogens and autoantibodies can perturb male fertility, as is commonly observed during orchitis and epididymitis (Trojian et al., 2009; Haidl et al., 2019). Interestingly, inflammatory cell infiltrates are detected in 30% of human testicular biopsies showing impaired spermatogenesis (Schuppe et al., 2001). These latter alterations are well reflected in a rodent model of experimental autoimmune orchitis (EAO) (Fijak et al., 2018).

1.2. Testicular morphology

The male genital tract consists of the testis, epididymis and vas deferens, which are responsible for the production, maturation, maintenance and transportation of spermatozoa, as well as the accessory sex glands including seminal vesicles, prostate and bulbourethral glands involved in the production of seminal plasma (Foster, 2016). The testis contains a series of lobules formed by seminiferous tubules. In seminiferous tubules, which are surrounded by myoid peritubular cells (PTCs), Sertoli cells (SCs) support and nourish different stages of developing germ cells, including spermatogonia, spermatocytes, round and elongated spermatids as well as spermatozoa, forming the germinal compartment (Dutta et al., 2021). The testicular interstitium located between seminiferous tubules contains the androgen-synthesizing Leydig cells (LCs), fibroblasts, blood vessels and immune cells such as macrophages, dendritic cells as well as T cells (Fijak and Meinhardt, 2006). These cells communicate and act together to form the immunosuppressive environment of the testis (Fijak et al., 2018). The schematic representation of testicular architecture is shown in **Fig. 1**.

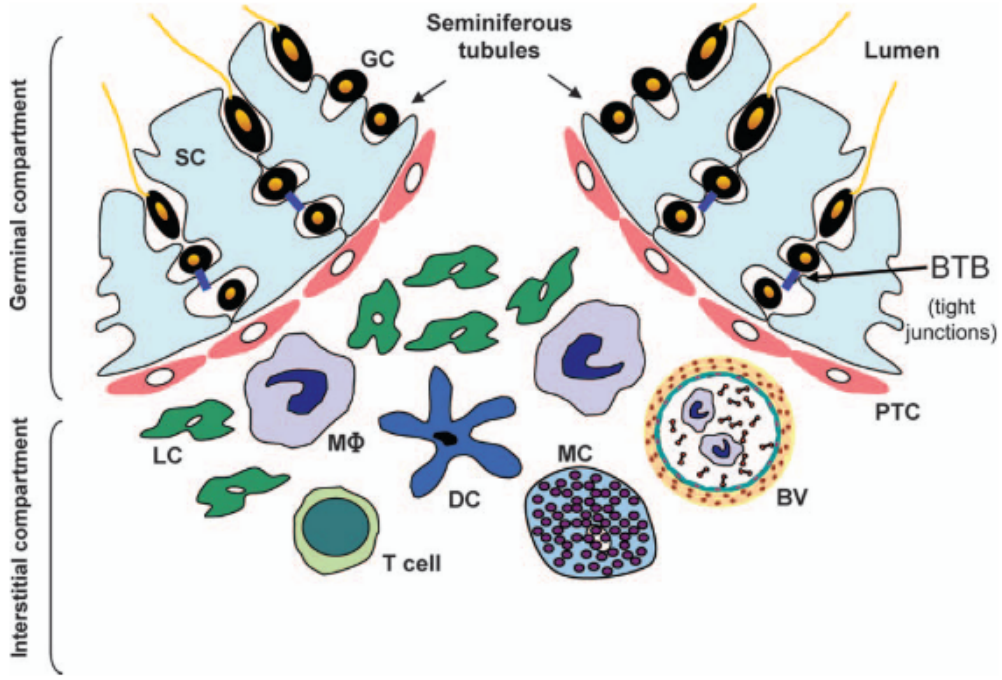

Figure 1. Testicular morphology under physiological conditions. BTB, blood-testis barrier; BV, blood vessel; DC, dendritic cell; GC, germ cell; LC, Leydig cell; MC, mast cell; PTC, peritubular cell; SC, Sertoli cell; Mφ, testicular macrophage. This figure is used with the permission of John Wiley and Sons, license number: 5273580184196 (Fijak and Meinhardt, 2006).

1.2.1. Germinal compartment

1.2.1.1. Germ cells (GCs)

Germ cells including spermatogonia, primary and secondary spermatocytes, round and elongated spermatids as well as spermatozoa are supported by SCs and located within the seminiferous tubules. During puberty, in response to increased androgen product triggered by pituitary gonadotropins, spermatogonia start to proliferate and differentiate into mature sperm in a complex process called spermatogenesis that includes mitotic and meiotic divisions (Stukenborg et al., 2014). Diploid spermatogonia located in the basal compartment of seminiferous tubules initiate mitosis and divide into primary spermatocytes, which subsequently undergo meiosis and give rise to haploid secondary spermatocytes (Stukenborg et al., 2014). After the second meiotic division, haploid round spermatids are formed and differentiate into elongated spermatids, which are finally released into the seminiferous lumen as spermatozoa. However, not all spermatogonia

differentiate into spermatocytes, some of which maintain the characteristics of stem cells and continue to divide and proliferate (Ehmcke et al., 2006).

1.2.1.2. Sertoli cells (SCs)

SCs are one of the somatic testicular cells showing an elongated pyramidal shape. The base of SCs adhere to the basal membrane, while the apical end extends into the lumen of the seminiferous tubules. Proliferation of immature SCs is activated by follicle-stimulating hormone (FSH), the insulin family of growth factors, activins, inhibins and other cytokines (Meroni et al., 2019). Cessation of proliferation and terminal maturation of SCs are regulated by androgens, thyroid hormones, estrogens and retinoic acid, accompanied by the expression of SRY-box transcription factor 9 (SOX9) (Fröjdman et al., 2000; Meroni et al., 2019). SCs have multiple functions. They support and nourish germ cells throughout the developmental stages and control spermatogonial stem cell maintenance and self-renewal as a part of the spermatogonial stem cell niche (França et al., 2016). Moreover, they are involved in the formation of the testicular immunosuppressive environment (Fijak and Meinhardt, 2006). SCs are capable of producing many factors for the interaction with germ cells and interstitial cells in an endocrine or paracrine manner. Factors include androgen binding protein, anti-Müllerian hormone, inhibin B and activin A (Iliadou et al., 2015; Kauerhof et al., 2019).

1.2.1.3. Myoid peritubular cells (PTCs)

PTCs surround the seminiferous tubules as smooth muscle cells, expressing smooth muscle actin, myosin, desmin, vimentin, and other cytoskeletal proteins (Maekawa et al., 1996). Due to their contractile properties they support the transportation of spermatozoa and fluid to the tubular lumen (Romano et al., 2005). Several studies demonstrated that PTCs secrete extracellular matrix (ECM) components (fibronectin, collagen I or IV, proteoglycans), growth factors (TGF-β, fibroblast growth factors, insulin-like growth factors [IGFs]) and signaling factors (interleukin-6 [IL-6], C-C motif chemokine ligand 2 [CCL2]), acting on germ cells, SCs, LCs and interstitial immune cells (Maekawa et al., 1996; Díez-

Torre et al., 2011; Mayerhofer, 2013). Therefore, while they are important elements of testicular structural integrity, they are also involved in the regulation of spermatogenesis and testicular homeostasis.

1.2.2. Interstitial compartment

1.2.2.1. Leydig cells (LCs)

LCs are a group of cells located in the testicular interstitium, which after stimulation with luteinizing hormone (LH) synthesize and secrete testosterone, an important hormone for the maturation of spermatozoa, formation of secondary sex characteristics and anabolic functions (Zirkin and Papadopoulos, 2018). In addition to testosterone, LCs also secrete interleukins, insulin-like 3 (INSL3), and a variety of growth factors such as activins, inhibins, TGFs or IGFs, which act together to directly influence the functions of SCs and PTCs as well as the process of spermatogenesis (Zhou et al., 2019). Insulin and IGFs derived from LCs are required for the SC proliferation and sperm production (Pitetti et al., 2013). LCs produce oxytocin or prostaglandins to induce the PTC contractility as a mean to transport sperm (Heinrich and DeFalco, 2020). Additionally, LCs are extensively and intimately connected to testicular macrophages (TMs) by interdigitations (Hutson, 1998). Colony stimulating factor 1 (CSF1) partially produced by LCs promotes the differentiation of immune cells, especially macrophages (Jones and Ricardo, 2013). Moreover, LCs form a negative feedback loop regulation with TMs. Testosterone inhibits the production of 25-hydroxycholesterol by TMs *in vitro*, which correspondingly reduces the testosterone production by LCs as 25-hydroxycholesterol is a precursor of steroidogenesis in LCs (Heinrich and DeFalco, 2020).

1.2.2.2. Testicular macrophages (TMs)

TMs constitute the principal immune cell population in the testis and play a critical role in organ homeostasis (Bhushan and Meinhardt, 2017). Tissue-resident macrophages such as TMs share common markers such as F4/80, CD11b, CD64 and macrophage-colony stimulating factor receptor (M-CSFR), as well as CX3CR1 (Gentek et al., 2014). In normal

mouse testis, there are roughly two subpopulations of macrophages described. One is the major subpopulation identified as M-CSFR^{hi}CD64^{hi}MHCII^{-} interstitial macrophages, which are localized in the interstitial space in close contact with LCs and show a rounded morphology (Mossadegh-Keller et al., 2017; Bhushan et al., 2020; Meinhardt et al., 2022). The second subpopulation consists of peritubular macrophages characterized by the expression of M-CSFR^{lo}CD64^{lo}MHCII^{+}, surrounding seminiferous tubules and exhibiting elongated morphology (Mossadegh-Keller et al., 2017; Bhushan et al., 2020; Meinhardt et al., 2022). Under physiological conditions, interstitial and peritubular macrophages are CD45^{+}Ly6C^{-}CD11c^{-}F4/80^{+}CD11b^{+} cells and both populations are positive for CX3CR1 (Mossadegh-Keller et al., 2017).

In general, macrophages are classified into two subpopulations (a) pro-inflammatory classically activated M1 macrophages and (b) anti-inflammatory alternatively activated M2 macrophages (Wang et al., 2017). M1 macrophages stimulated by interferon gamma (IFN-γ) or LPS produce high levels of pro-inflammatory cytokines including TNF and IL-6 with the ability to clear pathogens, while M2 macrophages under the stimulation of IL-10 or TGF-β release high levels of anti-inflammatory cytokines such as IL-10 to maintain tissue homeostasis and remodeling (Chávez-Galán et al., 2015). Most of tissue resident macrophages possess an M2 phenotype, for instance in liver, lung, brain or skin (Davies et al., 2013). Similarly, TMs express mainly M2 immunosuppressive genes in steady-state conditions. M2 macrophages constitute the major subpopulation of TMs (Bhushan and Meinhardt, 2017; Mossadegh-Keller et al., 2017). In addition to their role in the maintenance of tissue homeostasis, TMs also support steroidogenesis, promote spermatogenesis and preserve the blood-testis barrier (BTB) (Bhushan et al., 2020; Lustig et al., 2020).

1.3. Testicular immune privilege

The testis is vulnerable to inflammatory damage and generates actively an immunosuppressive microenvironment, which effectively protects the developing haploid germ cells from systemic autoimmune attack, as the body has already established immune tolerance mechanisms before puberty against sperm autoantigens (Zhao et al.,

2014). Many testicular cells including SCs, PTCs, LCs and interstitial immune cells as well as local immunosuppressive molecules participate in the formation of testicular immune privilege (Dutta et al., 2021).

SCs play a critical role in the maintenance of immune privilege, as well as survival and maturation of germ cells (Arck et al., 2014). They participate in the composition of the testicular immunosuppressive environment by expressing apoptosis inhibitors (SERPINA3N, SERPINB9), complement inhibitors (serping1, clusterin), immunomodulatory factors such as indoleamine 2,3-dioxygenase (IDO) or galectin-1, anti-inflammatory cytokines including transforming growth factor-β1 (TGF-β1), inhibitors of granzyme B and ligand B7-H1, which induces the apoptosis of lymphocytes (Meinhardt and Hedger, 2011; França et al., 2016). Furthermore, the tight junctions of SCs form the BTB, which prevents certain substances from entering the seminiferous epithelium, thus creating and maintaining a beneficial microenvironment for spermatogenesis (Marini et al., 2018).

LCs produce testosterone, which inhibits the production of pro-inflammatory cytokines by TMs, induces naïve T cells and M1 macrophages to differentiate into immunosuppressive regulatory T cells (Tregs) and M2 macrophages, respectively (Fijak et al., 2015; Meinhardt et al., 2018). Along with LCs, SCs and PTCs express the androgen receptor and are therefore regulated by testosterone to influence also the immune microenvironment of the testis. Some studies show that the specific deletion of the androgen receptor in SCs promotes BTB permeability, increases production of autoantibodies against germ cell antigens and recruits immune cells, while testosterone application inhibits the inflammatory responses in SCs and PTCs (Meng et al., 2011; Fijak et al., 2015). Altogether, these data indicate that testosterone is one of the important molecules involved in the maintenance of testicular immune privilege.

Compared to macrophages in other organs, TMs display a reduced capacity to express pro-inflammatory cytokines such as tumor necrosis factor (TNF) or IL-1β with concomitant elevated production of the anti-inflammatory factor IL-10 to support the immunosuppressive characteristics (Fijak and Meinhardt, 2006). In addition, TMs produce corticosterone to suppress inflammatory gene expression, polarize TMs into an M2

phenotype and expand the population of Tregs (Wang et al., 2017). Other immune cells such as dendritic cells (DCs), lymphocytes and mast cells together with TMs share their location in the testicular interstitial compartment, regulate immune responses and maintain the testicular immune privilege (Fijak and Meinhardt, 2006). DCs isolated from normal testis are immature with reduced capacity to stimulate T cells (Fijak and Meinhardt, 2006; Bhushan et al., 2020). Under physiological conditions, $CD8^+$ T cells are the major subpopulation of lymphocytes (Bhushan et al., 2020). A small population of $Foxp3^+$ Tregs was also identified in the testis where they function as a suppressor of T cell activation to maintain the tolerogenic environment (Jacobo et al., 2009).

1.4. Experimental autoimmune orchitis (EAO)

EAO is a rodent model of chronic testicular inflammation, which mimics the pathological changes found in some human biopsies with impaired spermatogenesis (Jacobo et al., 2011a; Lustig et al., 2020). EAO is induced by active immunization with testicular homogenate in complete Freund's adjuvant followed by the injection of *Bordetella pertussis* toxin (Fijak et al., 2018).

EAO pathology is characterized by progressive loss of germ cells, impairment of the BTB, atrophy of seminiferous tubules and thickening of the lamina propria (Pérez et al., 2012; Nicolas et al., 2017a). The progression of EAO pathogenesis is documented by testicular fibrosis visible as accumulation of collagen fibers and fibronectin. Similar changes are also frequently detected in biopsies from infertile men with impaired spermatogenesis and leukocytic infiltrates (Nicolas et al., 2017a; Kauerhof et al., 2019). Moreover, during EAO strong inflammatory responses are identified, including infiltration of the testicular interstitium with $CD45^+$ leukocytes (TMs, $CD3^+$ T cells, Tregs and dendritic cells) and elevated levels of inflammatory cytokines such as activins, TNF, CCL2, IL-1α, IL-1β, IL-10 or IFN-γ (Guazzone et al., 2009; Nicolas et al., 2017a; Fijak et al., 2018).

During testicular inflammation, increased numbers of TMs are accompanied by elevated levels of CCL2, which facilitates the infiltration of $CD68^+CD163^-$ monocytes expressing CCR2 into the testicular interstitium (Rival et al., 2008; Bhushan et al., 2020; Lustig et al.,

2020). Reduction in the number of TMs correlates with a decreased incidence and severity of the testicular damage under inflammatory condition (Rival et al., 2008). Immature DCs migrate to lymph nodes to proliferate, mature and present antigens to T cells, a process characterized by downregulation of the immature DC marker CCR2 and upregulation of bioactive IL-12 and CCR7 (Rival et al., 2007). In addition, TNF or IFN-γ expressing $CD4^+$ and $CD8^+$ T cells and Tregs accumulate in the inflamed testis (Jacobo et al., 2011b, 2015). Summary of EAO characteristics is shown in **Fig. 2**.

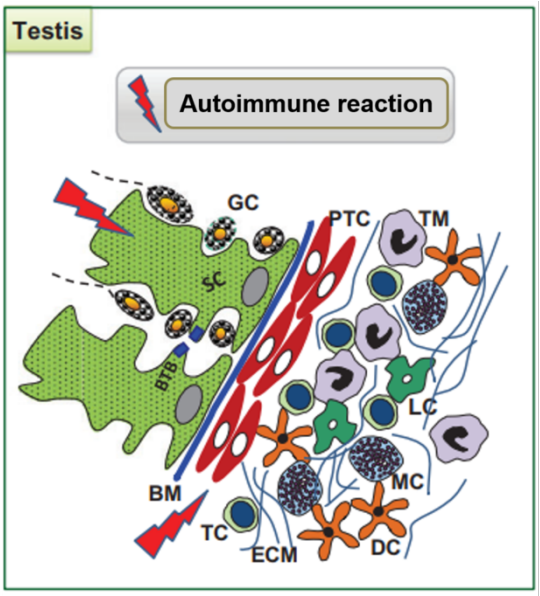

Common features
loss of germ cells
impairment of blood-testis-barrier
atrophy of seminiferous tubules, thickening of the seminiferous lamina propria
fibrosis, accumulation of collagen and fibronectin
infiltration of immune cells, including T cells, Treg, macrophages, DCs, and mast cells
Elevated levels of inflammatory mediators, such as CCL2, TNF, IL-1, IL-6, IL-10, and activin A

Figure 2. Pathological changes in the EAO testis. BM, basement membrane; DC, dendritic cell; ECM, extracellular matrix; GC, germ cell; LC, Leydig cell; MC, mast cell; PTC, peritubular cell; SC, Sertoli cell; TC, T cell; TM, testicular macrophage. This figure is used with the permission of Oxford University Press, license number: 5273561025685 (Fijak et al., 2018).

1.5. Chemokines and cytokines involved in testicular physiology and pathology

1.5.1. C-C motif chemokine ligand 2 (CCL2)

CCL2 and its main receptor C-C motif chemokine receptor type 2 (CCR2) have been implicated in pathological processes in diverse diseases in mediating the trafficking of lymphocytes, macrophages or bone marrow-derived fibroblasts to the sites of injury (Xia et al., 2013; Fantuzzi et al., 2019). CCL2, also known as monocyte chemoattractant protein-1 (MCP-1), belongs to the C-C chemokine family and is produced by a variety of

cell types, especially monocytes/ macrophages, fibroblasts, endothelial cells, epithelial cells, smooth muscle cells or tumor cells (Deshmane et al., 2009). CCL2 by binding to its receptor CCR2 or CCR4 is involved in enhancing survival, adhesion and cell-killing properties of myeloid cells. Moreover, it induces macrophage polarization and corresponding cytokine secretion and shows immunosuppressive effects, apart from the regulation of leukocyte migration (Gschwandtner et al., 2019).

CCL2 is involved in the control of a broad spectrum of disorders, including autoimmune diseases, cancer, obesity, atherosclerosis and neurodegeneration (O'Connor et al., 2015). CCL2-dependent macrophage recruitment promotes tissue inflammation and remodeling (Shen et al., 2014). Therapeutic blockade or genetic depletion of CCL2 not only confers resistance to disease, but also prevents their relapse, for example in multiple sclerosis, rheumatoid arthritis or atherosclerosis (O'Connor et al., 2015). Under pathological conditions, CCL2 is inducible after the exposure to inflammatory mediators such as IL-1, IL-6, TNF, TGF-β, IFN-γ or PDGFs (Yoshimura, 2018). Increased expression of CCL2 directly mediates pro-fibrotic effects on fibroblasts by inducing TGF-β signaling or recruiting immune cells, which both in turn excessively produce ECM proteins (Sahin and Wasmuth, 2013; Ruytinx et al., 2018).

In the testis, CCL2 expression is observed in mononuclear cells, LCs, PTCs and SCs (Gerdprasert et al., 2002; Lei et al., 2018). In the early phase of EAO, testicular mRNA expression of *Ccl2* is unchanged, whereas during the progression of inflammation levels of CCL2 are upregulated in the tissue, but also in isolated testicular fluid and in conditioned medium (CM) obtained from TMs (Guazzone et al., 2003; Nicolas et al., 2017a). In addition, increased CCL2 levels cause dysfunction, inhibition of steroidogenesis and apoptosis of LCs (Jiang et al., 2020b).

1.5.2. C-C motif chemokine receptor type 2 (CCR2)

CCR2 is a receptor for several ligands such as CCL2, CCL7, CCL8, CCL12 and CCL13, amongst which CCL2 is the most important chemokine (Bose and Cho, 2013). CCR2 is expressed on certain immune cell types, mainly monocytes, macrophages, natural killer

(NK) cells and T lymphocytes. During inflammation, CCR2 can also be induced in other cells such as endothelial cells, fibroblasts and regulatory T lymphocytes that perform either anti-inflammatory or pro-inflammatory functions (Chu et al., 2014; Angela Covino et al., 2015). CCR2 signaling is the key player in trafficking of monocytes/ macrophages or lymphocytes from bone marrow to the peripheral circulation and is implicated as a driver of tissue fibrosis (Fantuzzi et al., 2019). Recent studies showed that CCR2 is involved in the transmigration of bone marrow-derived fibroblasts and the differentiation of resident fibroblasts to myofibroblasts (Sahin and Wasmuth, 2013; Xia et al., 2013). CCR2 positive monocytes, macrophages and monocytic myeloid-derived suppressor cells can promote tissue fibrosis by producing TGF-β1, TIMP1, PDGF-B and collagens (Lebrun et al., 2017; Kuroda et al., 2019; Xu et al., 2019). Genetic deletion or pharmacological inhibition of CCR2 protects the tissue from damage and alleviates the progression of fibrotic responses (Sahin and Wasmuth, 2013).

In normal testis, CCR2 is expressed by mononuclear cells in the interstitial compartment (Guazzone et al., 2003). The number of $CCR2^+$ mononuclear cells is significantly higher in EAO testis, while the expression of *Ccr2* mRNA in dendritic cells from inflamed testis is decreased (Guazzone et al., 2003; Rival et al., 2007).

1.5.3. Activin A

Activin A, a member of the TGF-β superfamily of cytokines, was initially discovered as an inducer of FSH release (Vale et al., 1986). Activin A is formed as a homodimer of the inhibin βA subunit. It binds to the activin-specific type II receptor (ActRII) that oligomerizes the type I receptor (ActRI), which in turn phosphorylates specific serine/ threonine kinases (Hedger et al., 2011). In detail, activin A downstream signaling is induced by the phosphorylation of suppressor of mothers against decapentaplegic homolog 2/3 (Smad2/3) and the translocation of the Smad2/3-Smad4 complex to the nucleus (Morianos et al., 2019). In addition to the canonical activation pathway, activin A can also phosphorylate mitogen-activated protein (MAP) kinases, such as extracellular signal-regulated kinase 1/2 (ERK1/2), c-Jun N-terminal kinase (JNK) and p38, triggering downstream signaling (Hedger et al., 2011; Wijayarathna and de Kretser, 2016).

The activin A subunit inhibin βA is detected in most of tissues, e.g. bone marrow, liver, heart, central nervous system or fat, and is highly expressed in the male and female reproductive tract (Hedger and de Kretser, 2013). In normal testis, activin A is released mainly by SCs, and is also detected in PTCs, LCs, endothelial cells, TMs, mast cells, as well as spermatogonia, spermatocytes and round spermatids (Hedger and Winnall, 2012). In general, lipopolysaccharide (LPS) and several pro-inflammatory cytokines including TNF, IL-1β or TGF-β stimulate the synthesis and secretion of activin A in diverse cell types, such as monocytes/ macrophages, dendritic cells, neutrophils, B cells and T cells (Hedger et al., 2011).

Activin A is involved in the regulation of SC proliferation, BTB integrity, spermatogenesis and testicular steroidogenesis. Moreover, activin A also plays multiple biological functions in inflammation, immunity and fibrosis (Wijayarathna and de Kretser, 2016). In addition, activin A acts as an early pro-inflammatory mediator and also in an anti-inflammatory action when the inflammation is ongoing (de Kretser et al., 2012). Activin A recruits monocytes/ macrophages, mast cells or immature dendritic cells to the sites of injury. These cells then produce inflammatory mediators, including IL-1β, TNF, IL-6 or nitric oxide, while suppressing the potent anti-inflammatory cytokine IL-10 (Sierra-Filardi et al., 2011). On the other hand, activin A inhibits the conversion of IL-1β from the precursor to the activated form and the production of pro-inflammatory cytokines in monocytes/ macrophages (Hedger et al., 2011; de Kretser et al., 2012). Altogether, several studies indicate that activin A skews macrophages towards the M1 pro-inflammatory phenotype, while other reports suggest their role in promoting macrophage polarization towards the M2 anti-inflammatory phenotype (de Kretser et al., 2012; Hedger and de Kretser, 2013). Furthermore, activin A increases phagocytic and pinocytotic activities in macrophages, enhances reactive oxygen species production, IL-6 release and phagocytosis in neutrophils, stimulates immunoglobulin production by B cells and differentiation of monocytes to dendritic cells, promotes Tregs development, and inhibits IFN-γ production and cytotoxicity in NK cells (Hedger and de Kretser, 2013; Morianos et al., 2019).

Apart from the role in inflammation and immunity, activin A is involved in various tissues in fibrosis development. Activin A drives TGF-β1-induced renal fibrosis through STAT3 signaling pathway, activates hepatic stellate cells and contributes to the fibrogenesis through inducing TNF and TGF-β production by Kupffer cells, and induces the proliferation and differentiation of lung resident fibroblasts, leading to collagen deposition (Hardy et al., 2015; Kiagiadaki et al., 2018; Yuan et al., 2021). In addition, activin A increases the number of leukocytes, induces migration of fibroblasts and reprograms their transcriptome by increasing pro-fibrotic gene expression signatures, which act together to accelerate the process of tissue remodeling and fibrosis (Cangkrama et al., 2020; Wietecha et al., 2020).

Expression of the activin A subunit *Inhba* mRNA is elevated in human testis with impaired spermatogenesis and focal leukocytic infiltrates (Kauerhof et al., 2019). During testicular inflammation, stronger expression of activin A is observed in SCs and immune cells within inflammatory infiltrates (Nicolas et al., 2017a). Moreover, the concentration of activin A protein is increased in EAO testis, while no significant difference in activin βA subunit *Inhba* mRNA expression in EAO testis compared to controls is detected (Nicolas et al., 2017a).

1.5.4. Follistatin

Follistatin (FST), an activin A binding protein, has a high affinity to inhibit activin A bioactivity (de Kretser et al., 2012). There are two forms of follistatin, which are 288 (FST288) and 315 amino acids (FST315). FST288 is the tissue-bound form, binding to heparan-sulphate proteoglycans on cell surfaces, while FST315 is the circulating form, binding to the heparin site after it binds to activin A (Hedger and de Kretser, 2013). The binding between activin A and FST is irreversible, and finally leads to endocytosis and lysosomal degradation (Wijayarathna and Hedger, 2019).

Protein concentrations of FST are increased in EAO testis, while the mRNA expression of total *Fst*, *Fst288* and *Fst315* is not changed (Nicolas et al., 2017a). FST315 overexpression in mice reduces the induction rate and severity of EAO, decreases the expression of fibronectin, but does not prevent the disease development (Nicolas et al.,

2017b; Kauerhof et al., 2019). In mice lacking FST, serum activin A level is elevated and testicular weight is reduced (Wijayarathna et al., 2017).

1.6. Fibrosis

1.6.1. Mechanisms of fibrosis

Fibrosis is a pathological outcome in many chronic inflammatory disorders, in which normal parenchymal tissue is transformed into connective tissue composed of myofibroblasts/ fibroblasts concomitant with an excessive deposition of ECM components (Wynn and Ramalingam, 2012; Henderson et al., 2020). Myofibroblasts are an important source of ECM proteins during fibrogenesis. They are derived not only after transformation, activation or proliferation of resident fibroblasts, but also through infiltration and activation of circulating hematopoietic cells termed as fibrocytes, transdifferentiation and recruitment of pericytes, proliferation of vascular smooth muscle cells, as well as mesothelial-, epithelial- or endothelial-to-mesenchymal transition **(Fig. 3)** (Weiskirchen et al., 2019).

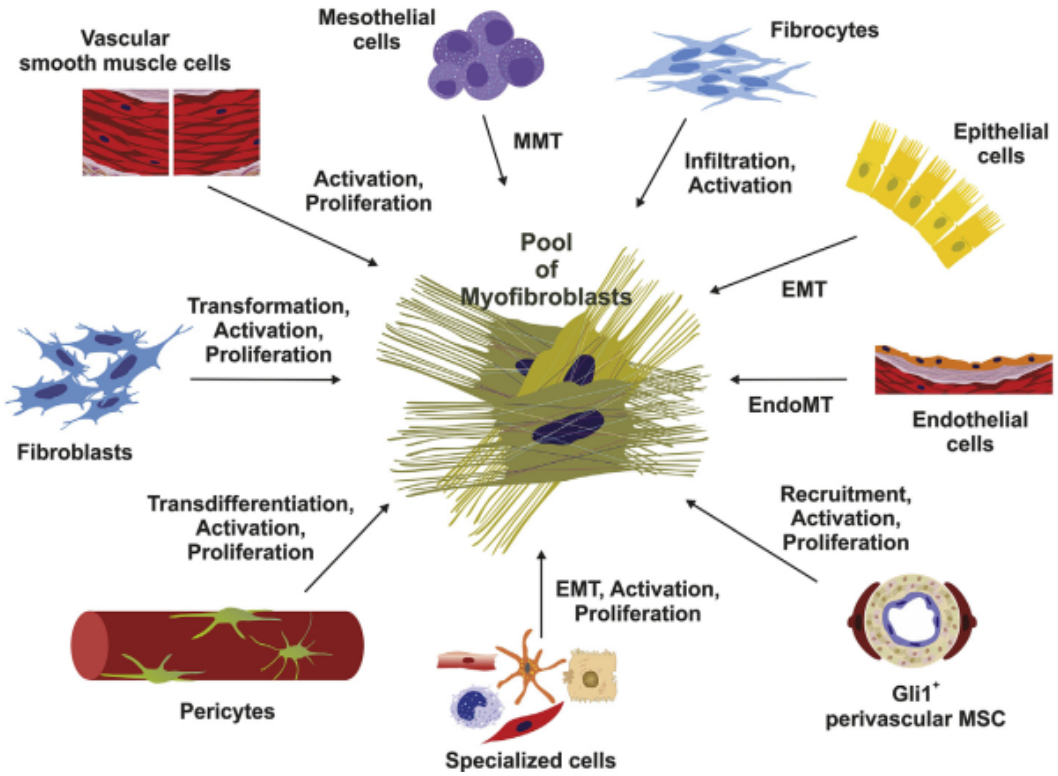

Figure 3. The origin of myofibroblasts leading to ECM component accumulation. This overview illustrates that myofibroblasts can derive from fibroblasts, fibrocytes, epithelial, endothelial, mesothelial cells, pericytes, vascular smooth muscle cells and perivascular mesenchymal stem cell-like cells. All of these cells contribute to the increase of the myofibroblast pool during fibrosis through transformation, activation, proliferation, infiltration, EMT, EndoMT or MMT. EMT, epithelial-to-mesenchymal transition; EndoMT, endothelial-to-mesenchymal transition; MMT, mesothelial-to-mesenchymal transition. This figure is used with the permission of Elsevier, license number: 5295980432293 (Weiskirchen et al., 2019).

Injury triggers the start of inflammation, followed by leukocyte infiltration, Th2 or M2 polarization and release of cytokines (Distler et al., 2019). Under the stimulation of type 2 cytokines secreted by injured epithelial cells or leukocytes, such as IL-4, IL-5, IL-13, IL-25 and IL-33, naïve $CD4^+$ T cells differentiate into Th2 cells, which correspondingly produce IL-4, IL-5 and IL-13 during lung, liver and skin fibrosis (Wynn and Ramalingam, 2012; Gieseck III et al., 2018). At the same time, monocytes or macrophages that are resident or recruited to the inflamed lesions, produce a variety of pro-fibrotic factors including TGF-β, platelet-derived growth factors (PDGFs), matrix metalloproteinases (MMPs) and fibronectin (Wynn and Vannella, 2016; Kishore and Petrek, 2021). All of these pro-fibrotic mediators produced either by leukocytes or mesenchymal cells promote the proliferation, differentiation, activation and migration of myofibroblasts or fibroblasts that facilitate fibrosis (Distler et al., 2019; Henderson et al., 2020). In addition, macrophage-myofibroblast transition is another important mechanism that promotes tissue remodeling. Macrophages derived from circulating monocytes originating from bone marrow transform into myofibroblasts by TGF-β/Smad, Wnt/β-catenin, NF-κB or STAT1/STAT3 signaling and contribute to renal and pulmonary fibrosis (Tang et al., 2020; Vierhout et al., 2021). Fibroblast-macrophage reciprocal interaction also influences the onset and progression of tissue fibrosis. Fibroblasts express CSF1, CCL2 and IL-6 to elicit the survival, migration and activation of macrophages. In turn, activated macrophages produce PDGF-A, TGF-β and IL-6 to promote the proliferation and activation of fibroblasts (Buechler et al., 2021).

1.6.2. Fibrocytes

The fibrocytes originally described as bone marrow-derived and fibroblast-like cells circulate in the peripheral blood, migrate to the injured tissues and contribute to the connective tissue scar formation (Bucala et al., 1994). Recently, these cells were identified to express the pan-hematopoietic cell marker CD45, the stem cell marker CD34 and mesenchymal cell markers such as collagen I, collagen III, fibronectin, or vimentin (Abe et al., 2001; Chong et al., 2019). Cultured fibrocytes from some organs such as liver, lung, heart, kidney or skin share the spindle-shaped morphology, produce collagens and αSMA proteins in response to TGF-β, IL-13, M-CSF or granulocyte-macrophage colony-stimulating factor (GM-CSF), differentiate into myofibroblasts and exert contractile force, suggesting a role in fibrotic tissue repair (Abe et al., 2001; Mack, 2018; de Oliveira and Wilson, 2020). During differentiation, fibrocytes gradually lose their expression of CD45 and CD34 (Quan et al., 2006; Chong et al., 2019).

In addition, fibrocytes also express chemokine receptors including CCR2, CCR5, CCR7 or CXCR4, which are involved in their migration from peripheral blood into fibrotic tissues (Wada et al., 2007; Mack, 2018). The studies show that the absence of CCR2 and the blockade of CCR7 signaling reduce the migration of fibrocytes into the injured organs (Sakai et al., 2006; Reich et al., 2013).

1.6.3. CXCL12/ CXCR4

C-X-C motif chemokine receptor 4 (CXCR4) is widely expressed in bone marrow-derived progenitor cells, which could differentiate into other cell types that are necessary for the tissue damage or repair, for instance fibrocytes, fibroblasts, epithelial or endothelial cells (Ridiandries et al., 2018; Kawaguchi et al., 2019; Jaffar et al., 2020). CXCR4 and its canonical C-X-C motif chemokine ligand 12 (CXCL12) regulate the homing and chemotaxis of immune cells including neutrophils, lymphocytes or fibrocytes from bone marrow to the target tissue, such as lung, kidney or heart (Wada et al., 2007; Döring et al., 2014; Xie and Zhao, 2017; Kawaguchi et al., 2019). CXCR4 expressing cells particularly $CXCR4^+$ macrophages are believed to be pro-fibrotic (Chen et al., 2021). Several studies demonstrated that blockade of CXCR4 or CXCL12 by using antibodies,

antagonists or genetic deletion reduces the infiltration of fibrocytes and shows lower levels of ECM protein deposition during inflammation and fibrosis (Phillips et al., 2004; Yuan et al., 2015; Xie and Zhao, 2017; Griffiths et al., 2018).

1.6.4. Extracellular matrix (ECM) components

The ECM is a dynamic network of proteins secreted by cells in all tissues and organs, consisting of collagens, fibronectin, laminin, elastin or proteoglycans (Yue, 2014). There are two main types of ECM based on their location and composition: (a) the interstitial connective tissue matrix supporting the tissue structure, including collagen type I, fibronectin, elastin and proteoglycans; and (b) the basement membrane located between epithelia and stromal layers consisting mainly of collagen type IV, laminin and heparan sulphate proteoglycans (Bonnans et al., 2014). The ECM regulates diverse cellular functions, including survival, proliferation, adhesion, migration or differentiation, and under pathological conditions functions as a driver of tissue fibrosis (Frantz et al., 2010; Herrera et al., 2018).

Collagens are the most abundant fibrous proteins in the ECM, in which collagen type I is the most prevalent component (Theocharis et al., 2016). The expression of collagen type I is generally increased in many fibrotic tissues, and plays a critical role in stimulating fibroblast migration and wound healing as well as the vascularization of endothelial cells (Kisling et al., 2019). Under physiological conditions in the rat testis, collagen type I is present in the capsule, interstitial space and basement membrane of the seminiferous tubules (Falade et al., 2017). The basement membrane of the seminiferous tubules in human testis also contains collagen type IV (Dobashi et al., 2003). Fibronectin is considered as a large glycoprotein that is involved in the connections between cells and interstitial ECM (Theocharis et al., 2016). Additionally, fibronectin is crucial not only for the cell attachment but also for the cell migration during disease development and wound healing through the binding to integrin receptors (Frantz et al., 2010). Excessive fibronectin deposition is associated with fibrosis and its inhibition attenuates liver fibrogenesis (Altrock et al., 2015). Furthermore, fibronectin regulates the expression of MMPs thus affects the tissue remodeling (Patten and Wang, 2021). In the normal testis,

fibronectin is clearly visible in basal membrane, PTC layer and blood vessels in the interstitial compartment (Santamaria et al., 1990; Başımoğlu Koca, 2019; Kauerhof et al., 2019).

1.6.5. Regulators of ECM

1.6.5.1. Matrix metalloproteinases (MMPs)

MMPs are mainly produced by fibroblasts, epithelial cells, endothelial cells or leukocytes and are capable of degrading ECM proteins such as collagens and fibronectin (Sengupta and MacDonald, 2007; Cui et al., 2017). MMPs are synthesized as a latent, inactive form (pro-MMPs), which is subsequently cleaved proteolytically by various proteinases in the extracellular space (Bonnans et al., 2014). In addition, cleavage of MMPs can lead to diverse biological activities, such as cell migration, differentiation, proliferation, apoptosis, or growth factor release and activation, which contribute to the tissue remodeling during physiological or pathological processes, for example angiogenesis, embryogenesis, inflammation, fibrosis or cancer (Nagase et al., 2006; Giannandrea and Parks, 2014; Cui et al., 2017).

1.6.5.1.1. MMP2

MMP2 belongs to the gelatinases also termed type IV collagenases and is mainly expressed in fibroblasts, smooth muscle cells, epithelial cells, or macrophages (Risinger et al., 2006; Yang et al., 2009; Kurzepa et al., 2014). In normal adult testis, MMP2 is detected in SCs, some interstitial cells and germ cells including spermatogonia, spermatocytes and round spermatids (Szarek et al., 2019). The latent form of pro-MMP2 is secreted and activated to MMP2 by the formation of the MMP14 - TIMP2 - pro-MMP2 trimolecular complex (Khokha et al., 2013). MMP2 is thought to be anti-fibrotic due to the ability of breaking down the ECM, resulting in the alleviation of fibrosis (Giannandrea and Parks, 2014). Loss of MMP2 increases the expression of collagen I, αSMA, TGF-β, MMP14, TIMP1 and PDGFRβ, which in turn enhance fibrosis (Onozuka et al., 2011; Radbill et al., 2011). However, MMP2 also shows pro-fibrotic functions. MMP2 expression

and activity are upregulated in several animal models of fibrosis (Giannandrea and Parks, 2014). Furthermore, immune as well as tumor cells produce MMP2, which is associated with the degradation of collagen IV, to enable them to cross the endothelium, thereby promoting the development of inflammation, fibrosis and cancer (Kurzepa et al., 2014).

1.6.5.1.2. MMP9

Similar to MMP2, MMP9 also belongs to the gelatinases and has the same ability to degrade collagen IV and facilitate leukocyte endothelial transmigration (Khokha et al., 2013). The expression of MMP9 was demonstrated in neutrophils, monocytes, macrophages, fibroblasts, or vascular endothelial cells (Opdenakker et al., 2001). Positive MMP9 staining was shown in SCs, spermatogonia and some PTCs in adult testis under physiological conditions (Szarek et al., 2019). MMP9, like MMP2, either reduces or promotes fibrosis (Giannandrea and Parks, 2014). On one hand, overexpression of MMP9 derived from macrophages attenuates the development of fibrosis, indicating the anti-fibrotic role of MMP9 during pathological conditions (Cabrera et al., 2007). On the other hand, MMP9 shows pro-fibrotic activity, which induces latent TGF-β1 and supports myofibroblast survival and activation (Yu and Stamenkovic, 2000; Wang et al., 2010).

1.6.5.2. Tissue inhibitor of matrix metalloproteinases (TIMPs)

The activity and function of MMPs can be regulated by TIMPs that are endogenous inhibitors of MMPs (Brew and Nagase, 2010). TIMPs inhibit many diverse biological processes caused by MMPs, for instance ECM proteolysis, TGF-β release and neutrophil chemotaxis (Arpino et al., 2015). The balance between MMPs and TIMPs determines the content of ECM in the tissue, leading either to ECM degradation or accumulation (Arpino et al., 2015; Cui et al., 2017). TIMP1 is a strong inhibitor of selected MMPs, especially MMP9 (Cabral-Pacheco et al., 2020). Several inflammatory cytokines are able to upregulate the expression of TIMP1, such as IL-1β, IL-6, TNF, and TGF-β (Hemmann et al., 2007). Due to the direct inhibition of ECM proteolysis, TIMP1 is generally considered as an important pro-fibrotic factor. $CCR2^+$ monocytes, fibrocytes or macrophages can

promote fibrosis through TIMP1 production by inhibiting collagen degradation (Kuroda et al., 2019; Chen et al., 2021). Neutralization of TIMP1 markedly reduces collagen accumulation and decreases fibroblast activation in a rat model of carbon tetrachloride (CCl_4)-induced liver fibrosis (Parsons et al., 2004). Conversely, mice lacking TIMP1 show enhanced acute lung injury after bleomycin exposure and increased inflammatory and fibrotic responses following CCl_4-induced liver injury, suggesting the role of TIMP1 in restricting inflammation and fibrosis (Brew and Nagase, 2010; Arpino et al., 2015).

1.6.5.3. Integrins

Integrins are heterodimeric transmembrane receptors consisting of an α and β subunit, which can bind to the ECM proteins extracellularly and link intracellularly to the cytoskeleton (Schnittert et al., 2018). According to the differences of their ligands, integrins are classified into four groups, (I) arginine-glycine-aspartate (RGD)-binding receptors, (II) leukocyte-specific receptors, (III) laminin receptors, and (IV) collagen receptors (Barczyk et al., 2010). The tripeptide RGD motif constitutes a major recognition site for integrin binding and can be found in ECM proteins such as fibrinogen, fibronectin or vitronectin (García-Gareta et al., 2019).

Integrins possess two main functions: (a) the attachment of cells to ECM or other cells, inducing ECM assembly and cell migration, and (b) the transduction of signals from ligands to cells, which leads to cell adhesion, proliferation, differentiation, survival or death (Marsico et al., 2018; Park et al., 2020). Through these various interactions between ECM and cells, integrins are directly or indirectly involved in the initiation and progression of fibrosis (Schnittert et al., 2018). For instance, αvβ3 integrin was upregulated in connective tissue growth factor-induced skin fibrosis, and blockade of αvβ3 integrin inhibited the contractility, differentiation and collagen synthesis in dermal fibroblasts (Hu et al., 2014). The expression of αvβ5 integrin was higher during rat cardiac fibrosis and in cardiac fibroblasts isolated from fibrotic tissue (Perrucci et al., 2018). Inhibition of αvβ5 integrin resulted in suppressed TGF-β1 release, collagen production and myofibroblast differentiation in cardiac fibroblasts during heart injury (Perrucci et al., 2018). Interestingly, increasing evidence points to the integrin - TGF-β crosstalk as a crucial factor for the

development and pathogenesis of fibrosis. TGF-β induces the expression of αvβ3 and αvβ5 integrins in fibroblasts, endothelial cells or carcinoma cells, promoting myofibroblast differentiation, re-epithelialization and angiogenesis during wound healing and fibrosis (Margadant and Sonnenberg, 2010). Moreover, αv-containing integrins such as αvβ3 or αvβ5 integrin enhance TGF-β activity and signaling in pulmonary fibrosis by MMP2, MMP9 or MMP14 cleavage (Wipff and Hinz, 2008; Margadant and Sonnenberg, 2010; Camelo et al., 2014).

1.6.5.4. Platelet-derived growth factors (PDGFs)

PDGF is one of the growth factors that regulates cell growth and division, and is composed of two subunit, forming five different isoforms, including PDGF-AA, -AB, -BB, -CC and -DD (Kardas et al., 2020). Multiple studies examining the effects of PDGF inhibition or overexpression have implicated that PDGFs promote fibrosis (Distler et al., 2019). Injured epithelial cells and/or endothelial cells as well as inflammatory immune cells produce PDGFs and stimulate PDGF receptor (PDGFRα or PDGFRβ)-expressing mesenchymal cells, such as fibroblasts, pericytes, or vascular smooth muscle cells, which give rise to myofibroblasts and produce exaggerated amount of ECM (Klinkhammer et al., 2018). In addition, PDGFs also drive chemotaxis and migration as well as exert anti-apoptotic and mitogenic effects in fibroblasts, activate cytoplasmic downstream signaling pathways or transcription factors and regulate stem cell pluripotency (Klinkhammer et al., 2018). During inflammation, elevated cytokines such as TGF-β or IL-1α upregulate the expression of PDGFs and PDGFR in fibroblasts or macrophages, leading to severe fibrosis (Andrae et al., 2008).

In adult rodent testis, LCs are the main source of PDGF-A, PDGF-B, PDGFRα and PDGFRβ, while SCs, PTCs, gonocytes and some interstitial cells such as immune cells express these factors and their receptors in small amounts (Mariani et al., 2002; Basciani et al., 2010). PDGF/ PDGFR signaling pathway regulates cell-cell interaction in the testis, for example, by promoting the proliferation and migration of PTC precursors, which induces the development of LCs, as well as establishes and maintains spermatogenesis (Mariani et al., 2002; Basciani et al., 2010).

1.6.6. Testicular fibrosis

Testicular fibrosis is a hallmark of a severe stage of EAO, which is accompanied by the accumulation of ECM components and the thickening of the α-smooth muscle actin (αSMA) positive layer in the seminiferous tubules (Nicolas et al., 2017a; Lustig et al., 2020). Total collagen content and *collagen I α-2* mRNA expression were elevated in EAO testis as compared to untreated and adjuvant controls (Kauerhof et al., 2019). Extensive deposition of fibronectin was found in the interstitium and around seminiferous tubules in EAO testis, and that was also positively correlated with the disease severity and fibrosis (Kauerhof et al., 2019; Lustig et al., 2020). Moreover, elevated levels of collagens were also detected in human testicular biopsies with impaired spermatogenesis and focal leukocytic infiltrates compared to control biopsies with intact spermatogenesis (Kauerhof et al., 2019).

Several factors may contribute to the development of testicular fibrosis following inflammation and injury. The stimulation of the TGF-β1/Smad2 or nuclear factor-erythroid factor 2-related factor 2 (Nrf2) signaling pathway is involved in testicular fibrosis (Yu et al., 2021; Zheng et al., 2021). In severe EAO testis, the appearance and progression of fibrosis is accompanied by an increase of activin A and CCL2 levels (Nicolas et al., 2017a). The expression of activin A subunit *Inhba* mRNA positively correlates with the total collagen content in patients with impaired spermatogenesis (Kauerhof et al., 2019). TNF stimulates activin A production by murine SCs *in vitro* (Kauerhof et al., 2019). Afterwards, activin A activates Smad2 signaling in PTCs and NIH 3T3 fibroblasts, which subsequently produce αSMA, fibronectin, collagen I or collagen IV *in vitro* (Kauerhof et al., 2019). Altogether, these results suggest that activin A could promote the progression of fibrosis during testicular inflammation probably through regulating the functions of macrophages, considering that this cell type is one of the target cells for activin A and migrates to the inflamed testis. However, the specific mechanisms leading to testicular fibrosis are not known as shown in **Fig. 4**.

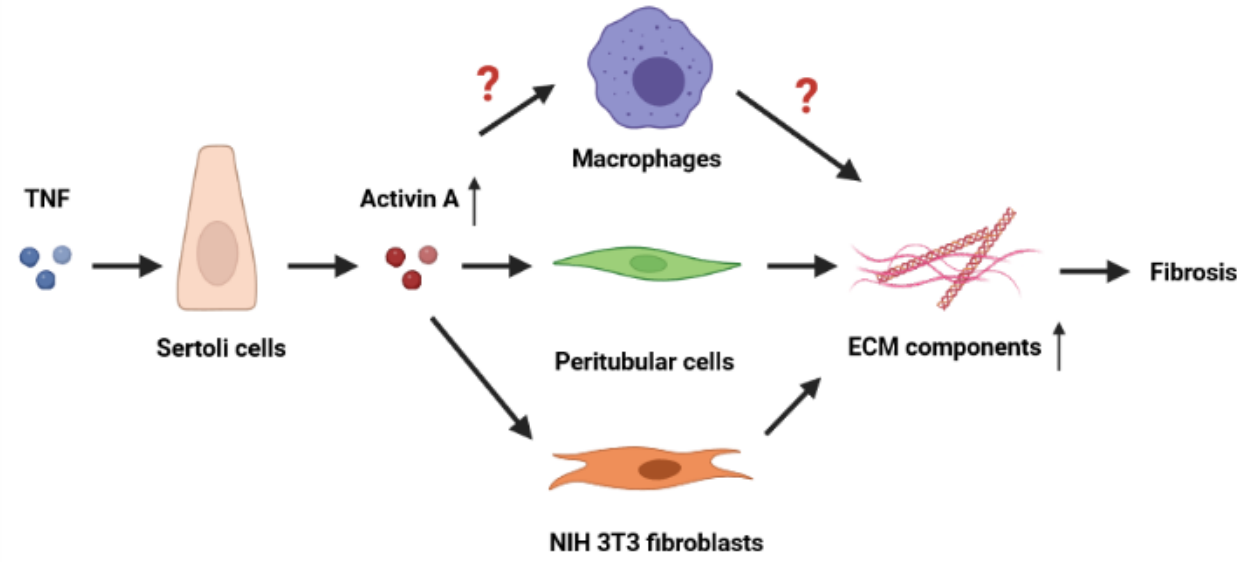

Figure 4. The simplified scheme of possible role of activin A in the development of fibrosis. TNF stimulates the synthesis of activin A by SCs, which in turn induces the production of ECM components by PTCs and NIH 3T3 fibroblasts. Whether activin A also affects the accumulation of ECM by influencing macrophages needs to be elucidated.

1.7. Aim of study

EAO is a mouse model of chronic testicular inflammation and fibrosis, well reflecting pathologies seen in some forms of spermatogenic disturbances in men. This model is characterized by the destruction of testicular morphology, infiltration of the testicular interstitium by leukocytes, elevated levels of pro-inflammatory cytokines/ chemokines such as TNF, CCL2 (ligand for CCR2) and activin A, as well as loss of germ cells, all leading to fibrosis and subsequent infertility (Fijak et al., 2018).

TMs constitute the principal immune cell population in the testis and these cells play a critical role in maintaining tissue homeostasis. Increased numbers of TMs during testicular inflammation correlate with a higher incidence and severity of testicular damage (Rival et al., 2008). Because resident or macrophages newly recruited to the inflammatory lesions can produce a variety of pro-fibrotic factors including CCL2, TGF-β, TNF, PDGFs, MMPs or TIMPs, they are key players in fibrotic remodeling (Wynn and Vannella, 2016).

CCL2 and CCR2 have a critical role in mediating the trafficking of monocytes, macrophages or bone marrow-derived fibroblasts to the site of injury. In the EAO model,

an increase of CCL2 is observed not only in the testicular tissue but also in testicular interstitial fluid and conditioned medium from cultured TMs (Guazzone et al., 2003). Furthermore, activin A, a member of the TGF-β superfamily of cytokines, released mainly by SCs is increased in EAO testis and levels correlate with the severity of disease (Nicolas et al., 2017b). Activin A stimulates resting macrophages to produce inflammatory mediators and promotes the expression of fibrosis specific genes in PTCs and NIH 3T3 fibroblasts *in vitro* (Kauerhof et al., 2019; Morianos et al., 2019).

Based on these findings, we hypothesize that activin A in concert with CCR2 influences the development of testicular fibrosis by regulating the properties of macrophages, which in turn are an important source of pro-fibrotic factors in EAO.

Therefore, the aims of this study are (1) to investigate the effect of CCR2 on the development of fibrosis during testicular inflammation, and (2) to analyze the influence of activin A on the fibrotic response in macrophages.

2. MATERIALS and METHODS

2.1. Materials

Table 1. Chemicals

2-Propanol	Sigma-Aldrich, Steinheim, Germany
β-mercaptoethanol	Sigma-Aldrich, Steinheim, Germany
Acetic acid	Merck, Darmstadt, Germany
Acrylamide 30% (w/v)	Carl Roth, Karlsruhe, Germany
Agarose	Invitrogen, Carlsbad, USA
Ammonium persulfate	Carl Roth, Karlsruhe, Germany
BlueEasy prestained protein marker	Nippon Genetics Europe, Dueren, Germany
Bordetella pertussis toxin	Calbiochem, Darmstadt, Germany
Bovine serum albumin (BSA)	Sigma-Aldrich, Steinheim, Germany
Bromophenol blue sodium salt	Sigma-Aldrich, Steinheim, Germany
Calcium chloride ($CaCl_2$)	Carl Roth, Karlsruhe, Germany
Complete Freund's adjuvant	Sigma-Aldrich, Saint Louis, USA
Coomassie Brilliant Blue R-250	Bio-Rad Laboratories, Munich, Germany
Ethanol	Sigma-Aldrich, Steinheim, Germany
Ethidium bromide	Carl Roth, Karlsruhe, Germany
Ethylene diamine tetra-acetic acid disodium salt (EDTA)	Merck, Darmstadt, Germany
Gelatin solution	Sigma-Aldrich, Steinheim, Germany
Glycerol	Carl Roth, Karlsruhe, Germany
Glycine	Carl Roth, Karlsruhe, Germany
Goat serum	BioLegend, San Diego, CA, USA
Hydrochloric acid, concentrated	Merck, Munich, Germany
Hydrochloric acid 37%	Carl Roth, Karlsruhe, Germany
MACS BSA stock solution	Miltenyi Biotec, Bergisch Gladbach, Germany

Methanol	Sigma-Aldrich, Steinheim, Germany
Isoflurane	Baxter, Unterschleißheim, Germany
Paraformaldehyde	Merck, Darmstadt, Germany
Picric acid solution, 1.3% in H_2O (saturated)	Sigma-Aldrich, Steinheim, Germany
ProLong Gold Antifade Mountant with DAPI	Life Technologies, Carlsbad, CA, USA
Proteinase K (30 units/mg)	Sigma-Aldrich, Steinheim, Germany
Tetramethylethylenediamine (TEMED)	Roth, Karlsruhe, Germany
Sirius red F3B (C.I. 35782)	Sigma-Aldrich, Steinheim, Germany
Sodium azide (NaN_3)	Merck, Darmstadt, Germany
Sodium Dodecylsulfate (SDS pellets)	Roth, Karlsruhe, Germany
Sodium chloride (NaCl)	Roth, Karlsruhe, Germany
Sudan Black B	Sigma-Aldrich, Steinheim, Germany
Tris	Carl Roth, Karlsruhe, Germany
Tris-hydrochloride	Carl Roth, Karlsruhe, Germany
Triton X-100	Sigma-Aldrich, Steinheim, Germany
Tween 20	Sigma-Aldrich, Steinheim, Germany
Xylene	Carl Roth, Karlsruhe, Germany
Zinc chloride ($ZnCl_2$)	Sigma-Aldrich, Steinheim, Germany

Table 2. PCR reagents

6 x Blue/orange DNA loading dye	Promega, Mannheim, Germany
Desoxyribonukleosidtriphosphate (dNTP) 10mM	Promega, Mannheim, Germany
DNA ladder	Promega, Mannheim, Germany
Go Taq G2 Flexi DNA polymerase	Promega, Mannheim, Germany
iTaq Universal SYBR Green Supermix	Bio-Rad Laboratories, Munich, Germany

Moloney Murine Leukemia Virus Reverse Transcriptase (M-MLV RT)	Promega, Mannheim, Germany
Oligo-dT15 primer	Promega, Mannheim, Germany
Recombinant RNasine Ribonuclease Inhibitor	Promega, Mannheim, Germany

Table 3. Cell culture reagents

4-(2-hydroxyethyl)-1-piperazineethanesulfonic acid (HEPES)	Gibco, Grand Island, NY, USA
β-mercaptoethanol	Gibco, Grand Island, NY, USA
Aqua	Fresenius Kabi, Bad Homburg, Germany
Arg-Gly-Asp-Ser (RGDS) tetrapeptide	Abcam, Cambridge, UK
Bovine serum albumin (BSA)	Sigma-Aldrich, Steinheim, Germany
Collagenase A	Roche Diagnostic, Mannheim, Germany
Dimethyl sulfoxide (DMSO)	Merck, Darmstadt, Germany
DMEM+GlutaMAX medium	Gibco, Grand Island, NY, USA
DMEM/F12+GlutaMAX medium	Gibco, Grand Island, NY, USA
DNase I	Roche Diagnostic, Mannheim, Germany
Dulbecco´s PBS	Gibco, Grand Island, NY, USA
Fetal Bovine Serum (FBS)	Gibco, Grand Island, NY, USA
Follistatin 288 (FST288)	Purified from HEK-293 cells transfected with human follistatin 288; Monash University, Melbourne, Australia
Hyaluronidase, from bovine testes	Sigma-Aldrich, Steinheim, Germany
Macrophage colony-stimulating factor (M-CSF)	Miltenyi Biotec, Bergisch Gladbach, Germany
MEM non-essential amino acids	Sigma-Aldrich, Steinheim, Germany
Penicillin/Streptomycin	Gibco, Grand Island, NY, USA
RBC lysis buffer	Qiagen, Hilden, Germany

Recombinant human activin A	Miltenyi Biotec, Bergisch Gladbach, Germany
Recombinant mouse TNF	PromoCell, Heidelberg, Germany
RPMI-1640 medium	Gibco, Grand Island, NY, USA
Sodium pyruvate	Gibco, Grand Island, NY, USA
Trypan blue solution 0.4%	Gibco, Grand Island, NY, USA
Trizma hydrochloride solution, pH7.5, 1 M	Sigma-Aldrich, Steinheim, Germany
Trypsin/EDTA solution, 0.25%	Gibco, Grand Island, NY, USA
Trypsin, from porcine pancreas	Sigma-Aldrich, Steinheim, Germany

Table 4. Kits

CFSE Cell Division Tracker Kit	Biolegend, San Diego, CA, USA
FoxP3 Staining Buffer Set	Miltenyi Biotec, Bergisch Gladbach, Germany
MACS Comp Bead Kit, anti-REA	Miltenyi Biotec, Bergisch Gladbach, Germany
QIAshredder Kit	Qiagen, Hilden, Germany
RNeasy Fibrous Tissue Mini Kit	Qiagen, Hilden, Germany
RNase-Free DNase Set	Qiagen, Hilden, Germany
RNeasy Mini Kit	Qiagen, Hilden, Germany
SuperScript III Reverse Transcriptase Kit	Life Technologies, Carlsbad, CA, USA
Total collagen assay Kit	QuickZyme Biosciences, Leiden, Netherlands
Total protein assay Kit	QuickZyme Biosciences, Leiden, Netherlands
VAHTS Stranded mRNA-seq Library Prep Kit	Vazyme, Nanjing, China

Table 5. Consumables

8 chamber polystyrene culture slides	Falcon, Corning Inc., Corning, NY, USA
Cell culture flask	Sarstedt, Nümbrecht, Germany
Cell culture plate, 6/ 12/ 24 well	Sarstedt, Nümbrecht, Germany
Cell strainer, 70 µm/ 100 µm	Greiner Bio-One, Frickenhausen, Germany
Cell scraper	Sarstedt, Nümbrecht, Germany
Cell strainer, 0.20 µm	BD Bioscience, Heidelberg, Germany
Culture-Insert 2 Well in µ-Dish 35 mm	ibidi, Martinsried, Germany
Cuvettes	Sarstedt, Nümbrecht, Germany
Falcon tube, 15/ 50 ml	Greiner Bio-One, Frickenhausen, Germany
Filter tips	Nerbe plus, Winsen/Luhe, Germany
Flow cytometry tubes	Sarstedt, Nümbrecht, Germany
Hard-shell 96-well PCR plates	Bio-Rad Laboratories, Munich, Germany
Microseal B adhesive seals (PCR plates)	Bio-Rad Laboratories, Munich, Germany
Needles, 24 G/ 30 G	BD, Franklin Lakes, NJ, USA
Nunc UpCell 6 Multidish	ThermoFisher Scientific, Waltham, MA, USA
Screw cap tubes, graduated and sterile	Greiner Bio-One, Frickenhausen, Germany
Stainless steel beads, 5 mm	Qiagen, Hilden, Germany
SuperFrost Plus microscope slides	R.Langenbrinck, Emmendingen, Germany
Syringes	BD Bioscience, Heidelberg, Germany
Tips and tubes	Sarstedt, Nümbrecht, Germany

Table 6. Software

Bio-Rad CFX Manager 3.1	Bio-Rad Laboratories, Munich, Germany
CorelDraw 2020	Corel Corporation, Ottawa, Ontario, Canada
FlowJo V10	FlowJo LLC, Oregon, USA
GraphPad Prism 7	GraphPad Software, San Diego, CA, USA
ImageJ	National Institutes of Health, Bethesda, Maryland, USA
Zeiss ZEN lite 3.3	Carl Zeiss, Göttingen, Germany

Table 7. Equipment

Cell culture CO_2 incubator	Binder, Tuttlingen, Germany
Centrifuge Labofuge 400R	Heraeus, Hanau, Germany
CFX96 touch thermal cycler	Bio-Rad Laboratories, Munich, Germany
Clean bench	BDK, Sonnenbühl-Genkingen, Germany
Confocal laser scanning microscope 710	Carl Zeiss, Göttingen, Germany
Cryostat CM30509	Leica, Wetzlar, Germany
Electronic balance SPB50	Ohaus, Giessen, Germany
Gel Jet Imager 2000 documentation system	Intas, Göttingen, Germany
Heat block DB-2A	Techne Inc., Cambridge, UK
Horizontal mini electrophoresis system	PEQLAB, Erlangen, Germany
Inverted microscope CKX41	Olympus, Hamburg, Germany
LabChip Gx Touch 24	Perkin Elmer, Waltham, USA
MACSQuant Analyzer 10	Miltenyi Biotec, Bergisch Gladbach, Germany
Microplate ELISA reader	Labsystems, Vantaa, Finland
Microtome RM2255	Leica, Wetzlar, Germany
Microwave oven	Samsung, Schwalbach, Germany

Mixer Mill MM 400	Retsch, Haan, Germany
NanoDrop ND 2000	Thermo Fisher Scientific, Waltham, USA
Neubauer Counting Chamber	Boeco, Hamburg, Germany
NextSeq500 instrument	Illumina, San Diego, USA
PCR thermocycler	Biozyme Scientific, Hessisch Oldendor, Germany
pH-meter 766	Knick, Berlin, Germany
Power supply units	PEQLAB, Erlangen, Germany
Precellys Evolution homogenizer	Bertin Technologies, Montigny-le-Bretonneux, France
SDS gel electrophoresis chambers	Consurs, Reiskirchen, Germany
Shaker 3005 orbital	GFL, Burgwedel, Germany
Vertical electrophoresis system	PEQLAB, Erlangen, Germany
Vertical microscope Leica DM750	Leica, Wetzlar, Germany

Table 8. Antibodies and isotype control antibodies used for flow cytometric analysis

Antibody	Company	Catalog No.	Clone	Dilution
Recombinant monoclonal anti-CD45 VioGreen REAfinity™	Miltenyi Biotec, Bergisch-Gladbach, Germany	130-110-803	REA737	1:50
Rabbit polyclonal anti-fibronectin	Abcam, Cambridge, UK	ab2413	-	1:100
Rabbit polyclonal anti-collagen I, biotin	Rockland, Limerick, USA	600-406-103	-	1:200
Recombinant monoclonal anti-CXCR4 PE REAfinity™	Miltenyi Biotec	130-118-682	REA107	1:50
Rat monoclonal anti-Ly6C PerCP	BioLegend	128027	HK1.4	1:80

Recombinant monoclonal anti-CD11c PE-Vio770 REAfinity™	Miltenyi Biotec	130-110-840	REA754	1:50
Recombinant monoclonal anti-F4/80 APC REAfinity™	Miltenyi Biotec	130-116-547	REA126	1:50
Recombinant monoclonal anti-CD11b APC-Vio770 REAfinity™	Miltenyi Biotec	130-113-803	REA592	1:50
Goat anti-rabbit Alexa Fluor 488	Invitrogen, Oregon, USA	A-11034	-	1:500
Streptavidin Alexa Fluor 488	BioLegend	405235	-	1:1000
Recombinant monoclonal REA control VioGreen	Miltenyi Biotec	130-104-624	REA293	1:50
Recombinant monoclonal REA control PE	Miltenyi Biotec	130-104-628	REA293	1:50
Recombinant monoclonal REA control PE-Vio770	Miltenyi Biotec	130-104-632	REA293	1:50
Recombinant monoclonal REA control APC	Miltenyi Biotec	130-104-630	REA293	1:50
Recombinant monoclonal REA control APC-Vio770	Miltenyi Biotec	130-104-634	REA293	1:50

Table 9. Primary and secondary antibodies used in immunofluorescence staining (IF)

Antibody	Company	Catalog No.	Dilution
Primary antibodies			
Rabbit polyclonal anti-fibronectin	Abcam	ab2413	1:300
Rabbit monoclonal anti-collagen I	Abcam	ab21286	1:300 (Frozen) 1:100 (Paraffin)

Rat monoclonal anti-CXCR4 Alexa Fluor 647	BioLegend	146503	1:100
Rat monoclonal anti-F4/80	Bio-Rad, Munich, Germany	MCA497G	1:200
Rat monoclonal anti-F4/80	BioLegend	123101	1:50
Rabbit monoclonal anti-SOX9	Abcam	Ab185230	1:200
Mouse monoclonal anti-aSMA FITC	Sigma-Aldrich, Saint Louis, USA	F3777	1:500
Secondary Antibodies			
Goat anti-rat IgG (H+L) Alexa Fluor 546	Invitrogen	A-11081	1:1500
Goat anti-rabbit IgG (H+L) Alexa Fluor 488	Invitrogen	A-11034	1:1500
Goat anti-rabbit IgG (H+L) Alexa Fluor 546	Invitrogen	A-11010	1:1500

Table 10. Primers used in qRT-PCR (F: forward primer, R: reverse primer)

Gene	Sequence (5'-3')	Amplicon size (bp)	Annealing temperature (°C)
18S rRNA	F: TACCACATCCAAGGAAGGCAGCA	180	55
	R: TGGAATTACCGCGGCTGCTGGCA		
Actb **(β-actin)**	F: TGACAGGATGCAGAAGGAGAT	156	55
	R: TACTCCTGCTTGCTGATCCAC		
Adgre1 **(F4/80)**	F: TCTGCAGTGTCAGCTCAGAA	277	60
	R: GAAGTCTGGGAATGGGAGCT		
Cxcl12	F: CAGTGACGGTAAACCAGTCAGC	68	64
	R: TGGCGATGTGGCTCTCG		
Cxcr4	F: GACTGGCATAGTCGGCAATG	131	60
	R: AGAAGGGGAGTGTGATGACAAA		

***Fn1* (fibronectin)**	F: AGAAGGCAGTAGCACAGA	110	55
	R: TCTCCTCCACAGCATAGATAG		
Hprt	F: CTGGTAAAAGGACCTC	110	55
	R: CTGAAGTACTCATTATAGTCAAG		
Itgav	F: AAGGCGCAGAATCAAGGGGA	182	60
	R: CCAGCCTTCATCGGGTTTCC		
Itgb3	F: TGGTGCTCAGATGAGACTTTGTC	86	60
	R: GACTCTGGAGCACAATTGTCCTT		
Itgb5	F: TGTTCAGCTACACAGAACTGCCCA	198	55
	R: TTTGGAACTTGGCAAACTCTCGGC		
Mmp2	F: CAGGGAATGAGTACTGGGTCTATT	119	60
	R: ACTCCAGTTAAAGGCAGCATCTAC		
Mmp9	F: AAGGACGGCCTTCTGGCACACGCCTTT	874	60
	R: GTGGTATAGTGGGACACATAGTGG		
Mmp14	F: TTACAAGTGACAGGCAAGG	112	60
	R: GCTTCCTCCGAACATTGG		
Pdgfa	F: CAAGACCAGGACGGTCATTT	223	55
	R: CCTCACCTGGACCTCTTTCA		
Pdgfb	F: CCCACAGTGGCTTTTCATTT	137	55
	R: GTGAACGTAGGGGAAGTGGA		
Pdgfrb	F: GAACGACCATGGCGATGAGA	146	60
	R: GCATCGGATAAGCCTCGAACA		
Timp1	F: CCCCAGAAATCAACGAGAC	156	55
	R: CTGGGACTTGTGGGCATATC		

2.2. Methods

2.2.1. Animals

Adult 10-12 weeks old *C57BL/6J* (*WT*; Charles River Laboratories, Sulzfeld, Germany) and *B6.129P2-Ccr2*$^{tm1Mae/tm1Mae}$ (*Ccr2*$^{-/-}$) mice were housed in specific pathogen free conditions (12 hours light/ dark cycle, 20-22°C), with access to water and food ad libitum at the animal facility of Justus Liebig University, Giessen, Germany (Boring et al., 1997). Animal experiments were approved by the responsible local committee on animal care (Regierungspraesidium Giessen GI 58/2014 — Nr. 735-GP). All experiments involving animals were carried out in strict accordance with the recommendations in the guide for the Care and Use of Laboratory Animals of the German law of animal welfare.

Femurs and tibias (isolation of bone marrow progenitor cells) as well as testes (isolation of SCs) were collected from adult or 21-day old male *C57BL/6J* mice, respectively. The local animal ethics authorities approved the collection of organs (684 M).

2.2.2. Induction of EAO in *WT* and *Ccr2*$^{-/-}$ mice

Periprocedural analgesia in mice was performed in a form of tramadol (STADApharm GmbH, Bad Vilbel, Germany) in drinking water (2.5 mg/ml) starting 24 hours before each immunization and kept for the following 3 days. During immunization, animals were anaesthetized by inhalation of 3-5% isoflurane.

To induce EAO, adult male *C57BL/6J* and *Ccr2*$^{-/-}$ mice were actively immunized with testicular homogenate (TH) in complete Freund's adjuvant (CFA) as previously described (n = 29) (Nicolas et al., 2017a). TH was prepared from decapsulated testes collected from adult *C57BL/6J* mice and homogenized in sterile 0.9% NaCl at a ratio of 1:1. Animals were immunized 3 times every 14 days with a mixture of TH in CFA, followed by *i.p.* injection of 100 ng *Bordetella pertussis* toxin in 100 µl Munõz Buffer (25 mM Tris, 0.5 M NaCl, 0.017% Triton X-100, pH 7.6) (Kohno et al., 1983). Each animal was immunized dorsally by four *s.c.* injections with a total volume of 200 µl (50 µl per injection site). Adjuvant control animals received CFA mixed with 0.9% NaCl instead of TH according to the same scheme

(n = 22). Age-matched untreated mice were also included (n = 21). The number of mice used for *in vivo* experiments is shown in Table 11.

Table 11. Summary of groups and number of animals used for EAO induction in the presented study

Mouse strain	Treatment group	Number of animals
WT	Untreated	10
	Adjuvant	11
	EAO	14
Ccr2$^{-/-}$	Untreated	11
	Adjuvant	11
	EAO	15

For euthanasia, animals were deeply anaesthetized by inhalation of 5% isoflurane and sacrificed by cervical dislocation 50 days after first immunization. A schematic diagram illustrating the time course of immunizations and time points for organ collection in the *in vivo* experiments is shown in **Fig. 5**. Both testes were removed, weighed, and either snap frozen in liquid nitrogen or fixed in Bouin's solution for embedding in paraffin. For flow cytometric analysis, fresh testes were used.

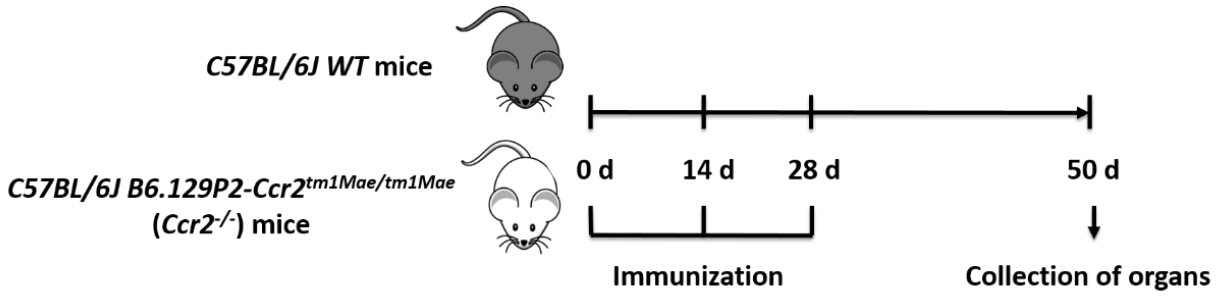

Figure 5. Schematic diagram representing the time points for EAO induction and organ collection in *C57BL/6J* (*WT*) and *B6.129P2-Ccr2*$^{tm1Mae/tm1Mae}$ (*Ccr2*$^{-/-}$) mice. Mice were immunized with TH in CFA three times every other week starting at day 0 and testes were collected at day 50. Adjuvant control mice received NaCl instead of TH. Untreated age-matched control mice were also included.

2.2.3. Induction of EAO in mice with elevated follistatin levels

30 days prior to the first immunization, *C57BL/6J* mice were injected *i.m.* with a non-replicative recombinant adeno-associated viral (rAAV) vector serotype 6 carrying a gene cassette of the circulating form of follistatin (FST315) or a vector with an empty gene cassette (empty vector [EV]). Adjuvant-only and untreated controls were included (Nicolas et al., 2017b). The number of mice used for *in vivo* experiments is shown in Table 12.

Table 12. Summary of groups and number of animals used for EAO induction after treatment with *rAAV-EV* and *rAAV-FST315*

Mouse strain	Treatment group	Number of animals
rAAV-EV	Untreated	4
	Adjuvant	4
	EAO	4
rAAV-FST315	Untreated	4
	Adjuvant	4
	EAO	5

The immunization protocol was modified according to the Monash University Animal Ethics committee requirements regarding the use of adjuvants: mice were immunized once with TH in CFA, prior to two further immunizations with TH in incomplete Freund's adjuvant followed by *B. pertussis* toxin injection. The animal experiments were approved by the Monash Medical Centre Animal Experimentation Committee. Approximately 75% of mice immunized by this protocol developed mild to severe EAO 50 days after first immunization. The application of *rAAV-FST315* increased serum follistatin levels 5 - fold at the time of first immunization (Nicolas et al., 2017b). Testes were either snap frozen in liquid nitrogen for immunofluorescence and RNA isolation or Bouin's fixed for paraffin embedding (Nicolas et al., 2017b). The samples were kindly provided by Prof. Mark P. Hedger from Monash University, Australia. Schematic diagram illustrating the time course of vector injection, immunizations and organ collection for the *in vivo* experiments is shown in **Fig. 6**.

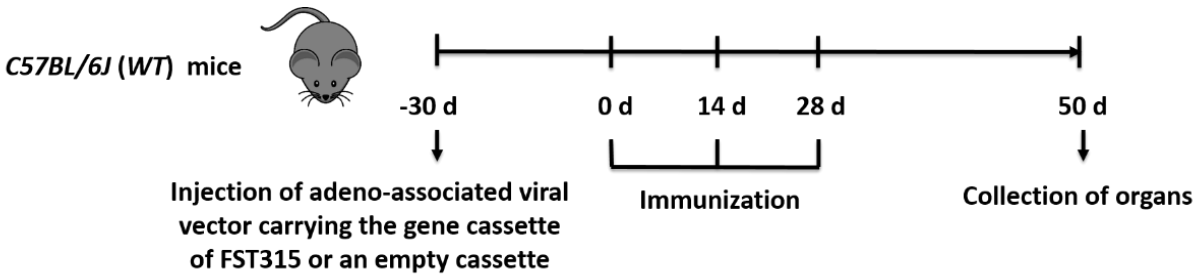

Figure 6. Schematic diagram representing the time points for vector administration, EAO induction and organ collection in *C57BL/6J* (*WT*). Mice were injected with rAAV carrying the gene cassette of FST315 (rAAV-FST315) or an empty vector (rAAV-EV) 30 days prior to first immunization, then immunized three times every other week starting at day 0 and testes were collected at day 50.

2.2.4. Picro-sirius red staining

Testicular histology and presence of collagen were assessed in untreated, adjuvant and EAO paraffin-embedded sections from *WT* and *Ccr2*$^{-/-}$ mice by picro-sirius red staining (Kiernan, 2008). Testicular sections were deparaffinized twice in xylene for 10 min and rehydrated in a series of gradually diluted ethanol (100%, 90%, 80%, 70% and 50%) for 5 min. Afterwards, the slides were stained in picro-sirius red solution for 1 h and rinsed twice with 0.5% acetic acid solution. Then, the sections were dehydrated in three changes of 100% ethanol, cleared in xylene and mounted in a resinous medium. Collagen fibers were stained in red.

Picro-sirius red solution
0.1% Sirius red F3B (C.I. 35782)
1.3% Picric acid solution, in H_2O (saturated)

2.2.5. Hydroxyproline assay

Total testicular collagen content was determined in untreated, adjuvant and EAO paraffin-embedded sections from *WT* and *Ccr2*$^{-/-}$ mice by chromogenic determination of hydroxyproline concentration using QuickZyme Total Collagen Assay Kit. Twelve testicular sections (10 µm) per group were hydrolyzed in 150 µl of 6 M HCl and incubated for 20 h at 95°C. After cooling to room temperature (RT), samples were centrifuged for

10 min at 13000 g. Then, supernatants (100 µl) were diluted with 50 µl ddH_2O. The collagen standard curve was prepared according to the manufacturer's instruction. All samples and standards diluted in the assay buffer were performed as duplicates and incubated for 20 min at RT with shaking. Afterwards, detection reagent (75 µl) was added and the plate was incubated for 60 min at 60°C. Finally, the samples were measured at 570 nm by spectrophotometer.

Total testicular collagen content was normalized to total testicular protein with QuickZyme Total Protein Assay Kit. Similar like for the measurement of total collagen, hydrolysis was performed in paraffin-embedded testicular sections. All samples and standards diluted in the assay buffer were prepared as duplicates. Subsequently, detection reagent (15 µl) was added and the plate was incubated for 60 min at 85°C. The samples were measured at 570 nm by spectrophotometer.

2.2.6. Flow cytometry

In *in vivo* experiments, testes were decapsulated and digested in phosphate buffered saline (PBS) containing 1.2 mg/ml collagenase A and 15 U/ml DNAse I in 34°C water bath for 15 min with agitation. After sedimentation of seminiferous tubules, supernatants containing interstitial cells were collected. In *in vitro* experiments, cells were seeded in the Nunc UpCell 6 Multidish plate and detached at RT for 30 min.

A total of 1×10^6 cells diluted in 100 µl PBS were stained with 1 µl Viobility 405/452 dye at RT for 15 min in the dark. For cell surface staining, after centrifugation cells were blocked with mouse FcR blocking reagent for 10 min at 4°C, followed by the incubation with appropriate antibodies (see Table 8 and 13 for antibody details) for 15 min at 4°C. Afterwards, for intracellular staining cells were permeabilized using Fix/ Permeabilization Staining Buffer Set for 30 min at 4°C according to the manufacturer's instructions and blocked again. Subsequently, cells were incubated with anti-fibronectin or anti-collagen I antibody for 45 min at 4°C and respective secondary antibody conjugated to Alexa Fluor 488 for 30 min at 4°C. Data were collected with the MACSQuant Analyzer 10 and analyzed

by the FlowJo V10 software. After gating out cell debris, doublets and nonviable cells, cell population of interest was selected according to the isotype control or negative control.

Table 13. Antibody panel for flow cytometry

Laser	Filter	Channel	Antibody or Dye
Violet 405 nm	450/50 nm	V1	Viobility 405/452
	525/50 nm	V2	CD45 VioGreen
Blue 488 nm	525/50 nm	B1	Fibronectin or Collagen I Alexa Fluor 488
	585/40 nm	B2	CXCR4 PE
	655-730 nm	B3	Ly6c PerCP
	750 nm LP	B4	CD11c PE-Vio770
Red 638 nm	655-730 nm	R1	F4/80 APC
	750 nm LP	R2	CD11b APC-Vio770

2.2.7. Immunofluorescence (IF) staining

2.2.7.1. IF on frozen testicular sections

Frozen testicular sections (10 µm) were fixed with ice-cold methanol for 10 min, and washed with Tris buffered saline containing 0.1% Tween-20 (TBST) 3 times for 5 min. Subsequently, slides were blocked with 5% bovine serum albumin (BSA) and 10% goat serum in TBST at RT for 1.5 h. Afterwards, slides were incubated with appropriate primary antibodies overnight (see Table 9 for antibody details). Next day, sections were washed with TBST and incubated with corresponding secondary antibodies at RT for 1 h. Finally, slides were mounted with ProLong Gold Antifade Mountant containing DAPI. Fluorescence images were taken with confocal laser scanning microscope (CLSM).

TBST (pH = 7.6)
15 mM Tris-HCl
137 mM NaCl
0.1 % Tween-20
ddH_2O

2.2.7.2. IF on paraffin-embedded testicular sections

Paraffin-embedded testicular sections (8 µm) were deparaffinized in xylene twice for 10 min and rehydrated in a series of gradually diluted ethanol (100%, 90%, 80%, 70% and 50%). After rinsing with distilled water, slides were incubated with pre-warmed proteinase K working solution (20 µg/ml proteinase K and 2.5% glycerol diluted in Tris-EDTA buffer) for 3 min at RT. Slides were then blocked with 5% BSA and 10% goat serum in TBS at RT for 1.5 h, and incubated with primary antibodies in blocking solution at RT for 4 h. After that, sections were washed with TBS and incubated with corresponding secondary antibodies at RT for 1 h, followed by the incubation with 0.3% Sudan Black B in 70% ethanol for 5 min to reduce autofluorescence. Finally, after several washes with TBS, sections were mounted with ProLong Gold Antifade Mountant containing DAPI, and photographed by using CLSM.

Tris-EDTA buffer (pH = 8)
50 mM Tris Base
1 mM EDTA
0.5% Triton X-100
ddH_2O

2.2.8. *In vitro* culture of primary SCs and PTCs

2.2.8.1. Isolation of primary SCs and PTCs

For each cell preparation, eight 21-day old male *C57BL/6J* mice were sacrificed by using 5% isoflurane and cervical dislocation. After removal, testes were decapsulated and incubated with 5 ml collagenase A solution (1 mg/ml in complete DMEM/F12-GlutaMAX medium containing 6 µg/ml DNase I) in a shaking water bath at 34°C for 20 min to dissociate tubules **(Fig. 7A)**. Tubules were settled down three times for 5 min after addition of complete DMEM/F12-GlutaMAX medium to discard interstitial cells present in the supernatant. Remaining tubules were subsequently resuspended in 5 ml trypsin solution (5 mg/ml in complete DMEM/F12-GlutaMAX medium containing 20 µg/ml DNase I) and further dissociated for 20 min in a shaking water bath at 34°C **(Fig. 7B)**. After that, 30 ml complete 10% FBS DMEM-GlutaMAX medium was added to the tubules to inactivate

trypsin. Dissociated tubules were settled down for 5 min and supernatant was collected and centrifuged at 400 x g for 10 min (PTCs fraction). This step was repeated three times. Cell clumps were removed by using a 70 µm strainer. Later, PTCs were plated in a 75 cm^2 flask and incubated at 37°C under 5% CO_2 until 90% confluence. In the meantime, dissociated tubules after trypsin digestion were incubated with 5 ml hyaluronidase solution (1 mg/ml in complete DMEM/F12-GlutaMAX medium containing 6 µg/ml DNase I) at 34°C for 15 min with shaking **(Fig. 7C)**.

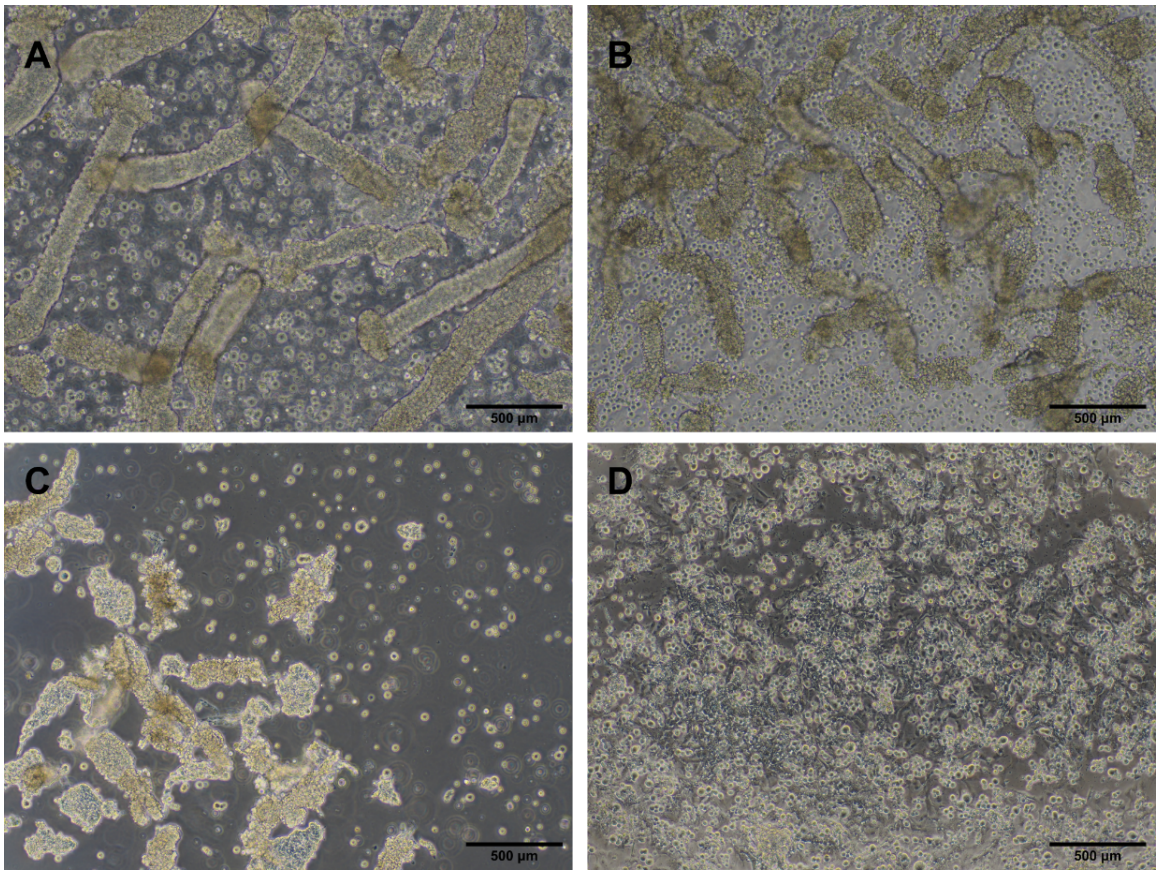

Figure 7. Isolation of SCs from immature mouse testes. After collagenase A digestion, seminiferous tubules and interstitial cells were dissociated **(A)**. PTCs were released from seminiferous tubules after trypsin digestion **(B)**. Further digestion of seminiferous tubules fragments by hyaluronidase led to formation of small tubule fragments and free SCs **(C)**. Contaminating germ cells were removed by hypotonic shock **(D)**.

Afterwards, cells were collected by centrifugation at 400 x g for 3 min, followed by the removal of clumps using a 100 µm strainer. Finally, SCs were resuspended to a

concentration of 1 × 10^6 cells/ml in 0.1% BSA DMEM-GlutaMAX medium in a 24-well cell culture plate, and were incubated at 32°C and under 5% CO_2. Two days after isolation, SCs were treated with cold hypotonic 20 mM Tris hydrochloride solution for 2 min to remove contaminating germ cells **(Fig. 7D)**.

Complete DMEM/F12-GlutaMAX medium
DMEM/F12-GlutaMAX medium
1% Penicillin/ Streptomycin
1% Non-essential amino acids

Complete DMEM-GlutaMAX medium (PTC cultivation)
DMEM-GlutaMAX medium
10% Fetal bovine serum (FBS)
1% Penicillin/ Streptomycin
1% Non-essential amino acids

0.1% BSA DMEM-GlutaMAX medium (SC cultivation)
DMEM-GlutaMAX medium
0.1% BSA
1% Penicillin/ Streptomycin
1% Non-essential amino acids

2.2.8.2. Purity evaluation of SCs and PTCs by IF staining

The purity of SCs (> 85%) was determined by triple fluorescence staining with SC marker SOX9, PTC marker αSMA and nuclear marker DAPI **(Fig. 8A - E)**. The staining of PTCs with αSMA and DAPI was used as a positive control **(Fig. 8F)**.

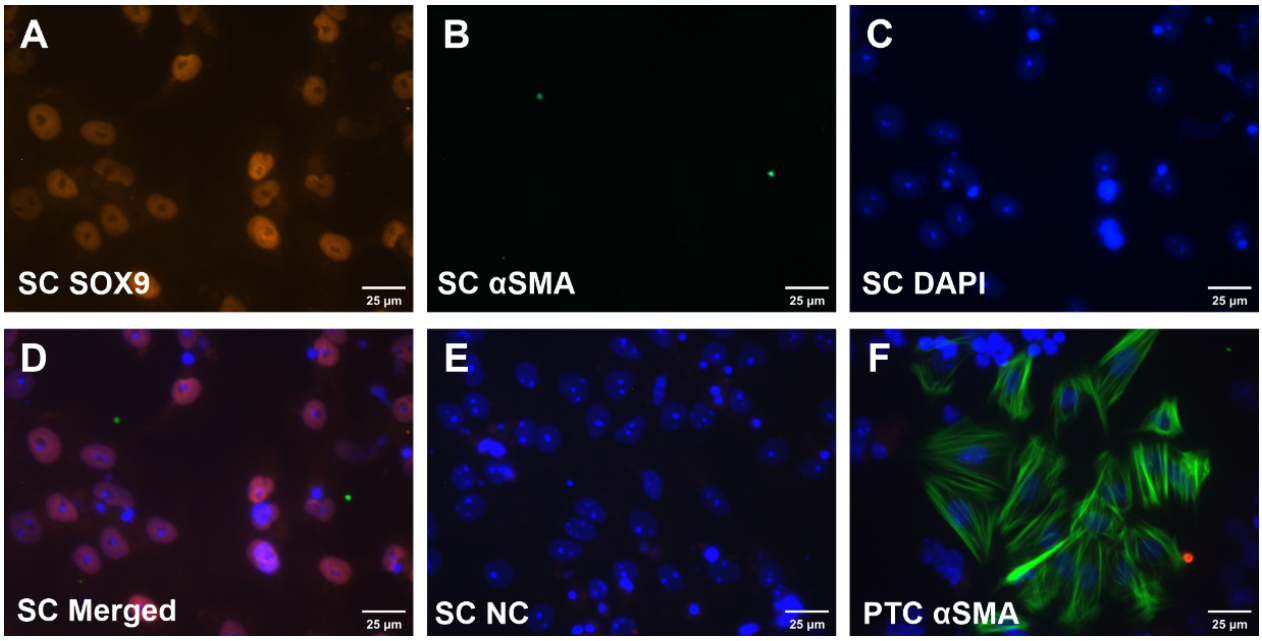

Figure 8. The purity of isolated SCs. Representative photomicrographs of SOX9 (orange), αSMA (green) and DAPI (blue) triple staining in isolated SCs. αSMA staining in PTCs was used as a positive control for αSMA. Immunofluorescence staining showed very high purity of SCs. NC: negative control.

Primary SCs or PTCs were fixed with cold 4% paraformaldehyde for 20 min and permeabilized with 0.5% Triton X for 20 min. After several washes with TBST, slides were blocked with 10% goat serum at RT for 1 h and incubated overnight with rabbit anti-SOX9 and mouse FITC-conjugated anti-αSMA antibodies. Afterwards, cells were washed with TBST and incubated with goat anti rabbit IgG-Alexa Fluor 546 at RT for 1 h. After several TBST washes, cells were mounted with ProLong Gold Antifade Mountant containing DAPI. The images were taken using CLSM.

2.2.8.3. Treatments of SCs

One day after hypotonic treatment, SCs were treated with 50 ng/ml recombinant mouse TNF, 250 ng/ml FST288 or a combination of both and SC conditioned medium (SCCM) was collected after 24 h.

2.2.9. Culture of bone marrow-derived macrophages (BMDMs)

2.2.9.1. Isolation of bone marrow progenitor cells

Bone marrow progenitor cells were isolated from adult male *C57BL/6J* mice according to the published protocol (Weischenfeldt and Porse, 2008). Mice were sacrificed, and intact femur as well as tibia were isolated. After several washing with PBS, both ends of femur and tibia were removed. After that, the syringe needle filled with PBS containing 50 µg/ml gentamycin was inserted into the bones. Bone marrow progenitor cells were flushed out and filtered with a 70 µm strainer. After centrifugation and red blood cells lysis, bone marrow progenitor cells were resuspended in complete RPMI-1640 medium containing 50 µM β-mercaptoethanol.

Complete RPMI-1640 medium
RPMI-1640 medium
10% FBS
1% Penicillin/ Streptomycin
1% Non-essential amino acids
1 mM Sodium pyruvate
10 mM HEPES buffer solution

2.2.9.2. Generation and treatments of BMDMs

On day 0, bone marrow progenitor cells were seeded in 6-well plates at a density of 3×10^6 cells/well for 3 days experiments or 1×10^6 cells/well for 6, 7 or 8 days experiments. BMDMs were generated by using 50 ng/ml mouse recombinant macrophage-colony stimulating factor (M-CSF) and stimulated with 25 or 50 ng/ml human recombinant activin A, 250 ng/ml human recombinant follistatin 288 (FST288) or a combination of both for 6 days. Cell culture medium was replaced on day 3. After 6 days, BMDMs were starved using serum-free RPMI-1640 medium and treated with 50 ng/ml M-CSF, 50 ng/ml activin A, 250 ng/ml FST288 or a combination of activin A and FST288. 1 day or 2 days later, BMDM conditioned medium (BMDM CM) was collected for gelatin-zymography, wound healing assay or proliferation assay.

For treatments with SCCM, BMDMs were generated by using 50 ng/ml M-CSF for 3 days and incubated subsequently with SCCM for additional 3 days.

2.2.10. Wound healing assay

NIH 3T3 cells were seeded on µ-Dish. Before treatments, cells were starved with 1% FBS DMEM-GlutaMAX medium for 24 h to keep cells under minimal maintenance conditions. NIH 3T3 fibroblasts were pretreated with 100 µg/ml fibronectin/ integrin binding inhibitor Arg-Gly-Asp-Ser (RGDS) tetrapeptide for 4 h, or directly treated with BMDM conditioned medium, 50 ng/ml activin A or 250 ng/ml FST288. The wound scratch area was photographed at 0 h and 24 h. The size of NIH 3T3 fibroblasts wound scratch area was analyzed by ImageJ software. The percentage of NIH 3T3 fibroblasts wound healing coverage area was calculated by using formula (1 - A1/A0) × 100%, where A0 represents the size of wound scratch area at 0 h and A1 represents the size of wound scratch area at 24 h.

2.2.11. Proliferation assay

Carboxyfluorescein succinimidyl ester (CFSE) is a dye that fluorescently labels living cells. CFSE easily penetrates cell membranes, binds to intracellular proteins and releases green fluorescence upon hydrolysis (Quah and Parish, 2010; Bocharov et al., 2013). The fluorescence intensity of CFSE gradually decreases as cells divide and proliferate, and the fluorescence can be equally distributed between the two daughter cells, where the subsequent fluorescence intensity is half that of the parental cells (Quah and Parish, 2010; Bocharov et al., 2013). Therefore, CFSE can be used for the analysis of cell division and proliferation. In this study, NIH 3T3 fibroblasts were starved with 1% FBS DMEM-GlutaMAX medium one day before labeling with 5 µM CFSE at 37°C for 20 min and treated with BMDM CM, 50 ng/ml activin A or 250 ng/ml FST288. The mean fluorescence intensity (MFI) of CFSE-labeled NIH 3T3 fibroblasts was measured after 48 h incubation by flow cytometry using the MACSQuant Analyzer 10.

2.2.12. Analysis of gene expression by quantitative reverse transcription polymerase chain reaction (qRT-PCR)

2.2.12.1. RNA isolation

Frozen testicular tissue (30 mg) or pelleted cells (cell number < 5×10^6) were collected and homogenized in 300 µl RLT lysis buffer containing 1% β-mercaptoethanol using stainless steel beads and Mixer Mill or in 350 µl RLT lysis buffer containing 1% β-mercaptoethanol using QIAshredder Kit, respectively. Afterwards, total RNA was isolated from frozen testes using RNeasy Fibrous Tissue Mini Kit and from cultured cells using RNeasy Mini Kit according to the manufacturer's instructions. During RNA purification, contaminating DNA was removed using RNase-Free DNase Set. The concentration and quality of RNA were measured by NanoDrop ND2000. An $A_{260/280}$ ratio of 1.8 to 2.0 as well as an $A_{260/230}$ ratio of 2.0 to 2.2 are indicators of good RNA quality. Lower ratios demonstrate the presence of protein, phenol or other contaminants in isolated RNA samples.

2.2.12.2. PCR analysis of genomic DNA contamination absence

After RNA isolation, the absence of genomic DNA contamination in RNA samples was checked by analyzing the amplification of β-actin transcript (156 bp) by PCR. The PCR reaction setup (Table 14) and PCR conditions (Table 15) are listed below.

Table 14. PCR reaction setup for amplification of β-actin

Component	Volume
RNA template	1 µl
5 X Green Go Taq Flexi Buffer	5 µl
25 mM $MgCl_2$	2 µl
10 mM dNTP	0.5 µl
5 units/µl Go Taq Polymerase Flexi	0.25 µl
10 pM β-actin forward primer	0.5 µl
10 pM β-actin reverse primer	0.5 µl
ddH_2O	15.25 µl

Total volume	25 µl

Table 15. PCR conditions

Number of cycles	Step	Temperature (°C)	Time
1	Denaturation	94	4 min
25	Denaturation	94	40 sec
	Annealing	55	40 sec
	Elongation	72	40 sec
1	Elongation	72	10 min

2.2.12.3. Agarose gel electrophoresis

After the completion of PCR amplification, 1.5% agarose gel was prepared by dissolving agarose in Tris-acetate-EDTA (TAE) buffer in the microwave. Before polymerization of agarose solution, ethidium bromide (250 µg/ml) was added. Afterwards, electrophoresis was performed at 150 V for 20 min.

TAE buffer
40 mM Tris Base
20 mM Acetic acid
1 mM EDTA

Finally, bands were visualized by ultraviolet - light and photographed using the Gel Jet Imager 2000 documentation system. The cDNA from splenocytes used as a positive control showed a transcript for β-actin with the expected transcript size of 156 bp, while RNA samples and negative control using RNase-free water demonstrated no presence of β-actin PCR product **(Fig. 9)**. This indicates the absence of genomic DNA contamination in isolated RNA samples.

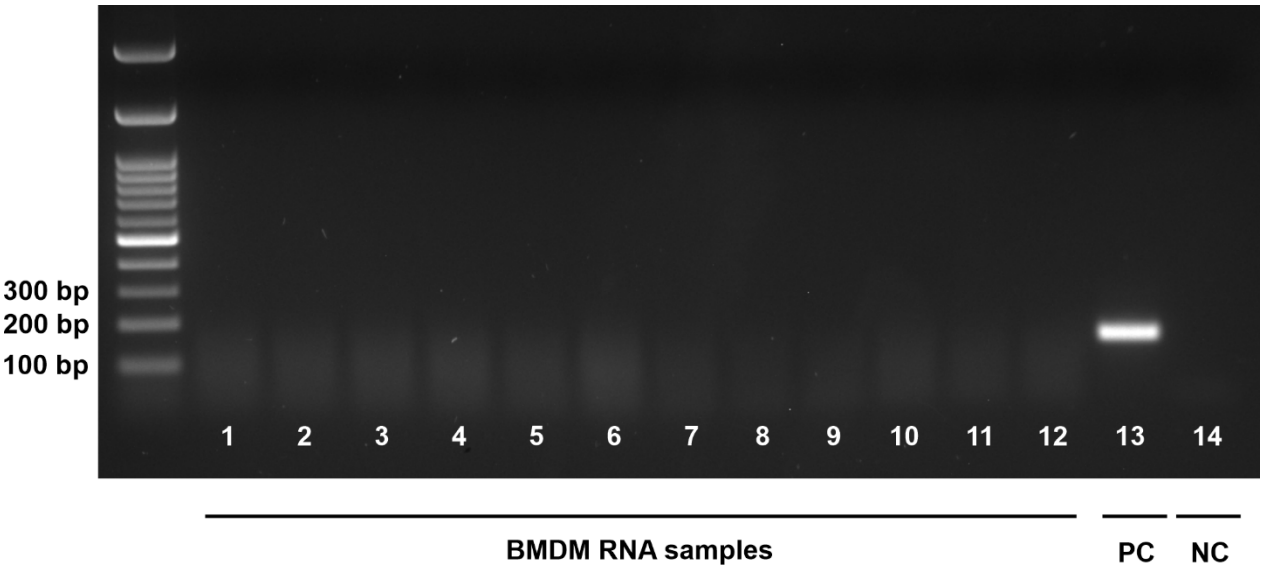

Figure 9. Verification of absence of genomic DNA contamination in total RNA samples from BMDMs. Total RNA was isolated from BMDMs 6 days after treatment with 25 or 50 ng/ml activin A, 250 ng/ml FST288 or a combination of both. The representative agarose gel of PCR amplicons for β-actin showed that no bands were detected in untreated (lane 1, 7), activin A-treated (lane 2, 3, 8, 9), activin A + FST288-treated (lane 4, 5, 10, 11) and FST288-treated (lane 6, 12) BMDM RNA samples (n = 12), which indicated that there was no genomic DNA contamination. The cDNA from splenocytes (lane 13) was used as a positive control and a negative control contained RNase-free water (lane 14) instead of RNA or cDNA template. The amplicon size of β-actin is 156 bp.

2.2.12.4. Reverse transcription

Total RNA was reversely transcribed using the established protocols in the lab (Nicolas et al., 2017b; Kauerhof et al., 2019). First of all, the PCR mix including 1 µg of total RNA, 2 µl of 10 pM oligo(dT)$_{20}$ and up to 22 µl RNase-free water was prepared and incubated at 70°C for 10 min. Afterwards, the master mix including 8 µl of M-MLV 5 X reverse transcription buffer, 2 µl of 10 mM dNTP, 1 µl of recombinant RNase inhibitor (40 units/ µl) and 7 µl of RNase-free water was mixed and pre-warmed for 2 min at 42°C. PCR mix, master mix and 1 µl of M-MLV reverse transcriptase (200 units/ µl) were added together and incubated for 75 min at 42°C. Subsequently, the reaction was inactivated by heating at 70°C for 15 min. The success of RNA reverse transcription was confirmed by amplification of β-actin product by PCR and agarose gel electrophoresis (see 2.2.12.2 and 2.2.12.3).

2.2.12.5. qRT-PCR analysis

qRT-PCR is an effective technique to monitor the entire PCR process in real time by adding fluorescent dyes such as SYBR Green to the PCR reaction system. During the exponential growth phase of the fluorescence signal, there is an inverse relationship between the value of the cycle threshold (Ct) and the amount of the starting template (Taylor et al., 2010). Therefore, the difference in the gene expression between different samples can be compared by this method. In this study, qRT-PCR was performed using iTaq Universal SYBR Green Supermix (Table 16) in a CFX96 Touch thermal cycler (Table 17).

Table 16. Reaction setup for qRT-PCR

Component	**Volume**
cDNA template	1 µl
10 pM forward primer	0.5 µl
10 pM reverse primer	0.5 µl
2 × iTaq™ Universal SYBR Green Supermix	10 µl
ddH_2O	8 µl
Total volume	20 µl

Table 17. qRT-PCR conditions

Number of cycles	**Step**	**Temperature (°C)**	**Time (sec)**
1	Denaturation	95	30
45	Denaturation	95	15
	Annealing	55 or 60 or 63	30
	Elongation	72	30
Melt curve	Dissociation	50-95	5

A single peak melting curve analysis allows the exclusion of the primer dimerisation and formation of non-specific PCR products. A representative melting curve is shown in

Fig. 10, which indicates a single specific peak for *Fn1* product during the amplification by qRT-PCR.

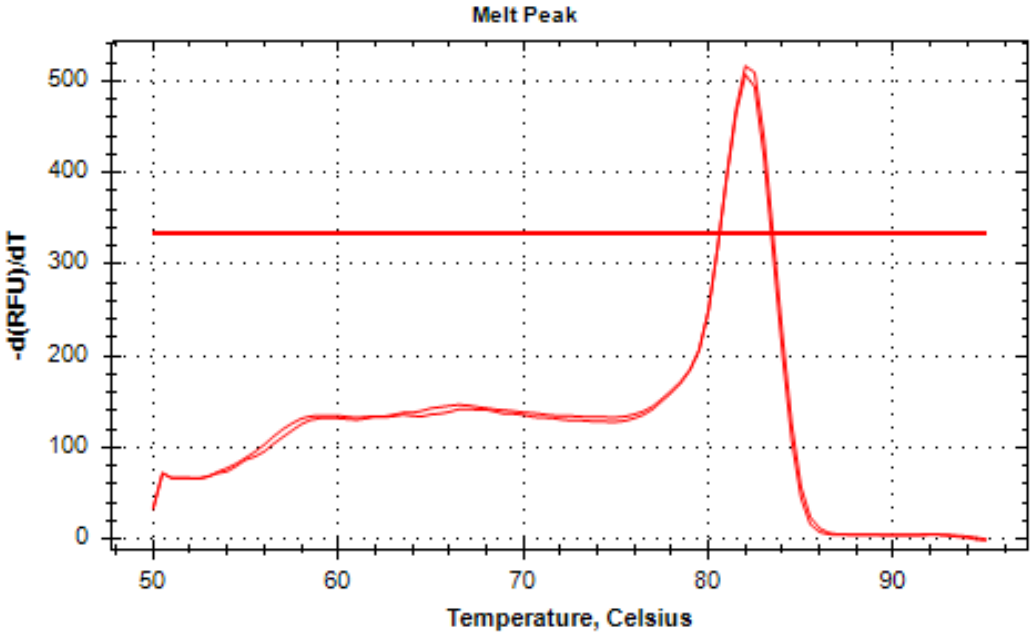

Figure 10. Representative melting curve for *Fn1* transcript by using cDNA template from NIH 3T3 fibroblasts. Single peak represents single amplicon from both *Fn1* duplicates at 82°C following melt curve analysis.

Primer efficiency was validated by setting a tenfold dilution series of cDNA samples. Afterwards, a linear standard curve was generated **(Fig. 11)**. Primer efficiency with 90% - 110% and R^2 value > 0.98 was used for the subsequent qRT-PCR analysis (Taylor et al., 2010).

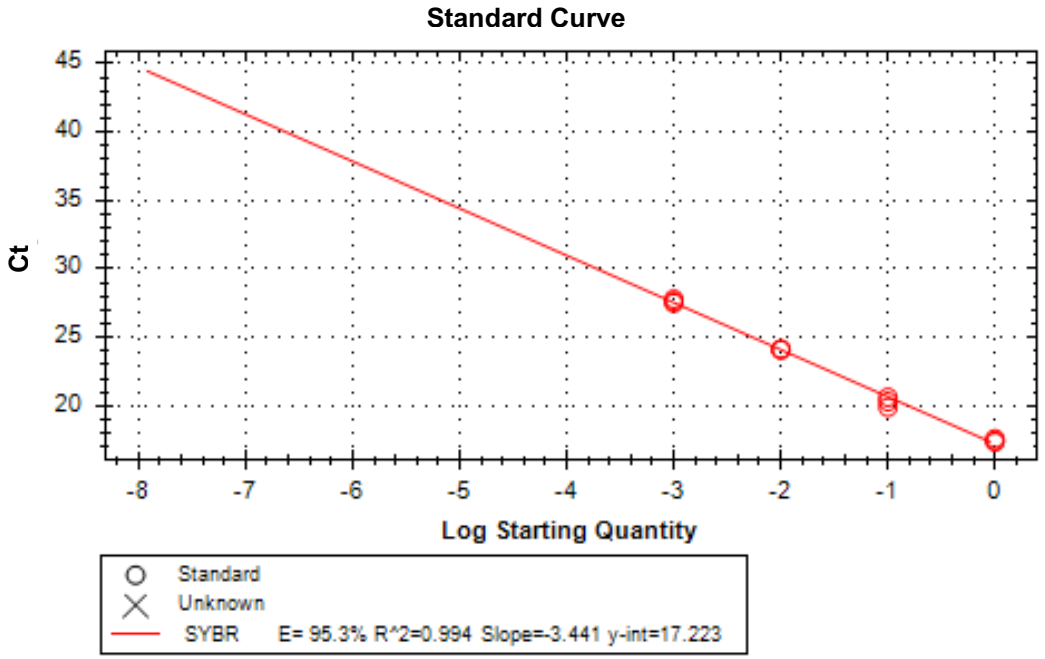

Figure 11. Representative qRT-PCR standard curve of *Fn1* primer by using cDNA template from NIH 3T3 fibroblasts. cDNA was diluted 10, 100 and 1000 times. Diluted (10, 100 and 1000 times) as well as undiluted cDNA were used as templates for *Fn1* qRT-PCR reaction. Ct values against the log of dilution series are plotted. Primer efficiency with 95.3% and R^2 value of 0.994 indicate the optimal qRT-PCR conditions.

The sequences of the primers and the annealing temperatures are listed in Table 10. *Hypoxanthin-guanin-phosphoribosyltransferase* (*Hprt*) and *18S rRNA* were selected as stable expressed housekeeping genes. All samples were performed as duplicates. The mRNA relative expression was calculated using the $2^{-\Delta\Delta Ct}$ method (Livak and Schmittgen, 2001). ΔCt = Ct (a target gene) – Ct (a housekeeping gene). ΔΔCt = ΔCt (a target sample) – ΔCt (a control sample). The relative gene expression is set to 1 for the control sample.

2.2.13. RNA sequencing

RNA sequencing was performed by Dr. Stefan Günther at ECCPS Bioinformatics and Deep Sequencing Platform in Max Planck Institute for Heart and Lung Research (Bad Nauheim, Germany). Total RNA was isolated according to the previous described methods. RNA and library preparation integrity were verified with LabChip Gx Touch 24

(Perkin Elmer, Waltham, USA). 4 µg of total RNA was used as input for VAHTS Stranded mRNA-seq Library preparation following manufacture's protocol (Vazyme, Nanjing, China). Sequencing was performed on NextSeq500 instrument (Illumina, San Diego, USA) using v2 chemistry with 1 x 75 bp single end setup. The resulting raw reads were assessed for quality, adapter content and duplication rates with FastQC (Andrews, 2010). Trimmomatic version 0.39 was employed to trim reads after a quality drop below a mean of Q20 in a window of 5 nucleotides (Bolger et al., 2014). Only reads between 30 and 150 nucleotides were cleared for further analyses. Trimmed and filtered reads were aligned versus the Ensembl mouse genome version mm10 (ensemble release 101) using STAR 2.7.9a with the parameter "--outFilterMismatchNoverLmax 0.1" to increase the maximum ratio of mismatches to mapped length to 10% (Dobin et al., 2013). The number of reads aligning to genes was counted with featureCounts 2.0.2 tool from the Subread package (Liao et al., 2014). Only reads mapping at least partially inside exons were admitted and aggregated per gene. Reads overlapping multiple genes or aligning to multiple regions were excluded. Differentially expressed genes (DEGs) were identified using DESeq2 version 1.30.0 (Love et al., 2014). Only genes with a minimum fold change of ± 2 (log2 = ±1), a maximum Benjamini-Hochberg corrected p-value of 0.05, and a minimum combined mean of 5 reads were deemed to be significantly differentially expressed. The Ensemble annotation was enriched with UniProt data (release 06.06.2014) based on Ensembl gene identifiers (UniProt Consortium, 2014).

2.2.14. Gelatin-zymography

Gelatin-zymography is a useful technique to analyze the proteolytic activity of activated or latent gelatinases (MMP2 and MMP9) expressed by different cell types, which can cleave gelatin as a gel substrate (Leber and Balkwill, 1997; Toth and Fridman, 2012). Coomassie brilliant blue staining demonstrates the site of proteolysis. The enzymatic activity of MMP2 and MMP9 was measured in conditioned medium after treatment of BMDMs with 50 ng/ml activin A, 250 ng/ml FST288 or a combination of both for 24 h. Gelatin-zymography was performed as reported (Leeman et al., 2002). Firstly, a separating gel (8%) containing 10% gelatin and a stacking gel (5%) without gelatin were prepared.

Separating gel (8%; pH = 8.8)	**Stacking gel (5%; pH = 6.8)**
375 mM Tris	250 mM Tris
0.1% SDS	0.1% SDS
25% Acrylamid	17% Acrylamid
10% Gelatin	-
1% APS	1.5% APS
0.1% TEMED	0.15% TEMED
ddH_2O	ddH_2O

After polymerization, the gels were mounted in the electrophoresis chamber filled with SDS running buffer. The conditioned medium samples (40 µl) mixed with 6 X Laemmli sample buffer were loaded into sample pockets, and the electrophoresis was performed at 90 V on ice.

10 X SDS running buffer
250 mM Tris
1.92 M Glycine
1% SDS
ddH_2O

6 X Laemmli sample buffer (pH = 6.8)
12% SDS
60% Glycerol
375 mM Tris-HCl (pH = 6.8)
0.012% Bromophenol blue
ddH_2O

Subsequently, separating gels were rinsed three times in ddH_2O and washed three times for 15 min in washing buffer with agitation. Gels were incubated in the fresh incubation buffer for 2 days at 37°C, and then stained with Coomassie brilliant blue solution for 1 h

with shaking, followed by washing with de-staining solution for 1 h. Gels were photographed using the Gel Jet Imager 2000 documentation system. The band intensity was quantified by ImageJ. The relative enzymatic activity of MMPs was calculated by normalizing the band intensity of untreated group to 1.

Washing buffer	**Incubation buffer**
1 M Tris (pH=7.6)	1 M Tris (pH=7.6)
2.5% Triton X	1% Triton X
1 M $CaCl_2 \times 2H_2O$	1 M $CaCl_2 \times 2H_2O$
1 mM $ZnCl_2$	1 mM $ZnCl_2$
-	0.1% Sodium azide
ddH_2O	ddH_2O

Staining solution	**De-staining solution**
0.25% Coomassie brilliant blue R	30% 2-propanol
40% Methanol	5% Acetic acid
10% Acetic acid	ddH_2O
ddH_2O	

2.2.15. Statistical analysis

Statistical data analysis was performed by using GraphPad Prism 7 software (GraphPad Software, San Diego, USA). Data are presented as mean ± standard error of the mean (SEM) and were tested for normal distribution by using the Kolmogorov-Smirnov test. Differences in multiple groups were calculated using the one-way or two-way Analysis of Variance (ANOVA) followed by Bonferroni's multiple comparisons test (Gaussian distribution) or the Kruskal-Wallis test followed by Dunn's multiple comparisons test (non-normal distribution). The correlation significance between two groups was analyzed using the Pearson coefficient (normal distribution) or Spearman coefficient (non-normal distribution). Statistical significance was set at $P < 0.05$.

3. RESULTS

3.1. *Ccr2* deficiency protects the testis from damage caused by EAO

Testicular weight as a first sign of successful EAO induction was collected in every group of mice 50 days after first immunization. In the EAO groups, the testis weight was reduced in both *WT* and *Ccr2*$^{-/-}$ mice strains as compared to untreated and adjuvant control groups, respectively **(Fig. 12A)**. However, the mean testis weight of *Ccr2*$^{-/-}$ EAO mice was significantly higher (0.089 ± 0.004 g) than that in *WT* EAO mice (0.045 ± 0.005 g) **(Fig. 12A)**, indicating less testicular damage due to EAO. In order to quantify fibrotic response, testicular collagen content was analyzed by hydroxyproline assay and picro-sirius red staining. The evaluation of total collagen content revealed significantly elevated levels in *WT* EAO testes compared to the *WT* untreated testes **(Fig. 12B)**. Although there was no statistical difference, the total collagen content in EAO testes from *Ccr2*$^{-/-}$ mice was 2.7 - fold lower than that of EAO testes from *WT* mice **(Fig. 12B)**.

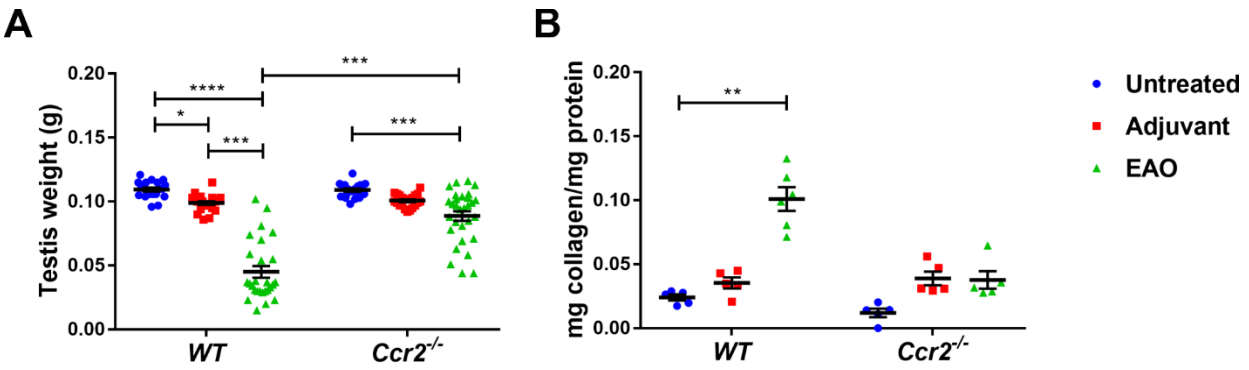

Figure 12. Testis weight and collagen deposition are reduced in *Ccr2*$^{-/-}$ EAO testes. Paired testis weight (g; n = 20 - 30) **(A)** and total collagen content determined by hydroxyproline assay (n = 5 - 6) **(B)** in untreated, adjuvant control and EAO testes from *WT* and *Ccr2*$^{-/-}$ mice. Values are mean ± SEM; the Kruskal-Wallis test followed by Dunn's multiple comparison test was employed for statistical analysis; **P* < 0.05, ***P* < 0.01, ****P* < 0.001, *****P* < 0.0001.

Histological examination of testicular sections revealed that in *WT* EAO testes, the testicular architecture was destroyed showing germ cell sloughing, atrophy of seminiferous tubules, thickening of the lamina propria of seminiferous tubules and an increase in the density of collagen fibers **(Fig. 13C)**. In contrast, in the *Ccr2*$^{-/-}$ EAO testes, most of the tissue remained intact, but there were still a few disrupted seminiferous tubules

visible in some testicular sections pointing to the crucial role of CCR2 in developing of testicular inflammation and following fibrotic remodeling **(Fig. 13F)**. In addition, *Ccr2* deficiency had no influence on testicular histology in untreated and adjuvant mice **(Fig. 13A, B, D and E)**.

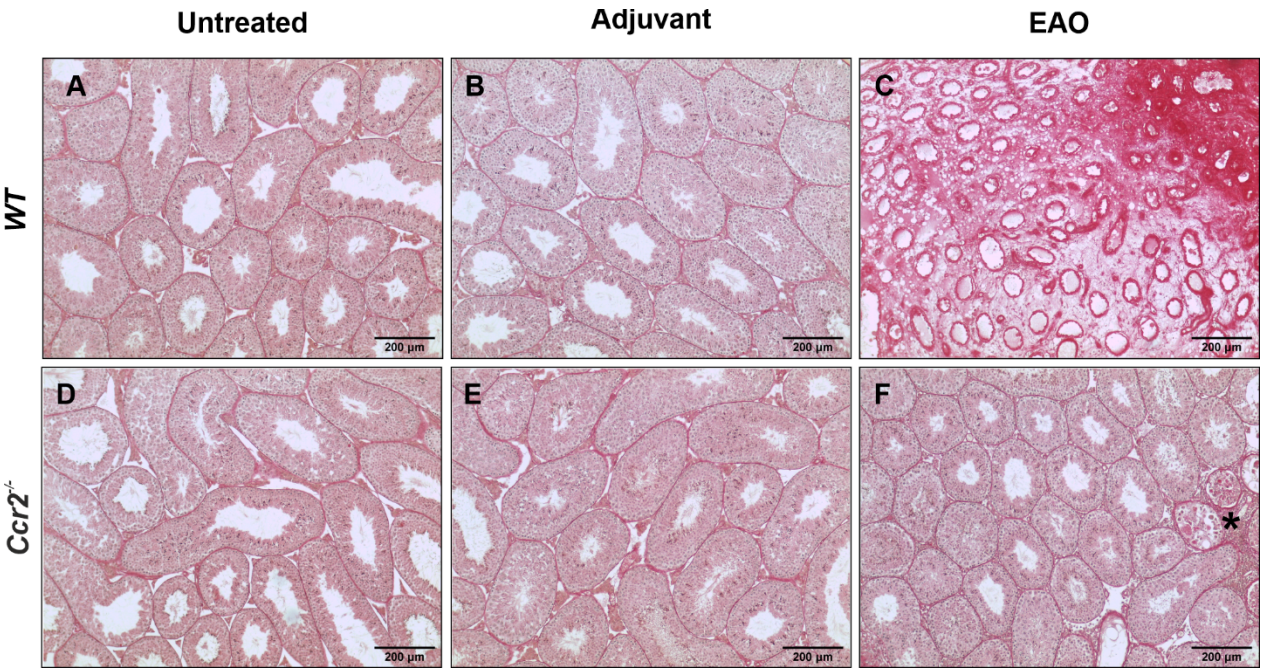

Figure 13. *Ccr2* deficient testes are protected from damage caused by EAO. Representative photomicrographs of picro-sirius red staining in paraffin-embedded sections from untreated **(A, D)**, adjuvant control **(B, E)** and EAO **(C, F)** testes in *WT* **(A - C)** and *Ccr2*$^{-/-}$ mice **(D - F)**. Asterisk points to the destroyed area.

3.2. Depletion of *Ccr2* reduces the immune cell infiltration in EAO testes

An increase in the number of CD45^{+} leukocytes and macrophages is an important hallmark of inflamed testes (Nicolas et al., 2017a; Lustig et al., 2020). To investigate whether the depletion of *Ccr2* affects testicular inflammatory response, the presence and number of immune cells were analyzed by flow cytometry after the exclusion of cellular debris, doublets and dead cells **(Fig. 14A)**. Flow cytometry results demonstrated that in *WT* EAO testes the number of CD45^{+} leukocytes **(Fig. 14B - C)** and CD45^{+}CD11b^{+}F4/80^{+} macrophages **(Fig. 14D)** in the population of single live cells was significantly increased as compared to untreated and adjuvant controls. The mean number of leukocytes and macrophages detected in *Ccr2* deficient EAO testes was 8 - fold and 5 - fold lower

respectively as compared to *WT* EAO testes, although not statistically significant **(Fig. 14B - D)**.

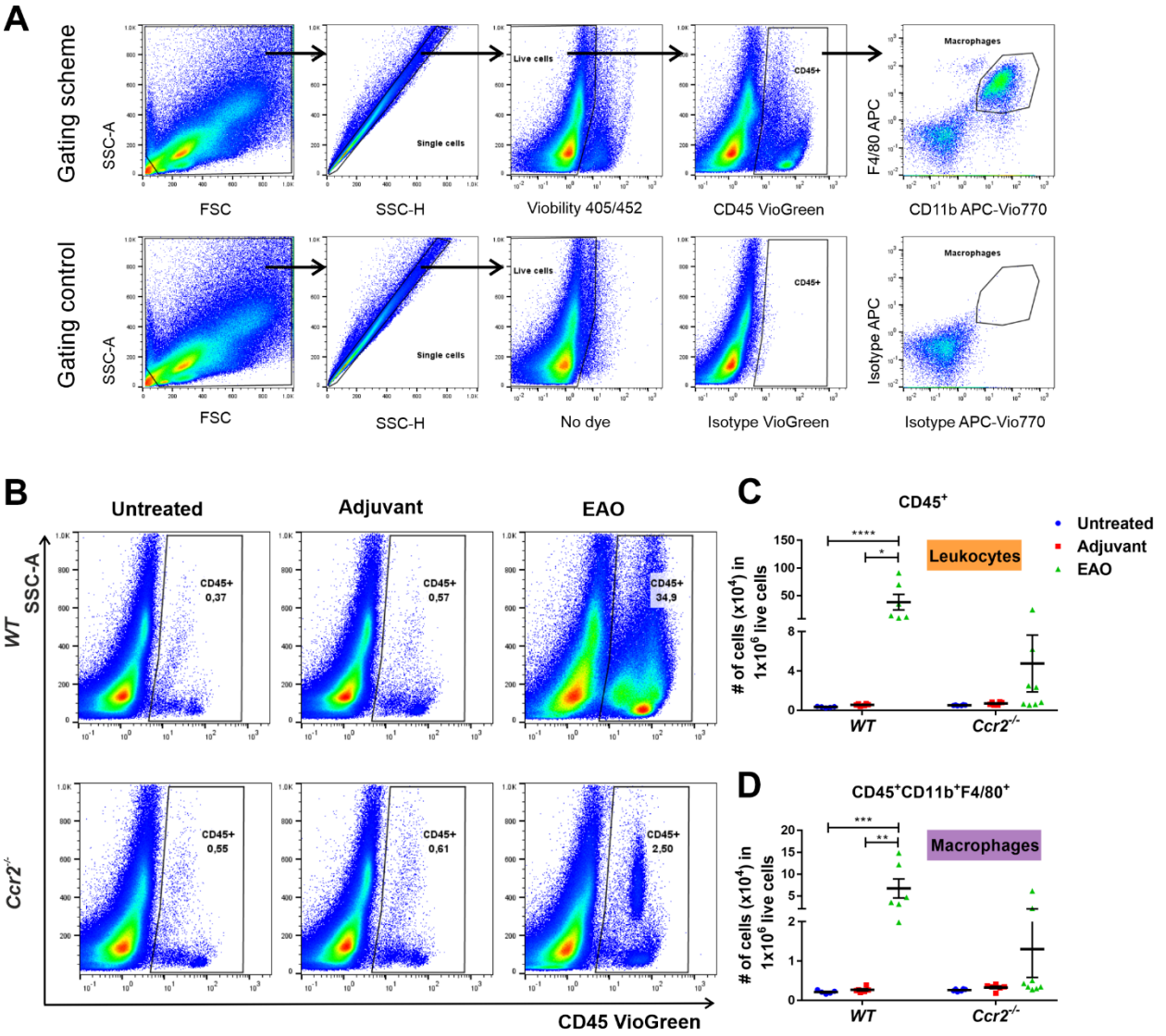

Figure 14. Diminished immune cell infiltration in *Ccr2*$^{-/-}$ EAO testes as compared to *WT* EAO testes. After exclusion of cellular debris, doublets and dead cells, CD45^{+} leukocytes and CD45^{+}CD11b^{+}F4/80^{+} macrophages were selected for further analysis **(A)**. Representative density plots of CD45^{+} leukocytes in untreated, adjuvant control and EAO testicular single cell suspensions from *WT* and *Ccr2*$^{-/-}$ mice **(B)**. The number of testicular CD45^{+} leukocytes **(C)** and CD45^{+}CD11b^{+}F4/80^{+} macrophages **(D)** was determined in untreated, adjuvant control and EAO testicular single cell suspensions from *WT* and *Ccr2*$^{-/-}$ mice by flow cytometry (n = 5 - 8). Values are mean ± SEM; the Kruskal-Wallis test followed by Dunn's multiple comparison test was employed for statistical analysis; **P* < 0.05, ***P* < 0.01, ****P* < 0.001, *****P* < 0.0001.

3.3. The number of ECM-expressing immune cells is decreased in EAO testes from *Ccr2*$^{-/-}$ mice

Since *Ccr2* depletion led to reduced accumulation of immune cells and inhibited fibrotic response in EAO testes, we aimed to check an involvement of immune cells in the development of testicular fibrotic remodeling. To explore whether immune cells, especially macrophages, are an important source of ECM proteins in testicular fibrosis, the number and the localization of ECM-expressing immune cells were analyzed in mouse testes by flow cytometry and immunofluorescence staining, respectively. CXCR4 is one of the important chemokine receptors present on ECM-producing immune cells (Mehrad et al., 2009). Our results showed that after gating out cellular debris, doublets and dead cells, the number of CD45$^+$fibronectin$^+$ cells and CD45$^+$fibronectin$^+$CXCR4$^+$ cells within CD45$^+$ leukocytes was increased in *WT* EAO testes, while *Ccr2* deficiency inhibited this effect **(Fig. 15A - C)**. Among immune cells, macrophages are an important source of ECM proteins (Mantovani et al., 2004). The number of fibronectin$^+$ macrophages in *WT* EAO testes was increased compared to testes from untreated and adjuvant controls **(Fig. 15D)**.

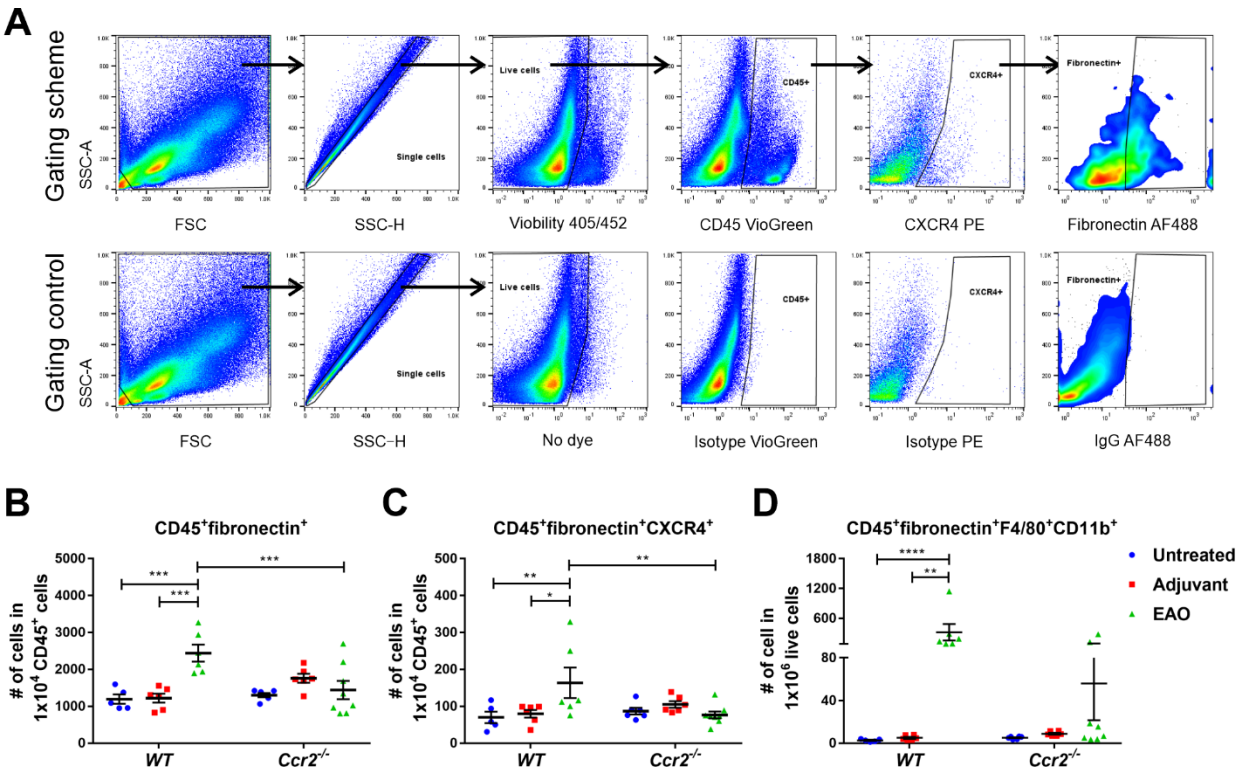

Figure 15. The number of immune cells expressing fibronectin is decreased in *Ccr2* deficient EAO testes. After gating out doublets and nonviable cells **(A)**, the number of testicular CD45$^+$fibronectin$^+$ cells **(B)** and CD45$^+$fibronectin$^+$CXCR4$^+$ cells **(C)** within CD45$^+$ leukocytes as well as the number of testicular CD45$^+$fibronectin$^+$F4/80$^+$CD11b$^+$ cells **(D)** in the population of live cells were analyzed in untreated, adjuvant control and EAO testicular single cell suspensions from *WT* and *Ccr2*$^{-/-}$ mice by flow cytometry (n = 5 - 8). Values are mean ± SEM; the Kruskal-Wallis test followed by Dunn's multiple comparison test or two-way ANOVA test followed by Bonferroni's multiple comparison test was employed for statistical analysis; *P < 0.05, **P < 0.01, ***P < 0.001.

Similar results were also observed for CD45$^+$collagen-I$^+$ cells, CD45$^+$collagen-I$^+$CXCR4$^+$ cells and CD45$^+$collagen-I$^+$F4/80$^+$CD11b$^+$ cells in untreated, adjuvant control and EAO testes from *WT* and *Ccr2*$^{-/-}$ mice **(Fig. 16)**.

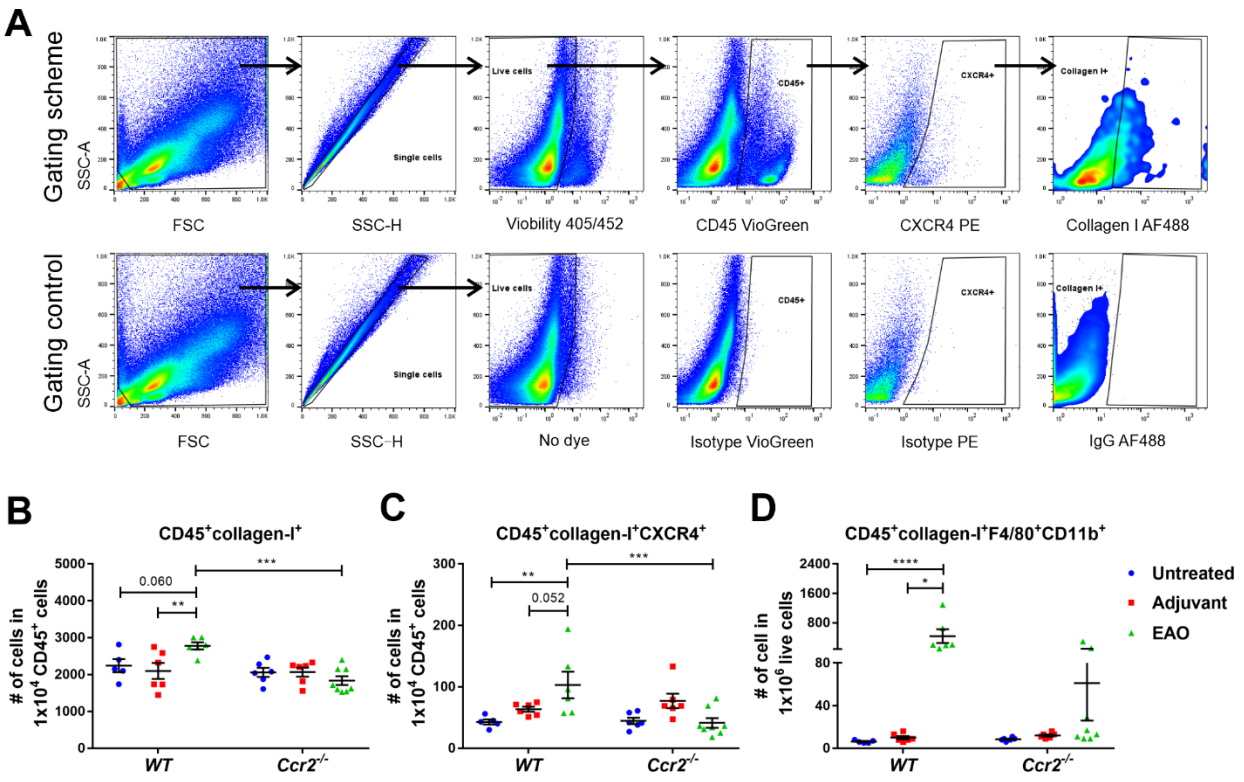

Figure 16. The number of immune cells expressing collagen I is decreased in *Ccr2* deficient EAO testes. After gating out doublets and nonviable cells **(A)**, the number of testicular CD45$^+$collagen-I$^+$ cells **(B)** and CD45$^+$collagen-I$^+$CXCR4$^+$ cells **(C)** within CD45$^+$ leukocytes as well as the number of CD45$^+$collagen-I$^+$F4/80$^+$CD11b$^+$ cells **(D)** in the population of live cells were analyzed in untreated, adjuvant control and EAO testicular single cell suspensions from *WT* and *Ccr2*$^{-/-}$ mice by flow cytometry (n = 5 - 8). Values are mean ± SEM; the Kruskal-Wallis test followed by Dunn's multiple comparison test or two-way ANOVA test followed by Bonferroni's multiple comparison test was employed for statistical analysis; *P < 0.05, **P < 0.01, ***P < 0.001.

Immunofluorescence analysis confirmed that only a few fibronectin^{+} TMs **(Fig. 17)** were detected in the testicular interstitium in untreated and adjuvant testes. In contrast, more fibronectin-expressing TMs were detected in *WT* EAO testes but less triple positive cells in *Ccr2*$^{-/-}$ EAO testes **(Fig. 17)**.

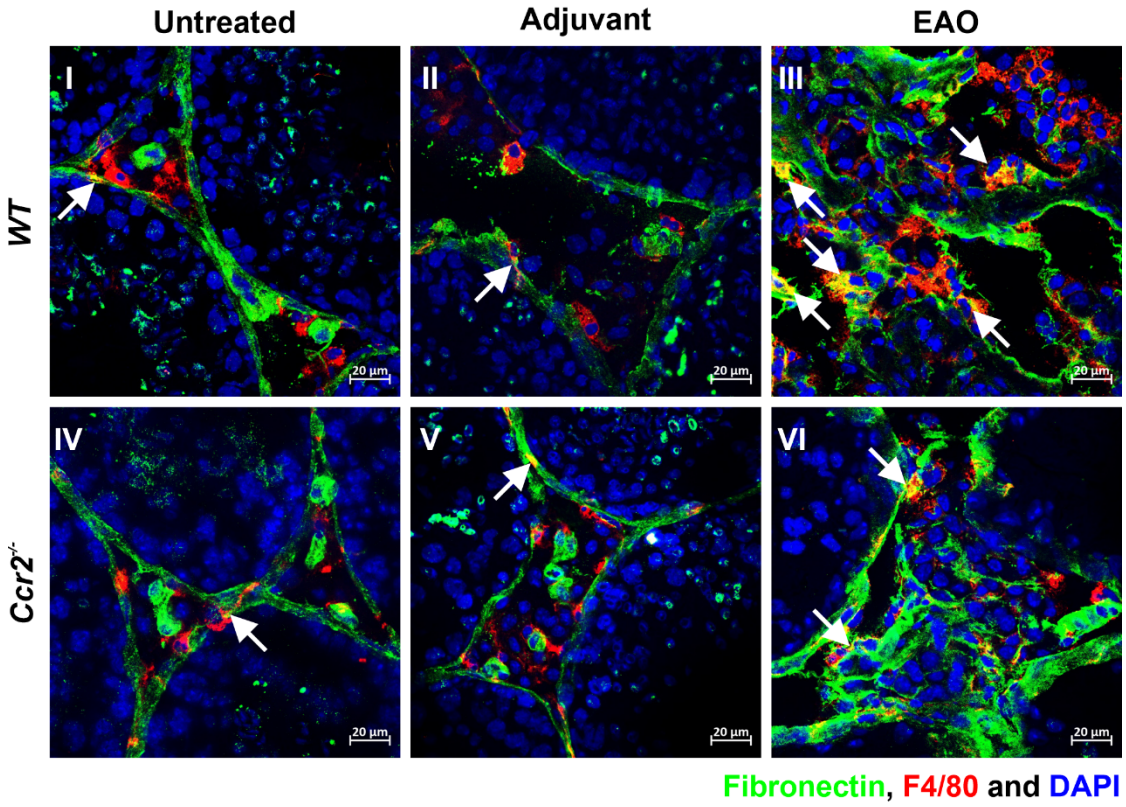

Figure 17. The presence of fibronectin-expressing TMs is lower in *Ccr2*$^{-/-}$ EAO testes as compared to *WT* EAO testes. Representative photomicrographs of fibronectin (green), F4/80 (red) and DAPI (blue) triple immunofluorescence staining in frozen sections from untreated **(I, IV)**, adjuvant control **(II, V)** and EAO **(III, VI)** testes in *WT* **(I - III)** and *Ccr2*$^{-/-}$ mice **(IV - VI)**. Arrow points to the fibronectin positive macrophages.

Similar results were found in collagen-I^{+} TMs during EAO **(Fig. 18)**. These results indicate that CCR2^{+} cells are involved in expression of ECM proteins during testicular inflammation and fibrotic remodeling.

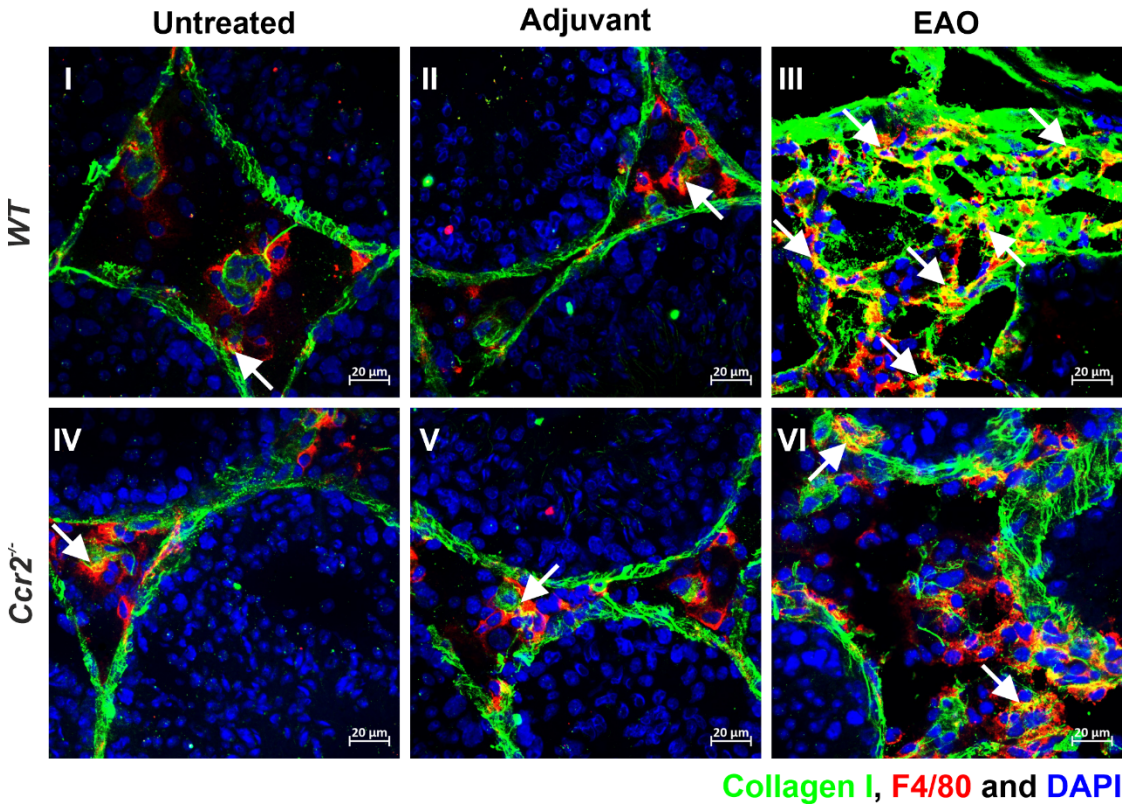

Figure 18. The presence of collagen I-expressing TMs is lower in *Ccr2*$^{-/-}$ EAO testes as compared to *WT* EAO testes. Representative photomicrographs of collagen I (green), F4/80 (red) and DAPI (blue) triple immunofluorescence staining in frozen sections from untreated **(I, IV)**, adjuvant control **(II, V)** and EAO **(III, VI)** testes in *WT* **(I - III)** and *Ccr2*$^{-/-}$ mice **(IV - VI)**. Arrow points to the collagen-I positive macrophages.

3.4. Loss of *Ccr2* inhibits the elevated levels of CXCL12/ CXCR4 during EAO

Because CXCR4 and its ligand CXCL12 contribute to the recruitment of circulating progenitors of active fibroblasts (Xu et al., 2007), the testicular expression of CXCR4 was also analyzed by flow cytometry, qRT-PCR and immunofluorescence in *WT* and *Ccr2*$^{-/-}$ EAO testes. Our results showed that absence of *Ccr2* not only led to the decrease in the number of CD45^{+}CXCR4^{+} cells within CD45^{+} leukocytes **(Fig. 19A)** but also demonstrated reduced *Cxcr4* **(Fig. 19B)** and *Cxcl12* **(Fig. 19C)** mRNA expression in *Ccr2*$^{-/-}$ EAO testes, although they both were increased in *WT* EAO testes (**Fig. 19A - C**). In the *WT* EAO testes not only the number of CXCR4^{+} TMs was increased, but also in general total number of CXCR4^{+} cells, while in the *Ccr2*$^{-/-}$ EAO testes the infiltration by CXCR4^{+} TMs was reduced **(Fig. 19D)**.

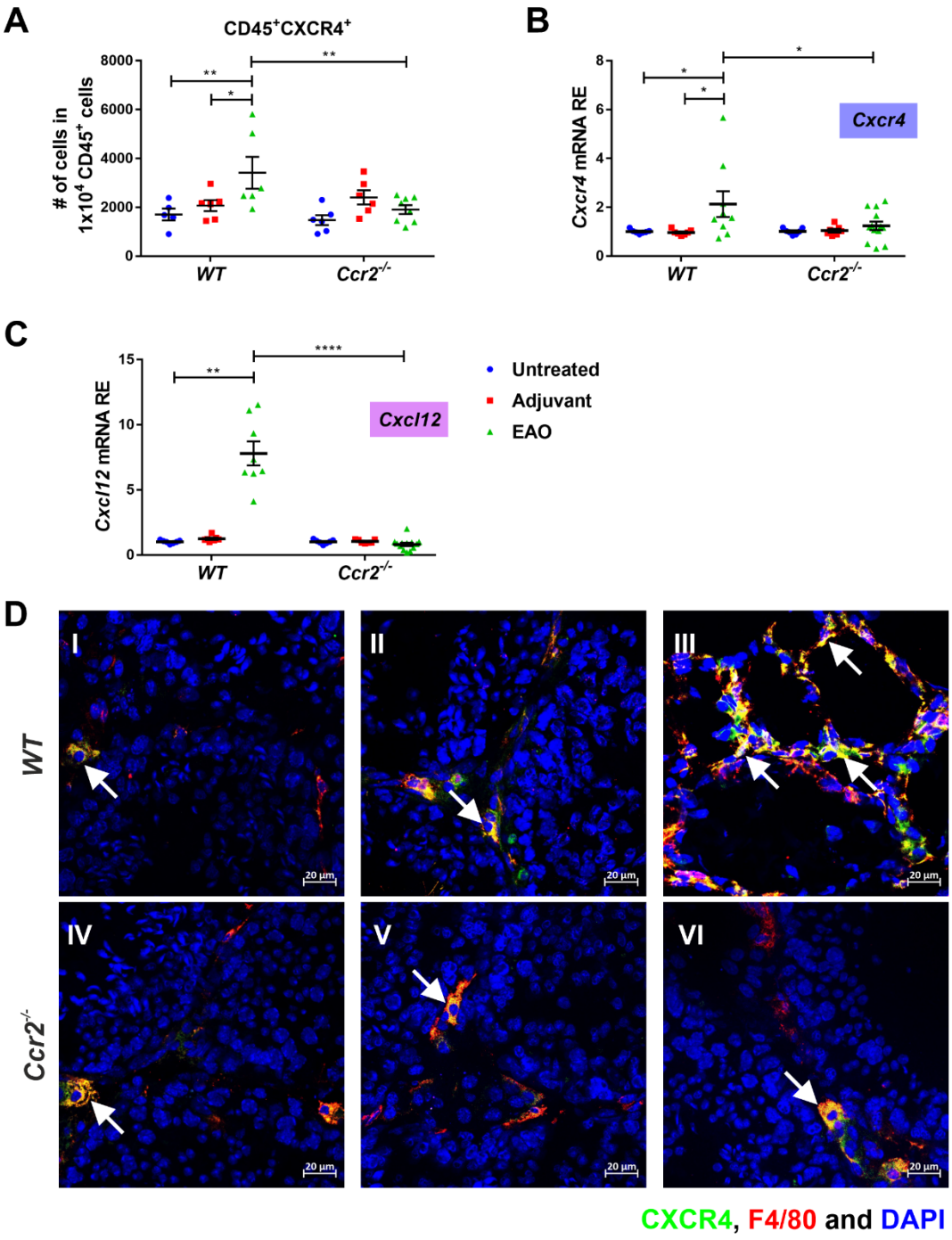

Figure 19. Expression of CXCR4 is reduced in *Ccr2*$^{-/-}$ EAO testes as compared to *WT* EAO testes. After gating out doublets and nonviable cells, the number of testicular CD45^{+}CXCR4^{+} cells in the population of CD45^{+} leukocytes was analyzed in untreated, adjuvant control and EAO testicular single cell suspensions from *WT* and *Ccr2*$^{-/-}$ mice by flow cytometry (n = 5 - 8) **(A)**. The relative expression (RE) of *Cxcr4* **(B)** and *Cxcl12* **(C)** mRNA was measured in untreated, adjuvant control and EAO testes from *WT* and *Ccr2*$^{-/-}$ mice by qRT-PCR and normalized to *18S rRNA* and *Hprt* (n = 7 - 13). Representative photomicrographs of CXCR4 (green), F4/80 (red) and DAPI (blue) triple immunofluorescence staining **(D)** in frozen sections from untreated **(I, IV)**, adjuvant control

(II, V) and EAO **(III, VI)** testes in *WT* **(I - III)** and *Ccr2*$^{-/-}$ mice **(IV - VI)**. Arrow points to the CXCR4 positive macrophages. Values are mean ± SEM, the Kruskal-Wallis test followed by Dunn's multiple comparison test or two-way ANOVA test followed by Bonferroni's multiple comparison test was employed for statistical analysis, **P* < 0.05, ***P* < 0.01, *****P* < 0.0001.

3.5. Activin A contributes to the production of collagen I by TMs during EAO

Our previous studies have reported that elevated levels of activin A, a known fibrotic agent, were accompanied by increased number of macrophages during the active phase of EAO (50 days). Furthermore, a positive correlation between the severity of disease and testicular activin A concentration was shown (Nicolas et al., 2017a, 2017b; Kauerhof et al., 2019). In order to prove the effect of activin A on expression of ECM in TMs, a mouse model overexpressing FST315 (activin A antagonist) to block activin A action was used **(Fig. 20A)**. The induction of EAO in *rAAV-EV* and *rAAV-FST315* mice was performed at the Monash University (Prof. Mark P. Hedger Lab, Hudson Institute of Medical Research). In the recently established EAO model in mice overexpressing FST315, only 40% of mice (2/5) showed the pathology of testicular inflammation, while 75% of mice (3/4) receiving *rAAV-EV* developed EAO (Nicolas et al., 2017b). Testicular FST levels were significantly higher in *rAAV-FST315* mice during EAO than those in *rAAV-EV* mice, while mean concentration of testicular activin A was decreased (Nicolas et al., 2017b). The immunostainings using paraffin-embedded testicular sections revealed that FST315 treatment also clearly reduced testicular infiltration by collagen-I^{+} TMs in mice undergoing EAO **(Fig. 20B)**. Collagen I was almost undetectable in TMs from untreated and adjuvant controls **(Fig. 20B)**.

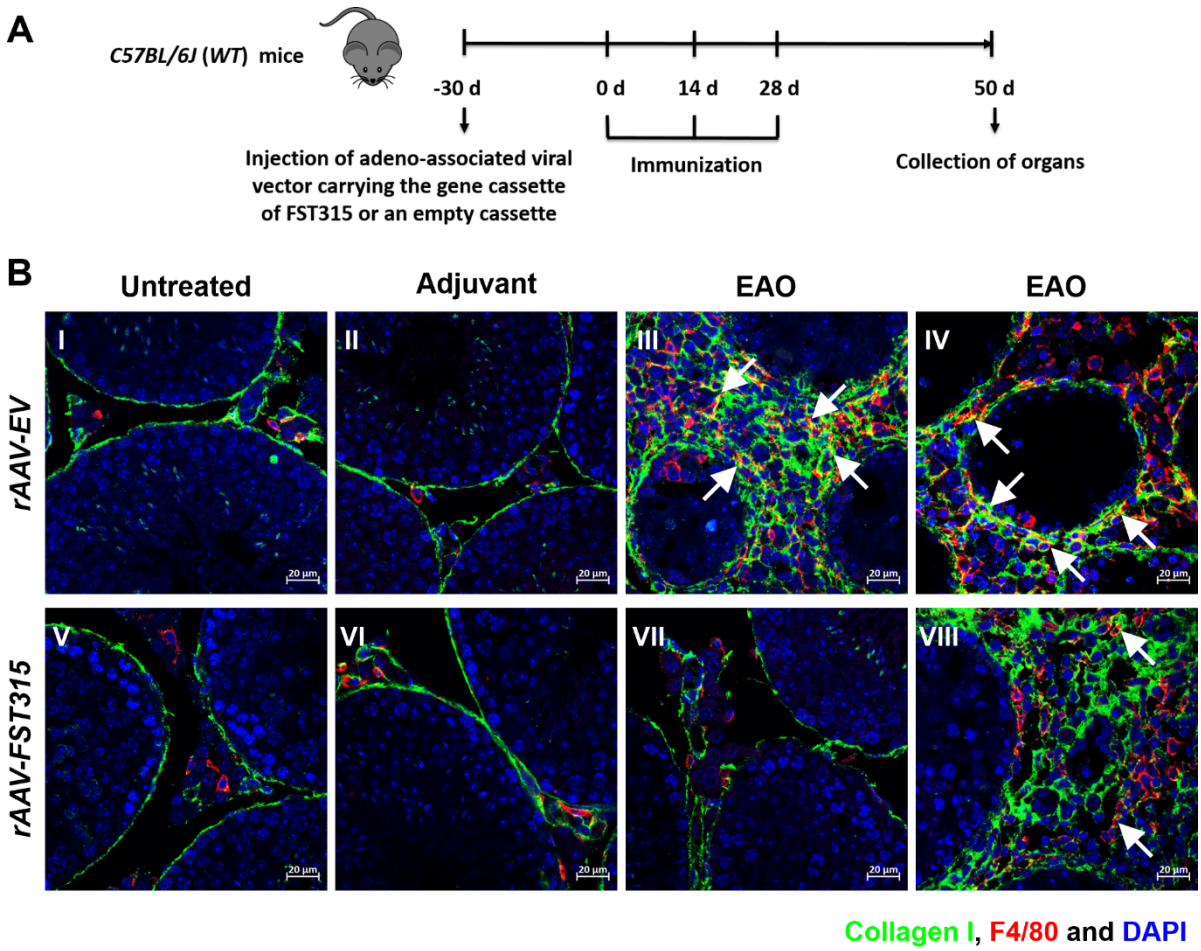

Figure 20. Activin A promotes macrophage-derived collagen I production during EAO. Schematic diagram representing the time points for recombinant adeno-associated viral vector (rAAV) injection, EAO induction and organ collection in *C57BL/6J* (*WT*) mice. Mice were injected with rAAV carrying the gene cassette of FST315 (*rAAV-FST315*) or an empty vector (*rAAV-EV*) 30 days prior to first immunization, then immunized three times every other week starting at day 0 and testes were collected at day 50 **(A)**. Representative photomicrographs of collagen I (green), F4/80 (red) and DAPI (blue) triple immunofluorescence staining in paraffin-embedded sections from untreated **(I, V)**, adjuvant control **(II, VI)** and EAO **(III, IV, VII, VIII)** testes in *rAAV-EV* **(I - IV)** and *rAAV-FST315* **(V - VIII)** mice**.** Arrow points to the triple positive cells **(B)**.

3.6. Analysis of the purity of cultured BMDMs

The above experiments point to a possible role of activin A associated with macrophages in fibrotic response during testicular inflammation. Therefore, the aim was to prove whether activin A through regulating and modulating macrophages contributes to inflammatory and fibrotic responses. As a surrogate of TMs, we used BMDMs generated in the presence of M-CSF stimulation.

Under the M-CSF conditions, myeloid cells may differentiate into monocytes, macrophages as well as a small proportion of dendritic cells (Francke et al., 2011). Therefore, in the first step, the cell composition of cultured bone marrow progenitor cells after M-CSF stimulation was investigated. Flow cytometry results demonstrated that after 3 days of culture 77% of live cells were $CD45^+$ leukocytes, and on day 6 almost all of viable cells were leukocytes **(Fig. 21A - B)**. The proportion of dendritic cells increased from 3.8% to 5.2% within live cells in the first three days of culture and then decreased to 2.0% at day 6 **(Fig. 21C)**. The percentage of $CD45^+CD11c^-Ly6C^+$ monocytes also dropped from 44% to 38% at the first three days of culture, but at day 6 only 4% of live cells were monocytes **(Fig. 21D)**. In the starting cell suspension (day 0), macrophages were almost absent (0.03%). After stimulation with M-CSF for 3 days, the population of $CD45^+CD11c^-Ly6C^-CD11b^+F4/80^+$ macrophages increased to 44% and reached ~ 90% after 6 days **(Fig. 21E)**.

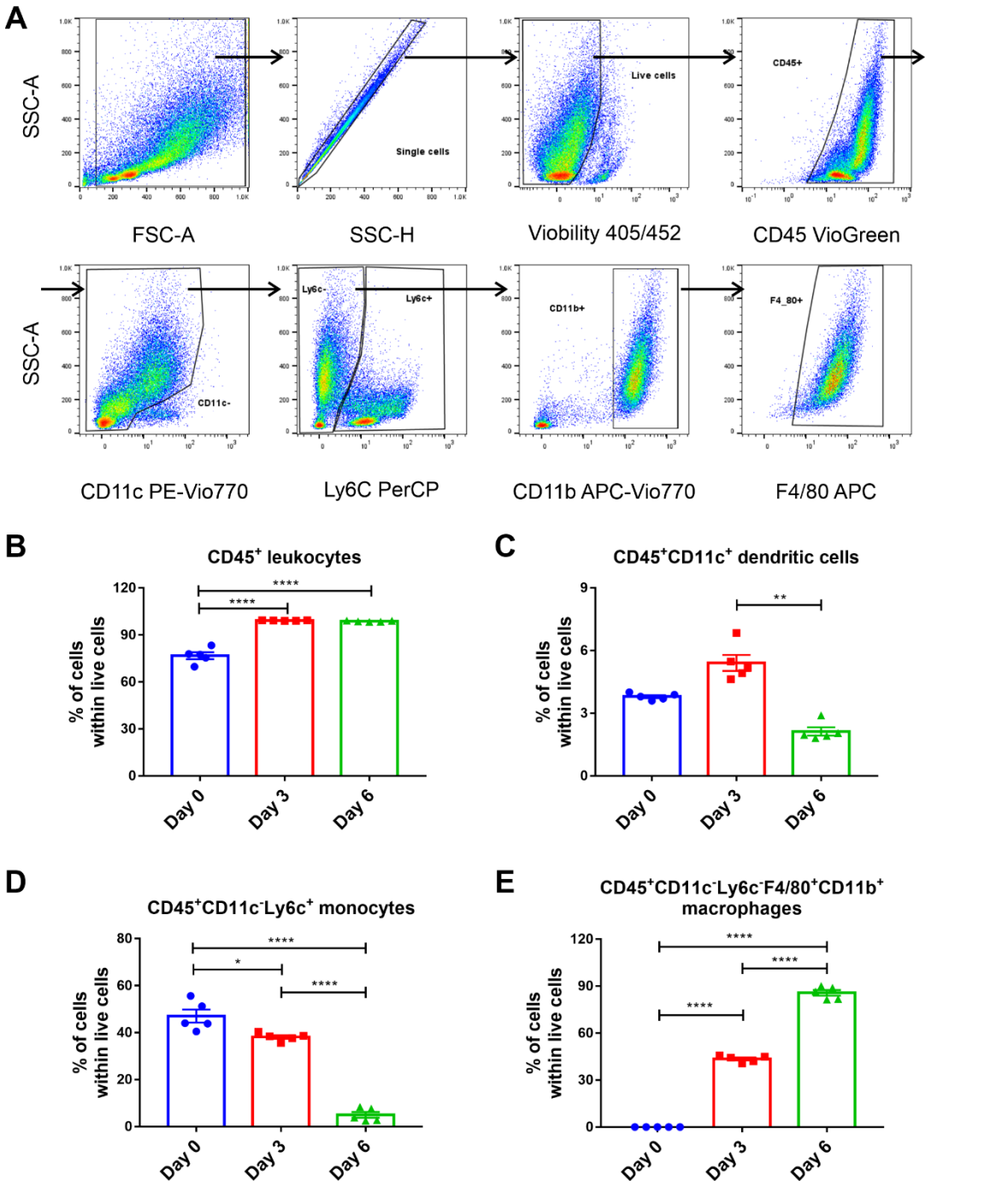

Figure 21. Analysis of cell content (leukocytes, dendritic cells, monocytes and macrophages) during cultivation of bone marrow progenitor cells in presence of M-CSF by flow cytometry. Representative flow cytometry plots show the gating strategy used for the analysis of different cell subpopulations in cultured bone marrow progenitor cells. After gating out debris, doublets and nonviable cells, $CD45^+$ leukocytes, $CD45^+CD11c^+$ dendritic cells, $CD45^+CD11c^-Ly6C^+$ monocytes and $CD45^+CD11c^-Ly6C^-F4/80^+CD11b^+$ macrophages were selected for further analysis **(A)**. The percentage of leukocytes **(B)**, dendritic cells **(C)**, monocytes **(D)** and macrophages **(E)** within live cells was analyzed by flow cytometry in bone marrow single

cell suspensions at day 0 and after 3 and 6 days in a presence of M-CSF (n = 5). Values are mean ± SEM, the Kruskal-Wallis test followed by Dunn's multiple comparison test or one-way ANOVA test followed by Bonferroni's multiple comparison test was employed for statistical analysis, **P* < 0.05, ***P* < 0.01, *****P* < 0.0001.

3.7. Activin A affects the phenotypical changes of BMDMs

Activin A treatment led also to changes in the morphology of BMDMs from round, oval or irregular form to elongated shape **(Fig. 22A)**.

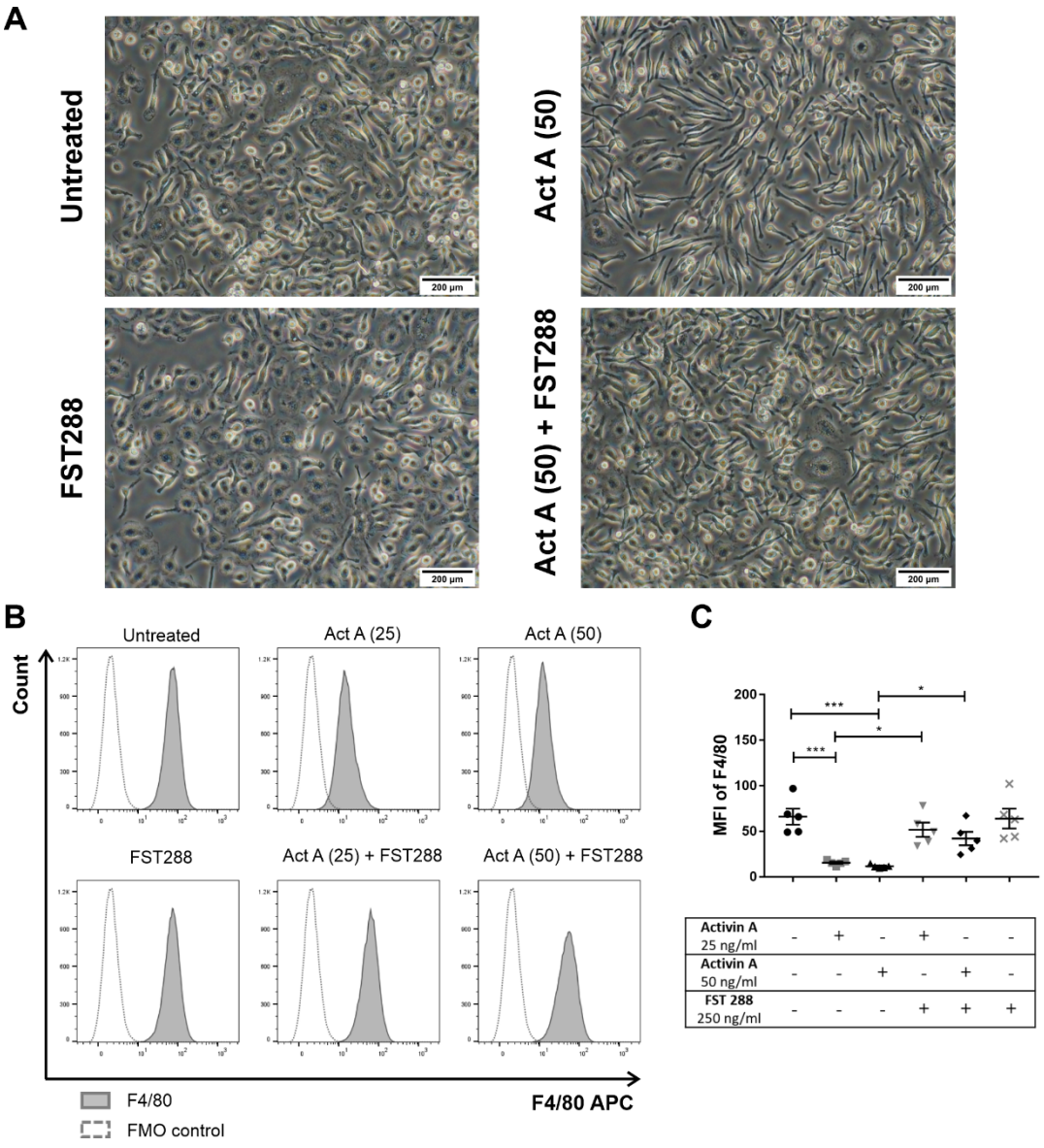

Figure 22. Activin A influences the morphology and phenotype of BMDMs. Representative photomicrographs of BMDMs after 6 days treatment with 50 ng/ml activin A, 250 ng/ml FST288 or

a combination of both **(A)**. After gating $CD45^+CD11c^-Ly6C^-F4/80^+CD11b^+$ macrophages, the mean fluorescence intensity (MFI) of F4/80 **(B, C)** was measured in BMDMs by flow cytometry (n = 5). Values are mean ± SEM; one-way ANOVA test followed by Bonferroni's multiple comparison test was employed for statistical analysis; $*P < 0.05$, $***P < 0.001$.

The influence of activin A on phenotypical changes of BMDMs was supported by the reduction of F4/80 mean fluorescence intensity (MFI) in macrophages upon 25 or 50 ng/ml activin A stimulation **(Fig. 22B - C)**. These effects were inhibited by FST288, which alone had no influence neither on the morphology nor on the MFI of F4/80 in BMDMs **(Fig. 22)**.

3.8. Activin A influences the transcriptome of BMDMs

Whole transcriptomic analysis was performed in BMDMs after the treatment with activin A, FST288 and a combination of both *in vitro* **(Fig. 23A)**. FST288 was used as an antagonist of activin A action. Generally, the samples from untreated, FST288 or FST288 + activin A-treated BMDMs showed similar gene expression pattern, which was visibly different from activin A-treated BMDMs **(Fig. 23B - D)**. Our data showed that there were 936 upregulated and 799 downregulated differentially expressed genes (DEGs) in activin A-stimulated BMDMs compared to the control group **(Fig. 23B - C)**. Further analysis of top 50 DEGs within the term "Inflammation mediated by chemokine and cytokine signaling pathway" from Panther database demonstrated that many cytokine and chemokine signaling related genes were regulated by activin A, e.g., *Ccr2* and *Cxcr4* were increased, while *Ccl2* was decreased **(Fig. 23E)**. Selection of Top50 significantly DEGs within the term "Extracellular matrix organization" from Reactome database indicated that the upregulated genes, such as *Tgfbr1*, *Mmp2* or *Mmp14*, were related to the TGF-β signaling and ECM organization **(Fig. 23F)**. ECM-related genes including *Fn1*, *Itgav*, *Pdgfa*, *Itgb5*, *Mmp14* and *Mmp2* were also elevated in BMDMs upon activin A treatment **(Fig. 23F)**. Therefore, we focused on the selected genes (*Ccr2*, *Cxcr4, Fn1, Mmp2*, *Mmp14*, *Pdgfa, Itgav, Itgb3*) in the further experiments.

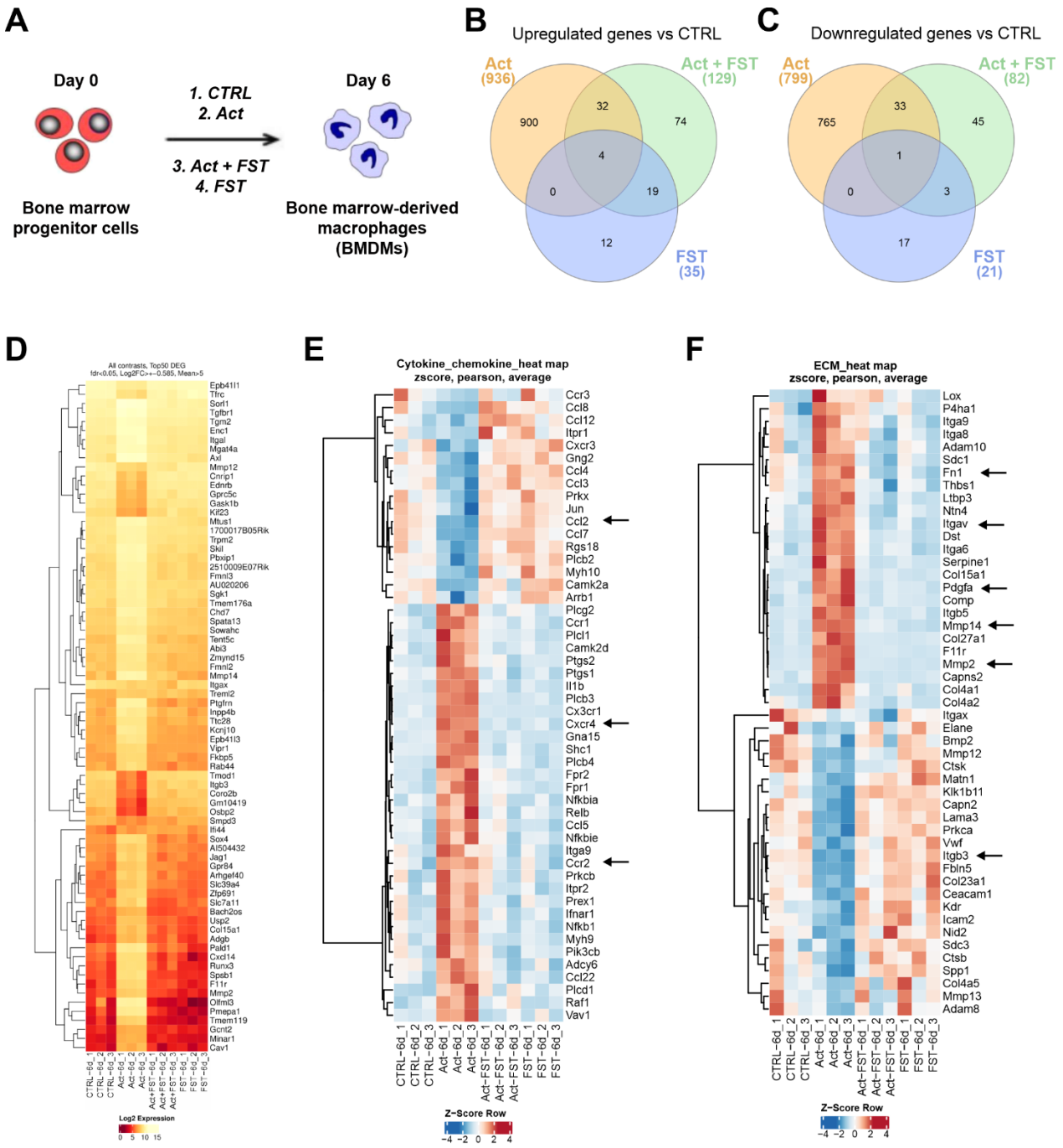

Figure 23. Whole transcriptome analysis of BMDMs upon activin A stimulation. Experimental set-up for transcriptome analysis in untreated (CTRL) or BMDMs (n = 3) stimulated with 50 ng/ml activin A (Act), 250 ng/ml FST288 (FST) or a combination of both (Act + FST) **(A)**. Venn diagram of up- **(B)** and downregulated-DEGs **(C)** in Act-, Act + FST- and FST-treated versus CTRL BMDMs. Heat map showing the expression of top 50 DEGs in CTRL, Act-, Act + FST- and FST-treated BMDMs (based on false discovery rate (FDR) > 0.05 and minimal count number > 5) **(D)**. Heat maps showing significantly DEGs within term "Inflammation mediated by chemokine and cytokine signaling pathway" **(E)** and "Extracellular matrix organization" **(F)** from Panther and Reactome

database, respectively in CTRL, Act-, Act+FST- and FST-treated BMDMs presented with Z-score normalization. Arrow points to the investigated genes.

3.9. Activin A increases fibronectin and CXCR4 expression in BMDMs

In vivo data demonstrated that both fibronectin$^+$ and CXCR4$^+$ macrophages were elevated in fibrotic lesions during the course of EAO **(Fig. 17 and 19)**. Moreover, RNA sequencing data confirmed that *Fn1* and *Cxcr4* gene expression were upregulated upon activin A stimulation in BMDMs **(Fig. 23E - F)**. In line with these findings, *Fn1* mRNA expression was increased in BMDMs after activin A treatment as confirmed by qRT-PCR **(Fig. 24A)**. This effect was inhibited by the addition of FST288 **(Fig. 24A)**.

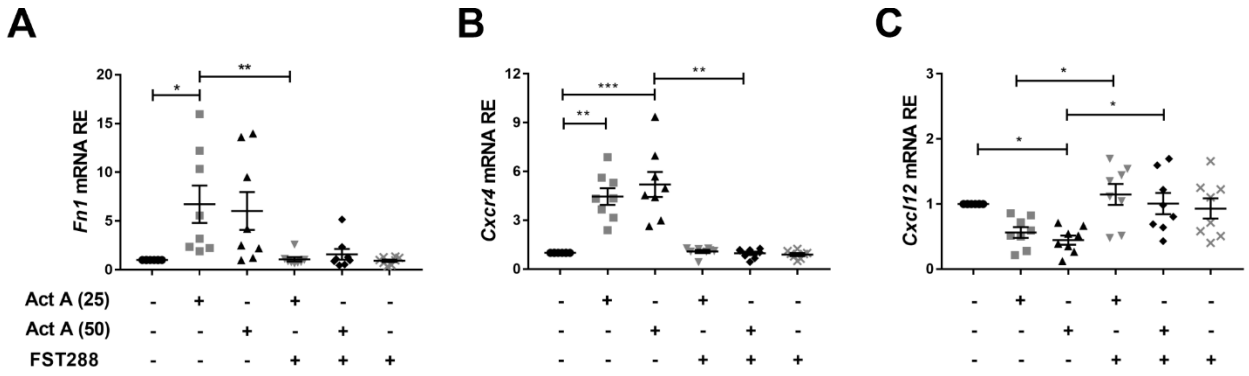

Figure 24. The expression of *Fn1*, *Cxcr4* and *Cxcl12* mRNA was elevated in BMDMs following the exposure to activin A. Total RNA was isolated from BMDMs 6 days after treatment with 25 or 50 ng/ml activin A, 250 ng/ml FST288 or a combination of both. The relative expression (RE) of *Fn1* **(A)**, *Cxcr4* **(B)** and *Cxcl12* **(C)** was measured by qRT-PCR and normalized to *Hprt* (n = 8). Values are mean ± SEM; the Kruskal-Wallis test followed by Dunn's multiple comparison test was employed for statistical analysis; **P* < 0.05, ***P* < 0.01, ****P* < 0.001.

Moreover, flow cytometry results showed that after gating CD45$^+$CD11c$^-$Ly6c$^-$CD11b$^+$F4/80$^+$ cell population, activin A increased the percentage of fibronectin$^+$ macrophages *in vitro* **(Fig. 25A - C)**. Similarly, the percentage of CXCR4$^+$ macrophages as well as the expression of *Cxcr4* mRNA were increased in activin A-treated BMDMs **(Fig. 24B and 25D - E)**. FST288 also suppressed the changes of CXCR4 in BMDMs caused by activin A **(Fig. 24B and 25D - E)**. In contrast, the mRNA expression of CXCR4 ligand *Cxcl12* was reduced in activin A-treated BMDMs **(Fig. 24C)**.

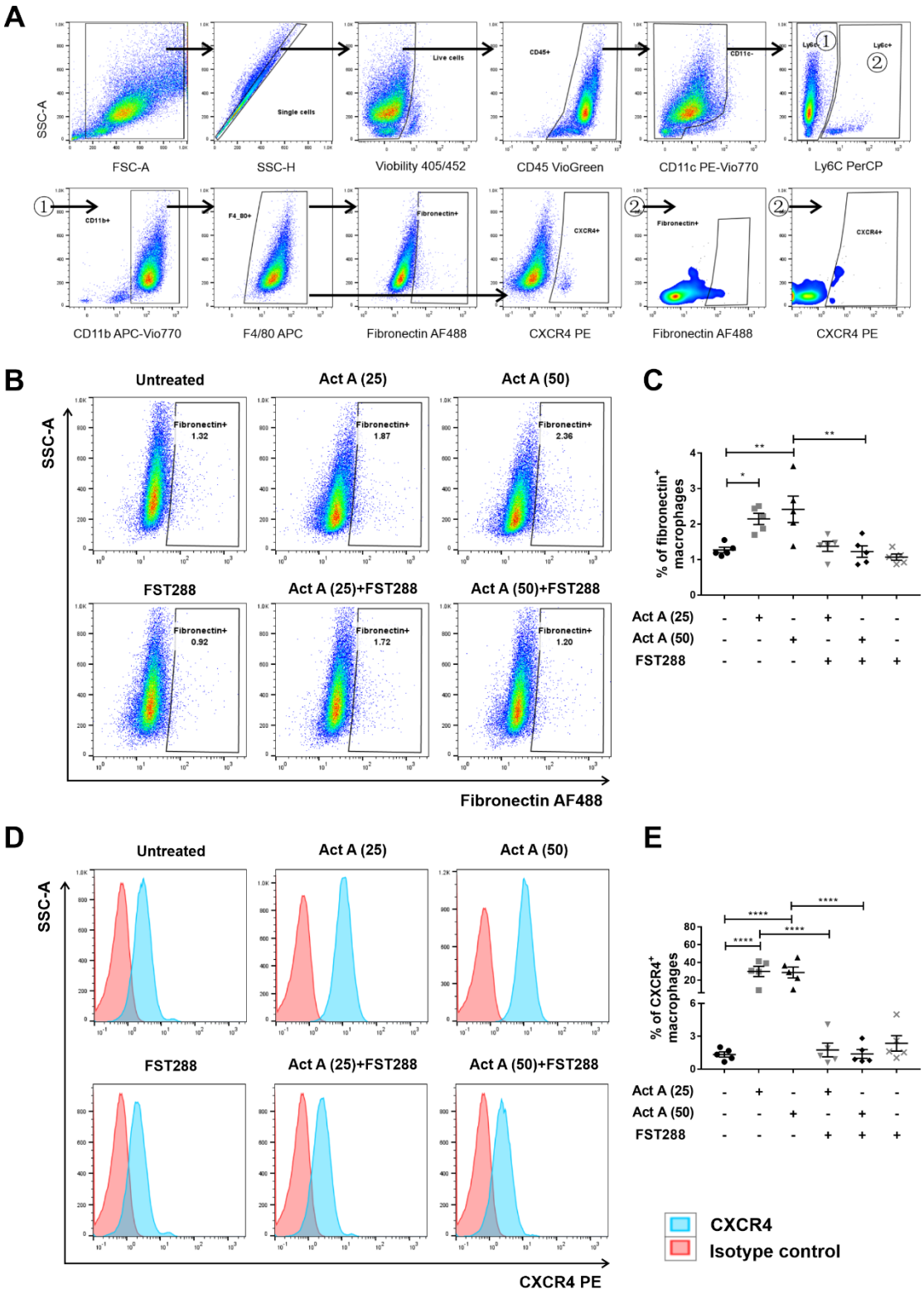

Figure 25. The percentage of fibronectin$^+$ and CXCR4$^+$ macrophages was increased in BMDMs following the exposure to activin A. After gating CD45$^+$CD11c$^-$Ly6C$^-$F4/80$^+$CD11b$^+$ macrophages **(A)**, the percentage of fibronectin$^+$ **(B, C)** and CXCR4$^+$ **(D, E)** macrophages after

treatment with 25 or 50 ng/ml activin A, 250 ng/ml FST288 or a combination of both were measured in BMDM single cell suspensions by flow cytometry (n = 5). Values are mean ± SEM; the one-way ANOVA test followed by Bonferroni's multiple comparison test was employed for statistical analysis; **P* < 0.05, ***P* < 0.01, ****P* < 0.001, *****P* < 0.0001.

3.10. The mRNA expression of MMPs, integrin subunits and PDGFs is affected by activin A in BMDMs

There is an evidence that MMPs and their inhibitors TIMPs are involved in the process of ECM degradation and tissue fibrosis (Robert et al., 2016). Our data from RNA sequencing analysis also revealed increased expression of *Mmp2* and *Mmp14* in BMDMs upon stimulation with activin A **(Fig. 23F)**. Therefore, the effect of activin A on the production of MMPs and TIMP1 in BMDMs *in vitro* was investigated. qRT-PCR results confirmed that activin A increased the mRNA expression of *Mmp2* and *Mmp14* in BMDMs, while the mRNA expression of *Mmp9* and *Timp1* was decreased **(Fig. 26A)**. In addition to the gene expression, activin A was involved in the upregulation of MMP2 and downregulation of MMP9 enzymatic activity, respectively **(Fig. 26B - C)**. This was in agreement with the qRT-PCR results **(Fig. 26A)**.

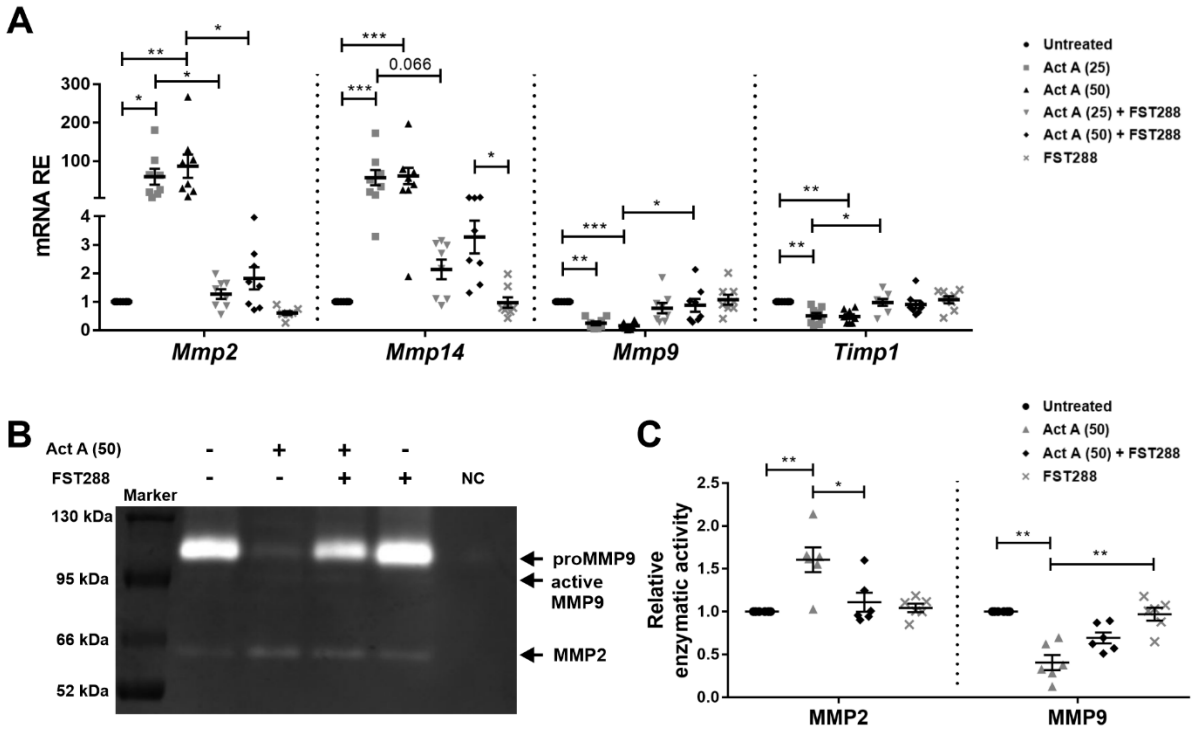

Figure 26. Activin A regulates the expression and enzymatic activity of MMPs in BMDMs. Total RNA was isolated from BMDMs 6 days after treatment with 25 or 50 ng/ml activin A, 250 ng/ml FST288 or a combination of both. The relative expression (RE) of *Mmp2*, *Mmp14*, *Mmp9* and *Timp1* mRNA was measured by qRT-PCR and normalized to *Hprt* (n = 8) **(A)**. Representative gelatin-zymography gel of BMDMs 7 days after treatment with 50 ng/ml activin A, 250 ng/ml FST288 or a combination of both. Serum-free RPMI-1640 medium was used as a negative control **(B)**. Six independent gelatin-zymography replicates were performed and the relative enzymatic activity of MMP2 and MMP9 was analyzed by quantifying the intensity of bands **(C)**. Values are mean ± SEM; the Kruskal-Wallis test followed by Dunn's multiple comparison test was employed for statistical analysis; **P* < 0.05, ***P* < 0.01, ****P* < 0.001.

Numerous studies have shown that integrins (receptors for ECM proteins) and PDGFs produced by immune cells contribute to the ECM deposition and fibrosis development (Margadant and Sonnenberg, 2010; Klinkhammer et al., 2018). The results from RNA sequencing analysis also suggested that several integrin subunits such as *Itgb3*, *Itgb5* and *Itgav*, as well as *Pdgfa* were regulated upon activin A treatment in BMDMs **(Fig. 23F)**. Therefore, the expression of integrins and PDGFs mRNA in activin A-treated BMDMs was determined. Activin A induced in a dose-dependent manner *Itgav*, *Itgb5*, *Pdgfa*, *Pdgfb* and *Pdgfrb* mRNA expression, while downregulated the expression of *Itgb3* mRNA in BMDMs **(Fig. 27)**. In contrast, expression levels of these genes after the treatment with combination of activin A and FST288 or FST288 alone were similar as in untreated BMDMs **(Fig. 27)**.

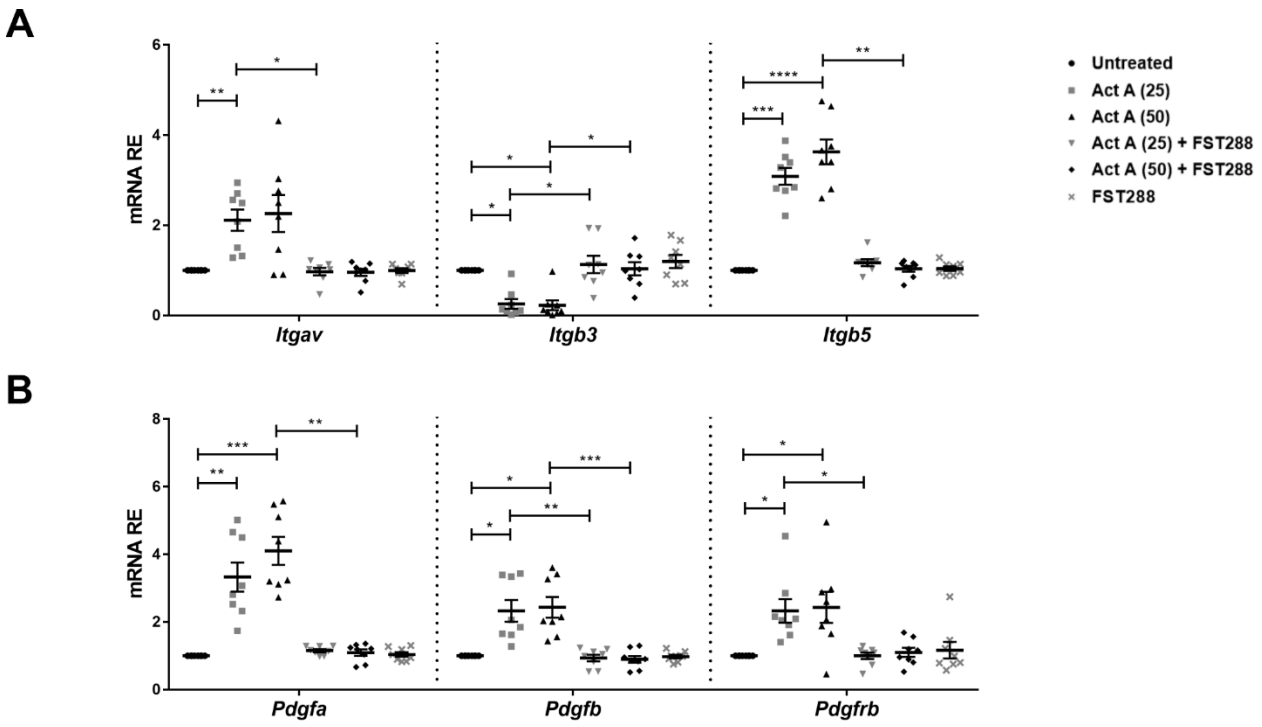

Figure 27. Activin A regulates mRNA expression of integrins and PDGFs in BMDMs. Total RNA was isolated from BMDMs 6 days after treatment with 25 or 50 ng/ml activin A, 250 ng/ml FST288 or a combination of both. The relative expression (RE) of *Itgav*, *Itgb3* and *Itgb5* mRNA **(A)**, *Pdgfa*, *Pdgfb* and *Pdgfrb* mRNA **(B)** was measured by qRT-PCR and normalized to *Hprt* (n = 8). Values are mean ± SEM; the Kruskal-Wallis test followed by Dunn's multiple comparison test was employed for statistical analysis; **P* < 0.05, ***P* < 0.01, ****P* < 0.001, *****P* < 0.0001.

3.11. SC - derived activin A increases fibronectin mRNA expression in BMDMs

Since our recent studies showed that TNF stimulates activin A secretion by mouse SCs *in vitro*, the SC conditioned medium (SCCM) was used here to evaluate the effect of activin A originating from testicular cells located in a direct neighborhood of macrophages (Kauerhof et al., 2019). The results of qRT-PCR confirmed that TNF-stimulated SCCM induced a significant increase in *Fn1* mRNA expression in BMDMs, while non-TNF-SCCM did not show any effects **(Fig. 28A)**. The specificity of activin A-induced *Fn1* mRNA expression was proven by inhibition of activin A action in SCCM by using FST288 (**Fig. 28A**). Although TNF-stimulated SCCM did not induced increased *Cxcr4* expression in BMDMs, the inclusion of FST288 resulted in reduced levels of *Cxcr4* mRNA **(Fig. 28B)**.

Treatment with TNF-stimulated SCCM also led to 50 - fold increased *Mmp2* expression **(Fig. 28C)**. Notably, treatment of BMDMs with conditioned medium from TNF-stimulated SCs also elevated the expression of *Mmp14* (46 - fold), *Mmp9* (16 - fold) and *Timp1* (1.5 - fold) mRNA; however, these increases were not abolished by FST288, pointing to regulation by SC-derived factors other than activin A **(Fig. 28D - F)**.

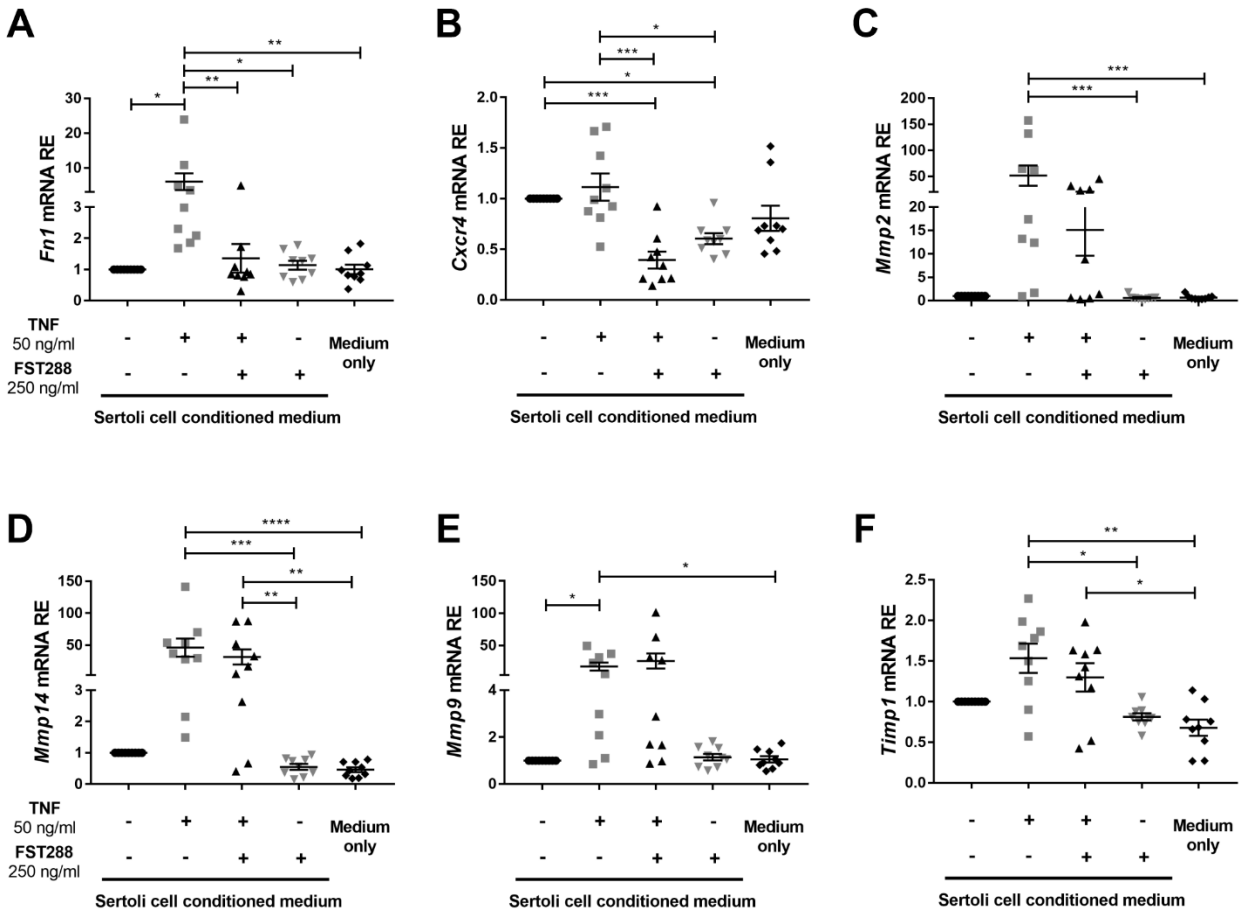

Figure 28. The expression of fibrotic-related genes in BMDMs after incubation with SCCM. The relative expression (RE) of *Fn1* **(A)**, *Cxcr4* **(B)**, *Mmp2* **(C)**, *Mmp14* **(D)**, *Mmp9* **(E)** and *Timp1* **(F)** was measured in BMDMs 3 days after treatment with conditioned medium from SCs cultured alone or in a presence of 50 ng/ml TNF, 250 ng/ml FST288 or combination of both by qRT-PCR and normalized to *Hprt* (n = 9). Values are mean ± SEM; the Kruskal-Wallis test followed by Dunn's multiple comparison test was employed for statistical analysis; **P* < 0.05, ***P* < 0.01, ****P* < 0.001, *****P* < 0.0001.

3.12. The mRNA expression of testicular MMPs, integrin subunits and PDGFs is dysregulated during EAO

Since activin A promoted the expression of some MMPs (*Mmp2*, *Mmp14*), integrin subunits (*Itgav*, *Itgb5*) and PDGFs (*Pdgfa*, *Pdgfb*) in BMDMs **(Fig. 26 - 27)**, we reasoned that increased levels of activin A measured during EAO may also influence the expression of these factors in inflamed testes. Therefore, the expression of MMPs, TIMP1, integrin subunits, PDGFs and PDGFRβ was investigated in *WT* and *Ccr2*$^{-/-}$ EAO testes. qRT-PCR results demonstrated that *Mmp2* **(Fig. 29A)**, *Mmp14* **(Fig. 29B)**, *Mmp9* **(Fig. 29C)**, *Timp1* **(Fig. 29D)**, *Itgav* **(Fig. 30A)**, *Itgb3* **(Fig. 30B)**, *Pdgfb* **(Fig. 30E)** and *Pdgfrb* **(Fig. 30F)** mRNA expression were elevated in *WT* EAO testes. In contrast, in *Ccr2*$^{-/-}$ EAO testes expression of *Mmp2* **(Fig. 29A)**, *Mmp14* **(Fig. 29B)**, *Itgav* **(Fig. 30A)**, *Itgb3* **(Fig. 30B)** and *Pdgfb* **(Fig. 30E)** mRNA was at levels comparable with the controls.

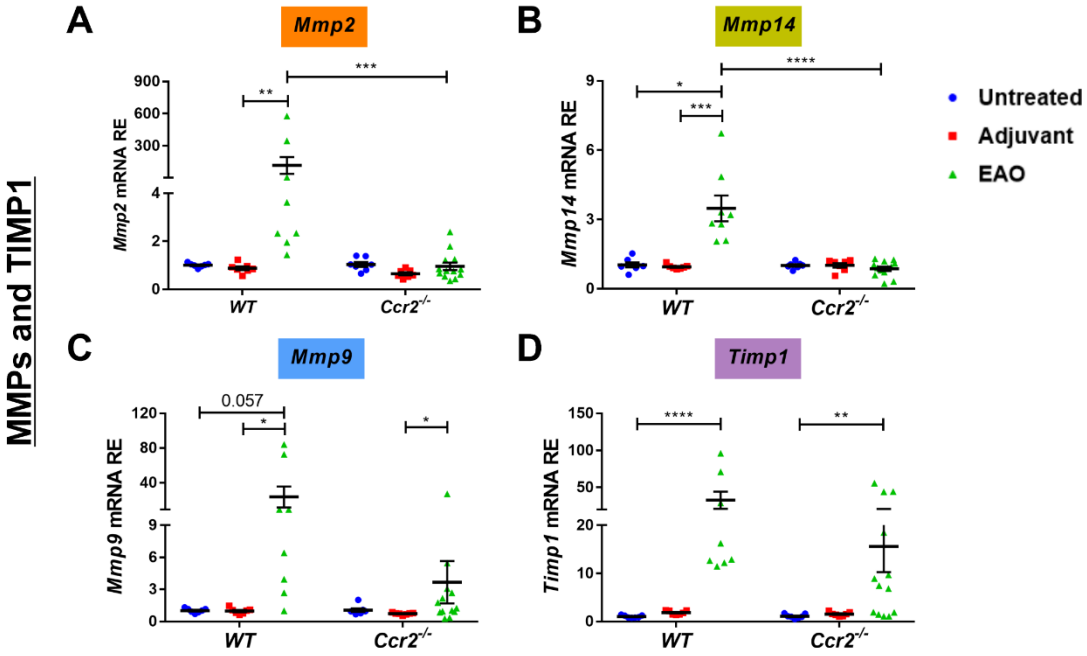

Figure 29. *Ccr2* deficiency inhibits the elevated mRNA expression of MMPs and TIMP1 caused by EAO. Total RNA was isolated from untreated, adjuvant control and EAO testes from *WT* and *Ccr2*$^{-/-}$ mice. The relative expression (RE) of *Mmp2* **(A)**, *Mmp14* **(B)**, *Mmp9* **(C)** and *Timp1* **(D)** mRNA was analyzed by qRT-PCR and normalized to *18S rRNA* and *Hprt* (n = 7-13). Values are mean ± SEM; the Kruskal-Wallis test followed by Dunn's multiple comparison test was employed for statistical analysis; **P* < 0.05, ***P* < 0.01, ****P* < 0.001, *****P* < 0.0001.

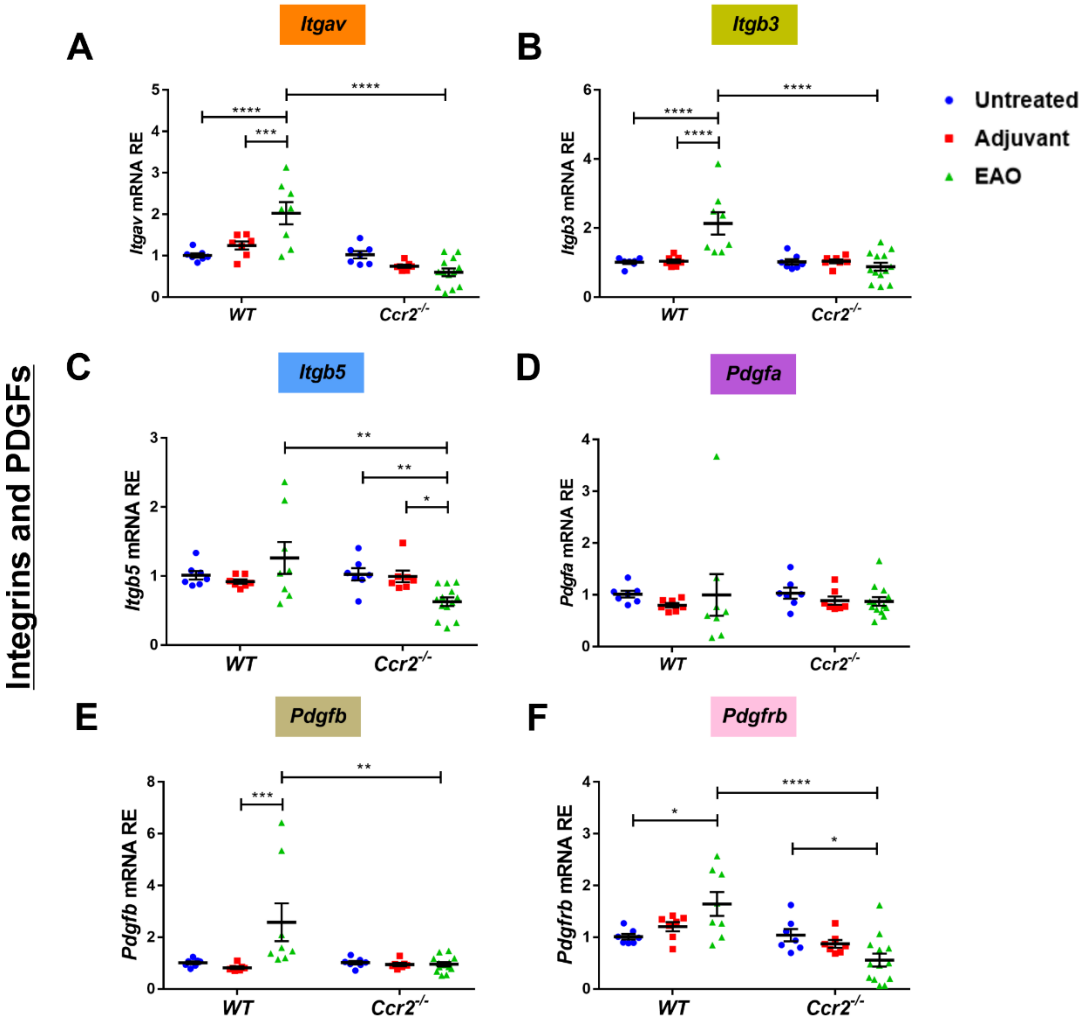

Figure 30. *Ccr2* deficiency inhibits the elevated mRNA expression of integrins and PDGFs caused by EAO. Total RNA was isolated from untreated, adjuvant control and EAO testes from *WT* and *Ccr2*$^{-/-}$ mice. The relative expression (RE) of *Itgav* **(A)**, *Itgb3* **(B)**, *Itgb5* **(C)**, *Pdgfa* **(D)**, *Pdgfb* **(E)** and *Pdgfrb* **(F)** mRNA was analyzed by qRT-PCR and normalized to *18S rRNA* and *Hprt* (n = 7-13). Values are mean ± SEM; the Kruskal-Wallis test followed by Dunn's multiple comparison test or two-way ANOVA test followed by Bonferroni's multiple comparison test was employed for statistical analysis; **P* < 0.05, ***P* < 0.01, ****P* < 0.001, *****P* < 0.0001.

Since some testes from *Ccr2*$^{-/-}$ EAO mice demonstrated higher *Mmp9* (1 of 13 mice) **(Fig. 29C)** and *Timp1* (3 of 13 mice) **(Fig. 29D)** mRNA expression, there were no significant statistical differences between *Ccr2*$^{-/-}$ and *WT* EAO testes, but the mRNA expression levels in *Ccr2*$^{-/-}$ EAO testes were still 6 - fold (*Mmp9* mRNA) and 2 - fold (*Timp1* mRNA) lower than those in *WT* EAO testes. *Itgb5* **(Fig. 30C)** and *Pdgfrb* **(Fig. 30F)** mRNA

expression were reduced in *Ccr2*$^{-/-}$ EAO testes as compared to not only *WT* EAO testes but also *Ccr2*$^{-/-}$ untreated testes. Moreover, the expression of *Pdgfa* mRNA was not changed in testes during EAO **(Fig. 30D)**.

Interestingly, the analysis of the *Adgre1* (gene coding for macrophage marker F4/80) mRNA expression in *WT* and *Ccr2*$^{-/-}$ EAO testes revealed significant positive correlation with the expression of *Mmp2*, *Mmp14*, *Mmp9*, *Timp1*, *Itgav* and *Pdgfrb* mRNA **(Fig. 31 and 32)**. In contrast, no significant correlation for *Itgb3*, *Itgb5*, *Pdgfa* and *Pdgfb* with *Adgre1* mRNA expression was observed **(Fig. 32)**.

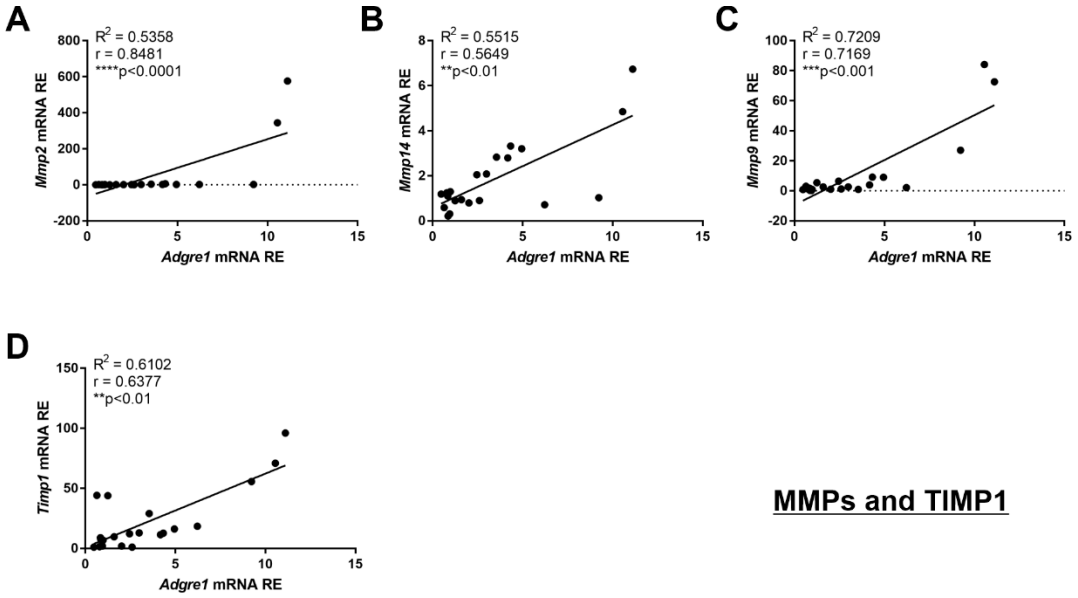

Figure 31. The expression of *Adgre1* mRNA positively correlates with mRNA expression of MMPs and TIMP1 in EAO testes. Total RNA was isolated from untreated, adjuvant control and EAO testes from *WT* and *Ccr2*$^{-/-}$ mice. The relative expression of *Adgre1* mRNA was analyzed by qRT-PCR and normalized to *18S rRNA* and *Hprt* (n = 7 - 13). The correlation between *Adgre1* mRNA and other transcripts of interest, including *Mmp2* **(A)**, *Mmp14* **(B)**, *Mmp9* **(C)** and *Timp1* **(D)**, was analyzed in *WT* and *Ccr2*$^{-/-}$ EAO testes. The correlation significance between two groups was analyzed by using Spearman coefficient; ***P* < 0.01, ****P* < 0.001, *****P* < 0.0001.

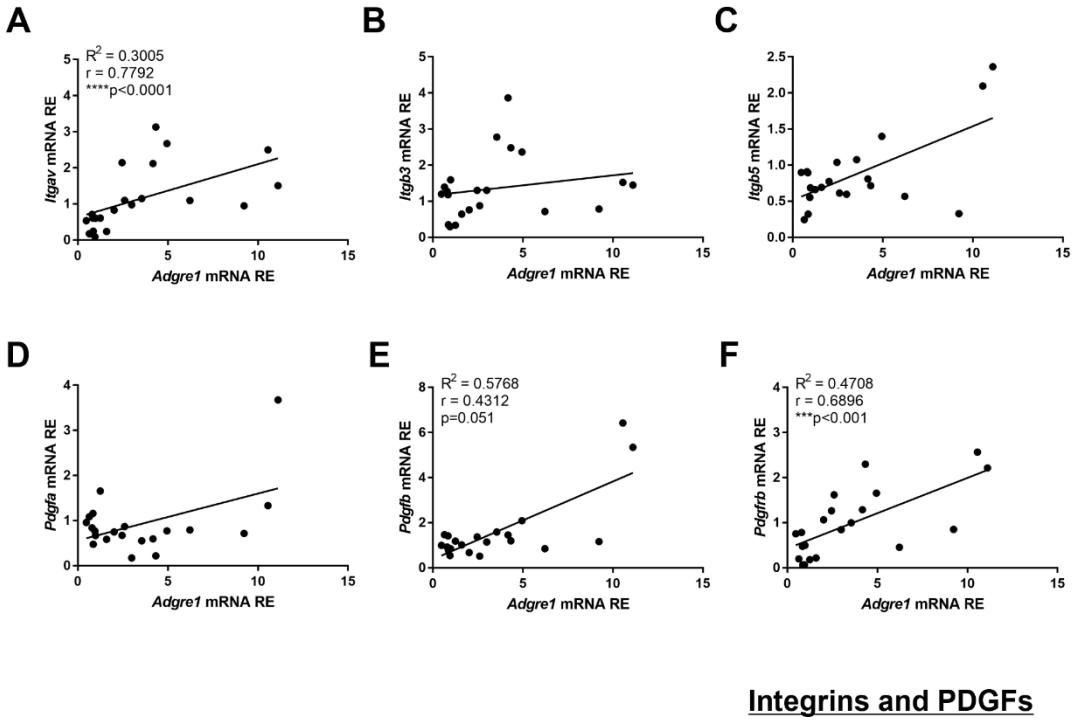

Figure 32. The expression of *Adgre1* mRNA positively correlates with mRNA expression of integrins and PDGFRβ in EAO testes. Total RNA was isolated from untreated, adjuvant control and EAO testes from *WT* and *Ccr2*$^{-/-}$ mice. The relative expression of *Adgre1* mRNA was analyzed by qRT-PCR and normalized to *18S rRNA* and *Hprt* (n = 7 - 13). The correlation between *Adgre1* mRNA and other transcripts of interest, including *Itgav* **(A)**, *Itgb3* **(B)**, *Itgb5* **(C)**, *Pdgfa* **(D)**, *Pdgfb* **(E)** and *Pdgfrb* **(F)**, was analyzed in *WT* and *Ccr2*$^{-/-}$ EAO testes. The correlation significance between two groups was analyzed by using Spearman coefficient; ***$P < 0.001$, ****$P < 0.0001$.

3.13. Activin A-stimulated BMDMs induce migration of NIH 3T3 fibroblasts

Our previous study demonstrated that activin A stimulated production of ECM proteins in NIH 3T3 fibroblasts *in vitro* (Kauerhof et al., 2019). Since activin A also induced expression of fibronectin, CXCR4, several MMPs, integrins and PDGFs in BMDMs **(Fig. 23 - 27)**, these data suggest that activin A-stimulated BMDMs could regulate the function of NIH 3T3 fibroblasts. In wound healing assays, conditioned medium (CM) from BMDMs treated with activin A or activin A alone induced the migration of NIH 3T3 fibroblasts and this effect was inhibited by FST288 **(Fig. 33A - C)**.

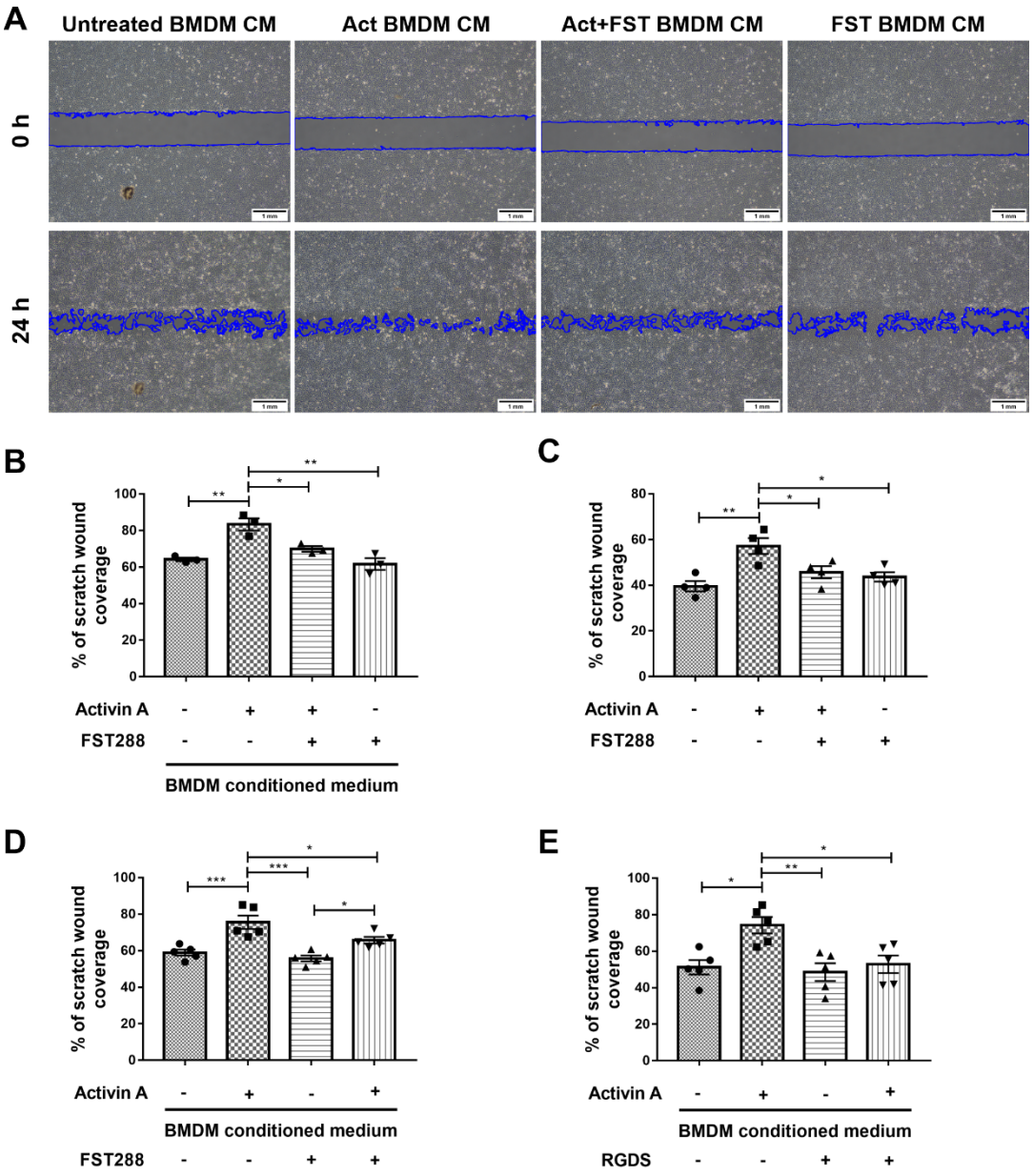

Figure 33. Conditioned medium from activin A-treated BMDMs promotes the migration of NIH 3T3 fibroblasts. Representative photomicrographs of wound scratch assay in NIH 3T3 fibroblasts cultivated in the presence of conditioned medium from untreated BMDMs (untreated BMDM CM) and BMDMs treated with 50 ng/ml activin A (Act BMDM CM), 250 ng/ml FST288 (FST BMDM CM) or a combination of both (Act+FST BMDM CM) for 24 h **(A)**. Three independent replicates were performed and the size of wound scratch coverage was measured by ImageJ (n = 3) **(B)**. The quantification of wound coverage percentage after 24 h incubation with 50 ng/ml activin A, 250 ng/ml FST288 or a combination of both in NIH 3T3 fibroblasts (n = 4) **(C)**. Before wound scratch, BMDM CM was pre-incubated with 250 ng/ml FST288 for 1 h (n = 5) **(D)** or NIH 3T3 fibroblasts were pre-incubated with 100 µg/ml RGDS for 4 h (n = 5) **(E)**, followed by the incubation with CM from untreated and 50 ng/ml activin A-treated BMDMs. The size of wound scratch coverage was measured by ImageJ after 24 h. Values are mean ± SEM; one-way ANOVA

test followed by Bonferroni's multiple comparison test was employed for statistical analysis; *$P < 0.05$, **$P < 0.01$, ***$P < 0.001$.

Furthermore, blockade of activin A by exogenous FST288 in activin A-stimulated BMDM CM led to suppression of NIH 3T3 fibroblast migration compared to BMDM CM from activin A-treated BMDMs **(Fig. 33D)**. Notably, in the presence of FST288, CM from activin A-stimulated BMDMs still induced, although at a lower level, the migration of NIH 3T3 as compared to the CM from untreated BMDMs, suggesting that other factors, in addition to activin A, could be involved in NIH 3T3 fibroblast migration **(Fig. 33D)**. Since activin A induced fibronectin expression in BMDMs and fibronectin is also known as a migration-stimulating factor, which requires binding to integrins (Clark et al., 2003), we tested whether inhibition of fibronectin could influence fibroblast migration. The results from wound healing assay showed that the fibronectin/ integrin binding inhibitor RGDS inhibited the migration of NIH 3T3 fibroblasts upon the treatment with CM from activin A-stimulated BMDMs **(Fig. 33E)**. All these observations together indicate that activin A alone and fibronectin derived from activin A-stimulated BMDMs have the ability to induce fibroblast migration.

3.14. Activin A induces proliferation of NIH 3T3 fibroblasts

In addition to migration, proliferation is another important property of fibroblasts during the fibrogenesis (Kendall and Feghali-Bostwick, 2014). CFSE, a cell division tracker, is widely used to monitor cell proliferation (Bocharov et al., 2013). In order to evaluate a direct effect of exogenous activin A or CM from activin A-stimulated BMDMs on the proliferation of NIH 3T3 fibroblasts, the CFSE fluorescence was measured by flow cytometry **(Fig. 34A)**. In contrast to the wound healing assay, activin A-stimulated BMDM CM did not affect the proliferation of NIH 3T3 fibroblasts **(Fig. 34B - C)**. Neither FST288-treated BMDM CM nor the inhibition of activin A in BMDM CM by addition of exogenous FST288 influenced the proliferation of NIH 3T3 fibroblasts **(Fig. 34B - C)**. However, exogenous activin A alone promoted this process (**Fig. 34D - E**). Inhibition of activin A action by FST288 reduced the

proliferation of NIH 3T3 fibroblasts, but not to the same level as in untreated and FST288-treated NIH 3T3 fibroblasts (**Fig. 34D - E**).

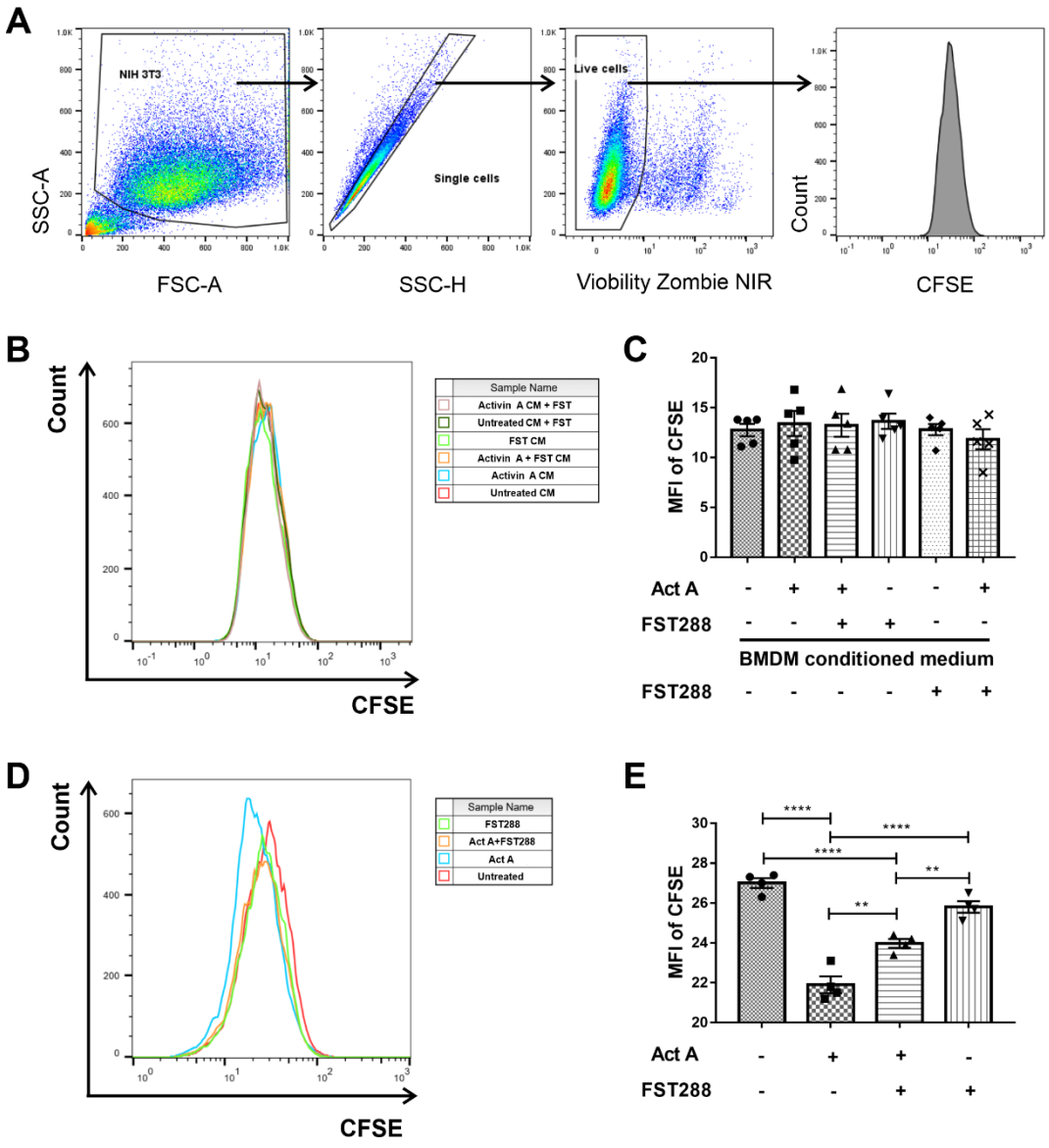

Figure 34. Activin A promotes the proliferation of NIH 3T3 fibroblasts. Starved NIH 3T3 fibroblasts were labelled with CFSE and incubated with BMDM CM (n = 5) **(B, C)** or 50 ng/ml activin A, 250 ng/ml FST288 or a combination of both (n = 4) **(D, E)** for 2 days. After gating out debris, doublets and dead cells **(A)**, the MFI of CFSE was analyzed by flow cytometry in CFSE-labelled NIH 3T3 fibroblast suspension **(B-E)**. Values are mean ± SEM; one-way ANOVA test followed by Bonferroni's multiple comparison test was employed for statistical analysis; $^{**}P < 0.01$, $^{****}P < 0.0001$.

4. DISCUSSION

Overall, this study revealed that CCR2 and activin A are important players involved in the progression of fibrosis in testicular inflammation. Furthermore, our findings underline a pro-fibrotic role of monocyte-derived macrophages in the development of testicular fibrosis. EAO is a well-established mouse model of autoimmune-based male infertility, where strong testicular deposition of ECM proteins including collagens and fibronectin is obvious, in addition to increased number of TMs and higher expression levels of inflammatory mediators such as TNF, CCL2 and activin A. All these pathological alterations lead to tissue destruction, inhibition of spermatogenesis and subsequent infertility (Nicolas et al., 2017a, 2017b; Fijak et al., 2018; Kauerhof et al., 2019).

4.1. *Ccr2* deficiency attenuates the development of fibrosis during testicular inflammation

CCR2 is a receptor for CCL2, a chemokine that mediates the chemotaxis of myeloid cells as well as adhesion or polarization of monocytes or macrophages in inflammatory diseases (Gschwandtner et al., 2019). After induction of testicular inflammation, loss of *Ccr2* not only preserved the testicular tissue from deposition of collagens or fibronectin, but also protected the testis from damage due to the reduced accumulation of macrophages. In spite of a few disrupted seminiferous tubules visible in some EAO testes from *Ccr2*$^{-/-}$ mice, the testicular structure was largely intact, indicating a crucial role for CCR2 in inflammation and damage following EAO.

This is in accordance with other reports demonstrating reduced inflammatory and fibrotic response in certain organs in the absence of CCR2 signaling. For instance, *Ccr2* ablation improves bleomycin-induced pulmonary fibrosis through inhibition of macrophage infiltration (Okuma et al., 2004). Genetic deletion of *Ccr2* inhibits total collagen deposition and results in the reduction of inflammatory cytokine expression and macrophage infiltration in renal fibrosis (Xia et al., 2013; Braga et al., 2018). Mice lacking *Ccr2* show attenuated monocyte/ macrophage accumulation in osteoarthritis and decreased collagen I production in colon fibrosis (Raghu et al., 2017; Kuroda et al., 2019).

Fibrotic remodeling is frequently observed in human infertile testes, especially in patients with non-obstructive azoospermia (Mayerhofer, 2013). Since the mechanisms leading to fibrotic responses and the production site of ECM proteins during the progression of testicular inflammation are unknown, we wanted to tackle this question. ECM-producing cells may originate from resident mesenchymal cells including resident fibroblasts or pericytes, epithelial or endothelial cells (due to epithelial/ endothelial-mesenchymal transition) or a population of bone marrow-derived circulating cells known as fibrocytes (Hinz et al., 2007; Mack and Yanagita, 2015). Fibrocytes are characterized by the co-expression of hematopoietic markers such as CD45, CD34 and CD11b, and mesenchymal markers such as collagen or vimentin (Reilkoff et al., 2011). These cells migrate to the injured sites mainly through activation of specific chemokine ligand/ receptor pathways, for instance the CCL2/ CCR2 or CXCL12/ CXCR4 axis (Reilkoff et al., 2011; Mack, 2018). Fibrocytes can also originate from a subpopulation of monocytes via monocyte-to-fibroblast transition (Niedermeier et al., 2009; Yang et al., 2013; Dong et al., 2016). Our results indicate that during the severe stage of EAO, immune cells, particularly macrophages are an important source of fibronectin and collagen I production as shown by flow cytometry and *in situ* by immunofluorescence. Since CCR2 participates also in the recruitment of fibrocytes, we demonstrated that inflamed *Ccr2*$^{-/-}$ testes accumulated significantly less CD45^{+} cells and TMs expressing fibronectin, collagen I and CXCR4 compared to *WT* EAO testes, highlighting the importance of CCR2 and CXCR4 signaling in testicular ECM expression. Considering that the CD34 marker was not included in our analysis, we cannot definitely exclude that a proportion of ECM-expressing CD45^{+} cells also belong to this population of fibrocytes.

These data are in agreement with published reports demonstrating CCR2 dependent inhibition of BMDM and fibrocyte infiltration in kidney injury, colonic or pulmonary fibrosis (Xia et al., 2013; Gurczynski et al., 2016; Do et al., 2019; Kuroda et al., 2019). *Ccr2* deficient mice show ameliorated glomerular injury and interstitial fibrosis during focal segmental glomerulosclerosis through decreased F4/80^{+} macrophage and CD45^{+}CD11b^{+}collagen-I^{+} fibrocyte infiltration (Wilkening et al., 2020). Moreover, pharmaceutical blockade of CCL2/ CCR2 pathway inhibits the infiltration of blood

peripheral CCR2$^+$ monocytes and reduces the accumulation of CD45$^+$collagen-I$^+$ fibrocytes in the inflamed colon (Hachiya et al., 2021).

Another important chemokine receptor involved in the trafficking of monocytes and fibrocytes to the site of injury is CXCR4. Many studies demonstrate that CXCR4 contributes to tissue fibrosis via binding to its ligand CXCL12. The expression of CXCR4 and the number of activated CXCR4$^+$CXCL12$^+$ cells are both elevated in the lung fibrotic tissues (Jaffar et al., 2020). CXCL12 stimulates αSMA expression and the formation of actin stress fibers in the lung fibroblasts via CXCR4 signaling (Lin et al., 2014). In addition, inhibition of CXCR4 by AMD3100 antagonist *in vitro* reduces the production of collagen I and connective tissue growth factor as well as the migratory ability of circulating fibrocytes after the stimulation with high concentration of glucose (Weng et al., 2019). Neutralization of CXCR4 signaling not only inhibits wound healing and collagen I secretion by fibroblasts, but also reduces the accumulation of CD45$^+$collagen-I$^+$CXCR4$^+$ fibrocytes during idiopathic pulmonary fibrosis (Griffiths et al., 2018). Other studies have reported that CXCR4$^+$ macrophages are the pro-fibrotic cell subpopulation, inducing fibrotic changes in other organs, e.g. kidney and lung (Yuan et al., 2015; Dupin et al., 2016; Chen et al., 2021). Similarly, results presented here demonstrate high levels of *Cxcl12* and *Cxcr4* mRNA and the persistence of CD45$^+$fibronectin$^+$CXCR4$^+$ cells in the *WT* EAO testes, which are significantly reduced in *Ccr2*$^{-/-}$ EAO testes.

MMPs as matrix-degrading enzymes play either pro-fibrotic or anti-fibrotic functions, augmenting or attenuating fibrosis (Giannandrea and Parks, 2014). MMP2 and MMP9 are gelatinases, which mainly cleave collagen IV, an important component of basement membrane, making it easier for leukocytes to transmigrate (Khokha et al., 2013; Kurzepa et al., 2014). The activation of MMP2 requires the involvement of MMP14, while TIMP1 inhibits the activity of MMPs showing high affinity for MMP9 (Yosef et al., 2018; Knight et al., 2019). Our results demonstrated that in *WT* EAO testes the mRNA expression of *Mmp2*, *Mmp14*, *Mmp9* and *Timp1* was increased pointing to the activation of ECM machinery. The aggregation of ECM proteins requires action of MMPs for degradation to prevent fibrosis. On the other hand, the increase of TIMP1 inhibits the degrading function of MMP proteins, thus exacerbating the fibrotic process. However, the elevated levels of

MMPs could also contribute to the immune cell migration, or activate PTCs or fibroblasts to produce more ECM proteins, thereby promoting the tissue fibrosis (Kobayashi et al., 2014; Song et al., 2015). It seems that the process of testicular fibrosis depends on the dynamic balance between MMPs (MMP2, MMP9, and MMP14) and TIMP1 activities. In *Ccr2*$^{-/-}$ EAO testes the elevated mRNA expression of *Mmp2* and *Mmp14* was abolished as compared to *WT* control testes. The expression of *Mmp9* and *Timp1* mRNA was lower in mice lacking CCR2 compared to *WT* mice during EAO although not statistically significant, showing similar expression levels as in the controls. Interestingly, the expression of these genes (*Mmp2*, *Mmp9*, *Mmp14*, *Timp1*) positively correlated with *Adgre1* mRNA, indicating the involvement of macrophages in their production thereby in promotion of testicular fibrosis during inflammatory response.

Integrins and PDGFs are two other important families of molecules involved in the promotion of tissue fibrosis (Margadant and Sonnenberg, 2010; Camelo et al., 2014; Klinkhammer et al., 2018; Schnittert et al., 2018). Among them, the αv-containing integrins facilitate fibrosis by activating myofibroblasts or TGF-β signaling in several organs, such as liver, lung and kidney (Henderson et al., 2013). PDGFRβ is mainly expressed on mesenchymal cells, such as fibroblasts or myofibroblasts, which are executors of fibrosis (Klinkhammer et al., 2018). The PDGF/ PDGFRβ axis is also expressed by testicular cells including PTCs or interstitial immune cells under physiological conditions (Basciani et al., 2002, 2010; Mariani et al., 2002). The mRNA expression of *Itgav*/ *Itgb3* (encoding αvβ3 integrin) and *Pdgfb/ Pdgfrb* was increased during EAO, possibly due to the infiltration of macrophages as *Ccr2*$^{-/-}$ mice showed decreased expression of *Itgav*, *Itgb3*, *Pdgfb* and *Pdgfrb* in EAO testes, and *Itgav* as well as *Pdgfrb* displayed positive correlation with *Adgre1* mRNA expression in inflamed testes. Furthermore, PDGF acts directly as a strong chemoattractant for fibrocytes in pulmonary fibrosis and pharmacological blockade of PDGF/ PDGFR axis is a promising treatment option (Aono et al., 2014).

Taken together, these *in vivo* data indicate that CCR2 is involved in the development of testicular fibrosis during inflammation. CCR2 mediates the infiltration of macrophages, production of ECM proteins by TMs and elevated expression of several molecules in EAO.

These molecules are associated with fibrotic remodeling, including CXCL12/ CXCR4 axis, MMPs, TIMP1, integrin αv subunit, PDGF-B and PDGFRβ.

4.2. Activin A promotes a pro-fibrotic phenotype of macrophages

In addition to CCR2, activin A is another important fibrotic regulator, which stimulates the expression of fibrosis-specific genes in mouse PTCs and NIH 3T3 fibroblasts (de Kretser et al., 2012; Kauerhof et al., 2019; Lustig et al., 2020). In the current study, activin A stimulated *Ccr2* expression in macrophages, while reducing *Ccl2* levels. Similar activin A effects on opposite expression levels of CCR2 and CCL2 were shown in human monocyte-derived macrophages (Sierra-Filardi et al., 2014). This indicates that activin A is increasing the responsiveness of inflammatory BMDMs to CCL2 by enhancing the expression of CCR2. Previously, we showed that the expression of activin βA subunit was increased not only in mouse inflamed testes, but also in human testes with impaired spermatogenesis and focal leukocytic infiltrates (Nicolas et al., 2017a; Kauerhof et al., 2019). Of note, the severity of induced inflammation and damage was directly proportional to the levels of activin A (Nicolas et al., 2017a; Kauerhof et al., 2019). These findings, together with reduced infiltration of macrophages and lower levels of ECM deposition during EAO caused by *Ccr2* deficiency, implement activin A as one of the important regulators of testicular inflammation and fibrosis through TMs. Therefore, it was hypothesized that activin A could regulate testicular inflammation and fibrosis via TMs.

Polarization of macrophages during injury by a variety of chemokines or cytokines, such as CCL2, TGF-β1, IL-4, IL-6 or IL-13, could lead to differentiation into a pro-fibrotic phenotype (Wynn and Vannella, 2016; Ayaub et al., 2017; Ruytinx et al., 2018). Similarly, activin A also induced pro-fibrotic properties of macrophages in our studies. During stimulation with activin A, BMDMs gradually lost their irregular morphology, and transformed into spindle-shaped cells similar to fibroblasts. Moreover, the expression of F4/80 (marker of macrophages) was diminished. In addition, activin A affected the transcriptome of BMDMs *in vitro*, inducing alterations in the expression of cytokines/ chemokines and ECM-related genes. Activin A increased the mRNA expression of *Fn1*, *Cxcr4*, *Mmp2*, *Mmp14*, *Itgav*, *Pdgfa*, *Pdgfb* and *Pdgfrb*, while it

decreased *Mmp9* and *Timp1* mRNA expression in BMDMs. Similarly, it was demonstrated that activin A reprograms pre-tumorigenic macrophages to a phenotype that resembles tumor-associated macrophages, promotes the conversion of $CD4^+CD25^-$ naïve T cell into regulatory T cells, and induces a pro-fibrotic transcriptome in fibroblasts thereby transforming them into myofibroblasts (Antsiferova et al., 2017; Cangkrama et al., 2020; Wietecha et al., 2020). Furthermore, macrophages from the synovia of patients with active rheumatoid arthritis exhibit an activin A-dependent pro-inflammatory profile, since activin A-neutralizing antibodies inhibited pro-inflammatory macrophage-polarizing ability of the synovial fluid (Palacios et al., 2015).

Numerous cytokines and chemokines are able to influence the expression of MMPs and their activity in macrophages (Ogawa et al., 2000). The enzymatic activity of MMP2 in BMDMs was enhanced after stimulation with activin A, while the MMP9 enzymatic activity was reduced. Generally, in contrast to MMP2, BMDMs mainly produce MMP9 at the basal level and have a stronger enzymatic activity based on the qRT-PCR and gelatin-zymography results. When BMDMs gradually lose their normal phenotype upon activin A stimulation, they may not be able to produce MMP9 as much as they normally do under physiological condition. Therefore, the expression and enzymatic activity of MMP2 and MMP9 are regulated differently in BMDMs upon activin A stimulation.

In addition to MMPs, activin A also increased *Itgav* (encoding integrin αv subunit) and *Pdgfb/ Pdgfrb* mRNA expression in BMDMs *in vitro*, which gives a hint that elevated levels of activin A in EAO testes could induce the production of integrin αv subunit, PDGF-B and PDGFRβ by TMs. This may be one of the reasons for the positive correlation of *Adgre1* with *Itgav* and *Pdgfrb* in EAO testes.

A previous study showed that TNF stimulates the synthesis of activin A by SCs (Kauerhof et al., 2019). Therefore, conditioned medium from TNF-treated SCs was used to analyze the effects of testis-derived activin A on the expression of fibrosis-related genes in BMDMs. Obtained results indicated that SC-derived activin A similar to the recombinant protein induced the expression of *Fn1* mRNA in BMDMs. Inhibition of activin A activity in conditioned medium from SCs by the addition of FST288 suppressed *Cxcr4* mRNA expression in BMDMs. However, addition of FST288 did not affect the expression of

Mmp2, *Mmp14*, *Mmp9* and *Timp1* mRNA upon stimulation with TNF-treated SCCM in BMDMs. This could be also explained by strong ability of TNF to induce MMPs or TIMP1 expression in macrophages (Amoah et al., 2015; Zhang et al., 2017a). All these results emphasize that increased levels of TNF during testicular inflammation stimulate SCs to synthesize and secrete activin A, which in turn can promote the production of fibronectin and CXCR4 in macrophages.

Combining these results, we claim that activin A promotes the progression of testicular fibrosis by inducing the expression of MMP2, MMP14, the integrin αv subunit, and genes of the PDGF-B/ PDGFRβ axis in TMs. Although activin A reduced the expression of *Itgb3* mRNA in BMDMs, other cells like fibroblasts can produce large amounts of β3 integrin in response to inflammatory stimuli (Balasubramanian et al., 2012), which could be the reason of the high level of αvβ3 integrin in EAO testes. From another point of view, fibroblasts and PTCs remain two other important sources of MMPs and TIMP1 in the testes (Yang et al., 2009; Szarek et al., 2019). Since activin A increases the production of fibrosis-related proteins, including MMP2 and fibronectin in L929 fibroblasts (Jiang et al., 2020a), it may also regulate the fibrotic responses through mediating MMPs, TIMP1 or αv-containing integrin expression in testicular resident fibroblast or PTCs.

The flow cytometric analysis revealed that cultured bone marrow cells in the presence of M-CSF contained a small proportion of $Ly6C^+$ monocytes. Several studies have also shown that monocytes contribute to the pathogenesis of tissue fibrosis during inflammation, and therapeutic inhibition of monocytes limits the development of fibrotic responses (Krenkel et al., 2018; Haub et al., 2019; Fraser et al., 2021). Monocyte-derived macrophages produce multiple growth factors and cytokines associated with the progression of fibrosis (Krenkel et al., 2018). The recruitment of inflammatory $Ly6C^+$ or $CCR2^+$ monocytes promotes fibrosis development, and inhibition of CCL2/ CCR2 signaling can protect the organs from fibrotic remodeling (Krenkel et al., 2018; Haub et al., 2019). Moreover, $CD64^{hi}$ monocytes in fibrotic tissue reveal the high expression of CCL2 and type I IFN, which in turn could drive chronic inflammation and fibrosis (Fraser et al., 2021).

Follistatin, applied here as an inhibitor of activin A, antagonizes its action *in vivo* and *in vitro*. *In vivo* blockade of activin A by overexpression of follistatin clearly demonstrated that apart from the CCL2/ CCR2 axis, activin A also contributes to the infiltration of collagen-I$^+$ TMs in the inflamed testes. This provides an additional evidence that activin A promoted the production of ECM components by macrophages and its inhibition is effective in reducing macrophage infiltration and fibrosis progression during EAO. However, overexpression of follistatin cannot fully prevent the development of EAO, although the severity of the disease was strongly reduced (Nicolas et al., 2017b).

Taken together, all these *in vitro* and *in vivo* results illustrate that activin A promotes the differentiation of macrophages into a pro-fibrotic phenotype through mediating the induction of fibronectin, collagen I, CXCR4, MMP2, MMP14, αvβ5 integrin, PDGF-A, PDGF-B and PDGFRβ expression, and this could serve as potential precursors of fibrocytes/ fibroblasts to facilitate tissue fibrosis.

4.3. Activin A induces the migration and proliferation of NIH 3T3 fibroblasts

Fibronectin, MMP2, MMP14, integrin αv subunit, PDGF-A and PDGF-B have been reported to induce the migration of fibroblasts (Li et al., 2004; Briggs, 2005; Schram et al., 2011; Missirlis et al., 2017). Since the expression of these factors was also induced in BMDMs by activin A, the migratory activity of fibroblasts in the presence of conditioned medium from BMDMs was analyzed. NIH 3T3 fibroblasts were used as a surrogate of testicular fibroblasts (Kauerhof et al., 2019). Wound healing assays showed that conditioned medium from activin A-stimulated BMDMs promoted fibroblast migration. In addition to multiple factors produced by activin A-treated BMDMs, the conditioned medium also contained activin A, which is also able to induce fibroblast migration (Jiang et al., 2020a). Considering this fact, we antagonized the action of activin A in conditioned medium from activin A-treated BMDMs by using FST288, our results revealed that activin A in conditioned medium from BMDMs had the ability to promote the migration of fibroblasts. Notably, under the condition of activin A inhibition by FST288, conditioned medium from activin A-treated BMDMs still promoted the migration of fibroblasts, which indicates that other factors in addition to activin A could induce this action.

Fibronectin, produced by BMDMs, could be another important regulator of fibroblast migration. RGDS peptide is an inhibitor of fibronectin-integrin interaction, which competes with fibronectin and binds to integrins, thus suppressing the attachment of cells to fibronectin (García-Gareta et al., 2019). RGDS inhibited the migration of NIH 3T3 fibroblasts during the incubation with conditioned medium from activin A-treated BMDMs. This reveals that an activin A-caused increase of fibronectin in BMDMs induces also NIH 3T3 cell migration, and thus possible migration of fibroblasts to the sites of injury.

Furthermore, activin A has been found to activate the proliferation of fibroblasts from lung, kidney or skin (Ohga et al., 1996; Yamashita et al., 2004; Wietecha et al., 2020). Our data confirmed that recombinant activin A promoted NIH 3T3 fibroblast proliferation *in vitro*. However, no alteration in the proliferative ability of NIH 3T3 fibroblasts was detected upon the incubation with the conditioned medium from BMDMs stimulated with activin A. This could be explained by the fact that both supernatants from untreated and activin A-treated BMDMs contain high levels of several factors that can induce the proliferation of fibroblasts, including fibronectin, MMP2, MMP9, TIMP1 or PDGF-B (Lu et al., 2011; Bates et al., 2015; Lee et al., 2016; Zhang et al., 2017b; Zhou et al., 2018). Therefore, inhibition of activin A alone is not sufficient to block the proliferation of NIH 3T3 fibroblasts.

4.4. Limitations of the study

Our approach does not fully allow to directly determine the local testicular environmental impact on macrophages and fibroblasts. Due to the limited number of TMs and testicular fibroblasts in normal mouse testis, *in vitro* experimentation would require an unreasonably high number of animals to isolate primary cells. Therefore, in accordance with 3R principles, TMs and testicular fibroblasts were replaced by BMDMs and NIH 3T3 fibroblasts, respectively, thus drastically reducing the number of experiments and animals required.

In addition, although our data indicate that CCR2, activin A and macrophages are responsible for the testicular fibrotic response, the precise immunological mechanism that regulates this process requires further investigation. Future studies are needed to address

the detail of a direct influence of activin A using targeted depletion of activin A receptors on monocytes/ macrophages to analyze their role in the inflammatory response and in fibrotic remodeling.

4.5. Hypothetical model of the role of the activin A - CCR2 - macrophage axis in the fibrotic response during testicular inflammation

Taken together, our findings suggest that CCR2 and activin A are required for the development of fibrosis through regulating macrophages during testicular inflammation (summarized in **Fig. 35**). Newly arriving monocytes/ macrophages expressing CCR2 infiltrate the inflamed testis in response to high concentration of CCL2 and produce TNF. TNF, in turn, stimulates SCs to release higher levels of activin A, which induces expression of CCR2 on bone marrow progenitor cells/ monocytes/ macrophages and drives macrophages to a pro-fibrotic phenotype through producing fibronectin, collagen I, CXCR4, MMPs, integrins and PDGFs, thereby promoting migration and proliferation of fibroblasts. Depletion of CCR2 as well as reduction in activin A levels by the overexpression of follistatin lead to a decrease in inflammation and fibrotic responses.

In conclusion, our data indicate that CCR2 and activin A regulate the development of fibrosis during testicular inflammation and underline a crucial pro-fibrotic function for the macrophages in inflammation-associated fibrotic remodeling in EAO. Future therapeutic targeting of CCR2 and/ or activin A may offer possible treatment strategy to address testicular fibrosis.

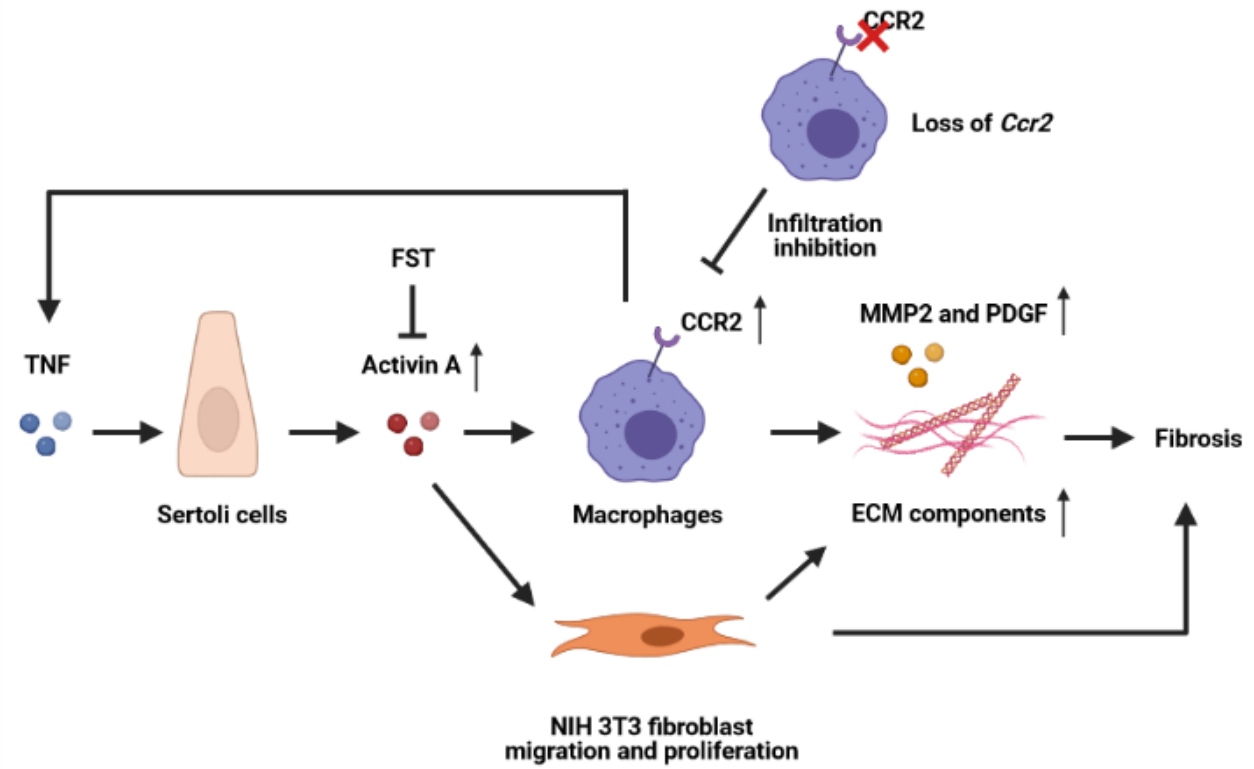

Figure 35. Simplified scheme summarizing the main findings in this study. Macrophages expressing CCR2 infiltrate the inflamed testes in response to high levels of CCL2 and produce TNF. TNF induces SCs to release higher levels of activin A, which drives macrophages to a pro-fibrotic phenotype through producing fibronectin, collagen I, CXCR4, MMPs, integrins and PDGFs, besides promoting migration and proliferation of fibroblasts. All processes together facilitate the development of fibrosis in EAO testes. The bioactivity of activin A is antagonized by FST.

5. SUMMARY

Approximately 8-12% of couples worldwide suffer from infertility, with men accounting for ~ 50% of cases. Multiple factors contribute to male infertility and testicular inflammation caused by bacteria, viruses or autoimmune diseases is a common contributor.

Experimental autoimmune orchitis (EAO) is a rodent model of chronic testicular inflammation, replicating observations seen in some forms of spermatogenic disturbances in men. During EAO levels of pro-inflammatory and pro-fibrotic mediators such as TNF, CCL2 (ligand for CCR2) and activin A are increased with a concomitant infiltration of leukocytes into the testicular parenchyma. Testicular fibrosis is a hallmark of progressive and severe EAO stages, accompanied by the accumulation of extracellular matrix (ECM) proteins.

Activin A correlates with the severity of EAO by promoting expression of fibrosis specific genes in peritubular cells and NIH 3T3 fibroblasts. Testicular macrophages (TMs) constitute a major immune cell population in the testis and these cells play a critical role in organ homeostasis. Generally, CCL2 and CCR2 mediate the trafficking of leukocytes and recruited macrophages express ECM components as well as CXCR4 in inflamed lesions.

Therefore, the involvement of macrophages, activin A and CCR2 in the development of testicular fibrosis during EAO was investigated. The disease was induced by active immunization with testicular homogenate in *wild type* (*WT*) and *Ccr2*$^{-/-}$ mice. Overall, *Ccr2* depletion led to the reduction of organ damage, collagen deposition and leukocyte infiltration with fibronectin^{+}, collagen-I^{+} or CXCR4^{+} TMs in EAO testes. Bone marrow-derived macrophages (BMDMs) were used as a surrogate for TMs to analyze the influence of activin A. BMDMs cultured in the presence of activin A expressed several pro-fibrotic mediators, including fibronectin, CXCR4, MMP2, MMP14, integrin αv subunit, PDGF-A, PDGF-B and PDGFRβ that were also found to be regulated in EAO testes. Follistatin, a potent activin A antagonist, inhibited these effects in activin A-stimulated BMDMs and suppressed collagen I production by TMs in EAO testes. Moreover, activin A induced the migration and proliferation of NIH 3T3 fibroblasts as shown in wound healing and proliferation assays.

Taken together, these data indicate that CCR2 and activin A are required for the development of fibrosis during testicular inflammation by regulating the function of macrophages. Inhibition of CCR2 or activin A protects the tissue from the progression of damage offering a promising tool for potential therapeutic intervention.

6. ZUSAMMENFASSUNG

Weltweit leiden ungefähr 8-12% der Paare an Unfruchtbarkeit, wobei männliche Faktoren etwa 50% der Fälle ausmachen. Mehrere Auslöser tragen zur männlichen Infertilität bei, wobei Hodenentzündungen, die durch Bakterien, Viren oder Autoimmunerkrankungen verursacht werden, zu den häufigsten Ursachen zählen.

Die experimentelle Autoimmun-Orchitis (EAO) ist ein Nagetiermodell chronische Hodenentzündungen, das bestimmte Formen idiopathische Spermatogenesestörungen bei Männern repliziert. Im Verlauf der EAO sind pro-inflammatorische und pro-fibrotische Mediatoren, wie TNF, CCL2 (Ligand für CCR2) und Aktivin A erhöht, bei gleichzeitiger Infiltration von Leukozyten in das Hodenparenchym. Eine testikuläre Fibrose ist ein Merkmal progressiver und schwerer EAO-Stadien, die durch die Akkumulation von extrazellulären Matrix Proteinen (ECM) charakterisiert sind.

Aktivin A korreliert mit dem Schweregrad der EAO, indem es die Expression Fibrose-spezifischer Gene in peritubulären Zellen und NIH 3T3-Fibroblasten fördert. Testikuläre Makrophagen (TMs) stellen eine wichtige Immunzellpopulation im Hoden dar und spielen eine entscheidende Rolle bei der Organhomöostase. CCL2 und CCR2 vermitteln die Migration von Leukozyten und rekrutieren Makrophagen zu den Entzündungsherden, wobei sie dann ECM-Komponenten sowie CXCR4 exprimieren, wodurch sie zur Fibrogenese in vielen Organen beitragen.

Daher wurde in dieser Arbeit die Beteiligung von Makrophagen, Aktivin A und CCR2 an der Entstehung der Hodenfibrose bei der Entwicklung einer EAO untersucht. Die EAO wurde durch aktive Immunisierung mit Hodenhomogenat in Wildtyp (WT) und *Ccr2*$^{-/-}$ Mäusen induziert. Die Depletion von *Ccr2* führte zu einer Verringerung der Organschäden, Kollagenablagerung und Leukozyteninfiltration, unter Einschluss von Fibronektin^{+}, Kollagen-I^{+} oder CXCR4^{+} TMs im EAO-Hoden. Aus dem Knochenmark stammende Makrophagen (BMDMs) wurden als Modell für TMs verwendet, um den Einfluss von Aktivin A zu analysieren. BMDMs, die in Gegenwart von Aktivin A kultiviert wurden, exprimierten pro-fibrotische Mediatoren, einschließlich Fibronektin, CXCR4, MMP2, MMP14, der Integrin-αv-Untereinheit, PDGF-A, PDGF-B und PDGFRβ, die auch im

EAO-Hoden fehlreguliert waren. Follistatin, ein potenter Aktivin-A-Antagonist, hemmte diese Wirkungen in Aktivin-A-stimulierten BMDMs und unterdrückte die Kollagen-I-Produktion durch TMs im EAO-Hoden. Darüber hinaus induzierte Aktivin A die Migration und Proliferation von NIH 3T3-Fibroblasten, wie in Wundheilungs- und Proliferationsassays demonstriert wurde.

Zusammengefasst weisen diese Daten darauf hin, dass CCR2 und Aktivin A für die Entwicklung der Fibrose während einer sterilen Hodenentzündung erforderlich sind, indem sie die Funktion von Makrophagen regulieren. Die Hemmung von CCR2 oder Aktivin A schützt das Gewebe vor dem Fortschreiten der Schädigung und bietet ein vielversprechendes Instrument für potenzielle therapeutische Interventionen.

7. ABBREVIATIONS

αSMA	Alpha smooth muscle actin
ActR	Activin-specific receptor
ANOVA	Analysis of variance
APS	Ammonium persulfate
BMDMs	Bone marrow-derived macrophages
BSA	Bovine serum albumin
BTB	Blood-testis barrier
CCL2	C-C motif chemokine ligand 2
CCR2	C-C motif chemokine receptor type 2
CD	Cluster of differentiation
cDNA	Complementary deoxyribonucleic acid
CFA	Complete Freund's adjuvant
CLSM	Confocal laser scanning microscope
CM	Conditioned medium
Ct	Cycle threshold
CSF1	Colony stimulating factor 1
CXCL12	C-X-C motif chemokine ligand 12
CXCR4	C-X-C motif chemokine receptor 4
DC	Dendritic cell
DEG	Differentially expressed genes
DMEM	Dulbecco's modified Eagle's medium
DNase	Deoxyribonuclease
dNTP	Deoxynucleoside triphosphate
DTT	Dithiothreitol
EAO	Experimental autoimmune orchitis
ECM	Extracellular matrix
EDTA	Ethylene diamine tetraacetic acid
ERK	Extracellular signal-regulated kinase

EV	Empty vector
FBS	Fetal bovine serum
FSH	Follicle-stimulating hormone
FST	Follistatin
HEPES	4-(2-hydroxyethyl)-1-piperazineethanesulfonic acid
HPRT	Hypoxanthine guanine phosphoribosyl transferase
IDO	Indoleamine 2,3-dioxygenase
IFN-γ	Interferon gamma
IGF	Insulin-like growth factor
IL	Interleukin
JNK	c-Jun N-terminal kinase
LC	Leydig cell
LH	Luteinizing hormone
LPS	Lipopolysaccharide
MACS	Magnetic-activated cell sorting
MAP	Mitogen-activated protein
MC	Mast cell
MCP-1	Monocyte chemoattractant protein-1
M-CSF	Macrophage-colony stimulating factor
MFI	Mean fluorescence intensity
MHCII	Major histocompatibility complex class II
MMP	Matrix metalloproteinase
mRNA	Messenger ribonucleic acid
NK	Natural killer
PBS	Phosphate buffered saline
PCR	Polymerase chain reaction
PDGF	Platelet-derived growth factor
PTC	Peritubular cell
qRT-PCR	Quantitative reverse transcription-PCR

RBC	Red blood cell
RE	Relative expression
RGDS	Tetrapeptide Arg-Gly-Asp-Ser
RPMI	Roswell park memorial institute
RT	Room temperature
SC	Sertoli cell
SCCM	Sertoli cell conditioned medium
SEM	Standard error of the mean
Smad	Suppressor of mothers against decapentaplegic
SOX9	SRY-box transcription factor 9
SRY	Sex-determining region Y
TAE	Tris-acetate-EDTA
TBST	Tris-buffered saline containing 0.1% Tween-20
TEMED	Tetramethylethylenediamine
TGF-β	Transforming growth factor beta
TH	Testicular homogenate
TNF	Tumor necrosis factor
TM	Testicular macrophage
TIMP	Tissue inhibitor of metalloproteinase
Treg	Regulatory T cell
WT	Wild type
w/v	Weight per volume

8. REFERENCES

Abe, R., Donnelly, S. C., Peng, T., Bucala, R., and Metz, C. N. (2001). Peripheral Blood Fibrocytes: Differentiation Pathway and Migration to Wound Sites. *J. Immunol.* 166, 7556–7562. doi:10.4049/jimmunol.166.12.7556.

Agarwal, A., Baskaran, S., Parekh, N., Cho, C. L., Henkel, R., Vij, S., et al. (2021). Male infertility. *Lancet* 397, 319–333. doi:10.1016/S0140-6736(20)32667-2.

Altrock, E., Sens, C., Wuerfel, C., Vasel, M., Kawelke, N., Dooley, S., et al. (2015). Inhibition of fibronectin deposition improves experimental liver fibrosis. *J. Hepatol.* 62, 625–633. doi:10.1016/j.jhep.2014.06.010.

Amoah, B. P., Yang, H., Zhang, P., Su, Z., and Xu, H. (2015). Immunopathogenesis of Myocarditis: The Interplay Between Cardiac Fibroblast Cells, Dendritic Cells, Macrophages and CD4+T Cells. *Scand. J. Immunol.* 82, 1–9. doi:10.1111/sji.12298.

Andrae, J., Gallini, R., and Betsholtz, C. (2008). Role of platelet-derived growth factors in physiology and medicine. *Genes Dev.* 22, 1276–1312. doi:10.1101/gad.1653708.

Andrews, S. (2010). FASTQC. A quality control tool for high throughput sequence data. https://www.bioinformatics.babraham.ac.uk/projects.

Angela Covino, D., Sabbatucci, M., and Fantuzzi, L. (2015). The CCL2/CCR2 Axis in the Pathogenesis of HIV-1 Infection: A New Cellular Target for Therapy? *Curr. Drug Targets* 17, 76–110. doi:10.2174/1389450117011512171109 17.

Antsiferova, M., Piwko-Czuchra, A., Cangkrama, M., Wietecha, M., Sahin, D., Birkner, K., et al. (2017). Activin promotes skin carcinogenesis by attraction and reprogramming of macrophages. *EMBO Mol. Med.* 9, 27–45. doi:10.15252/emmm.201606493.

Aono, Y., Kishi, M., Yokota, Y., Azuma, M., Kinoshita, K., Takezaki, A., et al. (2014). Role of platelet-derived growth factor/platelet-derived growth factor receptor axis in the trafficking of circulating fibrocytes in pulmonary fibrosis. *Am. J. Respir. Cell Mol. Biol.* 51, 793–801. doi:10.1165/rcmb.2013-0455OC.

Arck, P., Solano, M. E., Walecki, M., and Meinhardt, A. (2014). The immune privilege of testis and gravid uterus: Same difference? *Mol. Cell. Endocrinol.* 382, 509–520. doi:10.1016/j.mce.2013.09.022.

Arpino, V., Brock, M., and Gill, S. E. (2015). The role of TIMPs in regulation of extracellular matrix proteolysis. *Matrix Biol.* 44–46, 247–254. doi:10.1016/j.matbio.2015.03.005.

Ayaub, E. A., Dubey, A., Imani, J., Botelho, F., Kol, M. R. J., Richards, C. D., et al. (2017). Overexpression of OSM and IL-6 impacts the polarization of pro- fibrotic macrophages and the development of bleomycin-induced lung fibrosis. *Sci. Rep.* 7, 13281. doi:10.1038/s41598-017-13511-z.

Balasubramanian, S., Quinones, L., Kasiganesan, H., Zhang, Y., Pleasant, D. L.,

Sundararaj, K. P., et al. (2012). β3 Integrin in Cardiac Fibroblast Is Critical for Extracellular Matrix Accumulation during Pressure Overload Hypertrophy in Mouse. *PLoS One* 7, e45076. doi:10.1371/journal.pone.0045076.

Barczyk, M., Carracedo, S., and Gullberg, D. (2010). Integrins. *Cell Tissue Res.* 339, 269–280. doi:10.1007/s00441-009-0834-6.

Basciani, S., Mariani, S., Arizzi, M., Ulisse, S., Rucci, N., Jannini, E. A., et al. (2002). Expression of platelet-derived growth factor-A (PDGF-A), PDGF-B, and PDGF receptor-alpha and -beta during human testicular development and disease. *J. Clin. Endocrinol. Metab.* 87, 2310–2319. doi:10.1210/jcem.87.5.8476.

Basciani, S., Mariani, S., Spera, G., and Gnessi, L. (2010). Role of Platelet-Derived Growth Factors in the Testis. *Endocr. Rev.* 31, 916–939. doi:10.1210/er.2010-0004.

Başımoğlu Koca, Y. (2019). Localization of Laminin and Fibronectin in Rat Testes after Diisobutyl Phthalate Exposure: Histopathologic and Immunohistochemical Study. *Celal Bayar Üniversitesi Fen Bilim. Derg.* 15, 293–300. doi:10.18466/cbayarfbe.570613.

Bates, A. L., Pickup, M. W., Hallett, M. A., Dozier, E. A., Thomas, S., and Fingleton, B. (2015). Stromal matrix metalloproteinase 2 regulates collagen expression and promotes the outgrowth of experimental metastases. *J. Pathol.* 235, 773–783. doi:10.1002/path.4493.

Bhushan, S., and Meinhardt, A. (2017). The macrophages in testis function. *J. Reprod. Immunol.* 119, 107–112. doi:10.1016/j.jri.2016.06.008.

Bhushan, S., Theas, M. S., Guazzone, V. A., Jacobo, P., Wang, M., Fijak, M., et al. (2020). Immune Cell Subtypes and Their Function in the Testis. *Front. Immunol.* 11, 583304. doi:10.3389/fimmu.2020.583304.

Bocharov, G., Luzyanina, T., Cupovic, J., and Ludewig, B. (2013). Asymmetry of cell division in CFSE-based lymphocyte proliferation analysis. *Front. Immunol.* 4, 1–8. doi:10.3389/fimmu.2013.00264.

Bolger, A. M., Lohse, M., and Usadel, B. (2014). Trimmomatic: A flexible trimmer for Illumina sequence data. *Bioinformatics* 30, 2114–2120. doi:10.1093/bioinformatics/btu170.

Bonnans, C., Chou, J., and Werb, Z. (2014). Remodelling the extracellular matrix in development and disease. *Nat. Rev. Mol. Cell Biol.* 15, 786–801. doi:10.1038/nrm3904.

Boring, L., Gosling, J., Chensue, S. W., Kunkel, S. L., Farese, R. V., Broxmeyer, H. E., et al. (1997). Impaired monocyte migration and reduced type 1 (Th1) cytokine responses in C-C chemokine receptor 2 knockout mice. *J. Clin. Invest.* 100, 2552–2561. doi:10.1172/JCI119798.

Bose, S., and Cho, J. (2013). Role of chemokine CCL2 and its receptor CCR2 in neurodegenerative diseases. *Arch. Pharm. Res.* 36, 1039–1050.

doi:10.1007/s12272-013-0161-z.

Braga, T. T., Correa-Costa, M., Silva, R. C., Cruz, M. C., Hiyane, M. I., da Silva, J. S., et al. (2018). CCR2 contributes to the recruitment of monocytes and leads to kidney inflammation and fibrosis development. *Inflammopharmacology* 26, 403–411. doi:10.1007/s10787-017-0317-4.

Brew, K., and Nagase, H. (2010). The tissue inhibitors of metalloproteinases (TIMPs): An ancient family with structural and functional diversity. *Biochim. Biophys. Acta - Mol. Cell Res.* 1803, 55–71. doi:10.1016/j.bbamcr.2010.01.003.

Briggs, S. (2005). The role of fibronectin in fibroblast migration during tissue repair. *J. Wound Care* 14, 284–287. doi:10.12968/jowc.2005.14.6.26789.

Bucala, R., Spiegel, L. A., Chesney, J., Hogan, M., and Cerami, A. (1994). Circulating fibrocytes define a new leukocyte subpopulation that mediates tissue repair. *Mol. Med.* 1, 71–81. doi:10.1007/bf03403533.

Buechler, M. B., Fu, W., and Turley, S. J. (2021). Fibroblast-macrophage reciprocal interactions in health, fibrosis, and cancer. *Immunity* 54, 903–915. doi:10.1016/j.immuni.2021.04.021.

Cabral-Pacheco, G. A., Garza-Veloz, I., Rosa, C. C. D. La, Ramirez-Acuña, J. M., Perez-Romero, B. A., Guerrero-Rodriguez, J. F., et al. (2020). The roles of matrix metalloproteinases and their inhibitors in human diseases. *Int. J. Mol. Sci.* 21, 9739. doi:10.3390/ijms21249739.

Cabrera, S., Gaxiola, M., Ram, R., Jara, P., Armiento, J. D., Richards, T., et al. (2007). Overexpression of MMP9 in macrophages attenuates pulmonary fibrosis induced by bleomycin. *Int. J. Biochem. Cell Biol.* 39, 2324–2338. doi:10.1016/j.biocel.2007.06.022.

Camelo, A., Dunmore, R., Sleeman, M. A., and Clarke, D. L. (2014). The epithelium in idiopathic pulmonary fibrosis: Breaking the barrier. *Front. Pharmacol.* 4, 173. doi:10.3389/fphar.2013.00173.

Cangkrama, M., Wietecha, M., and Werner, S. (2020). Wound Repair, Scar Formation, and Cancer: Converging on Activin. *Trends Mol. Med.* 26, 1107–1117. doi:10.1016/j.molmed.2020.07.009.

Chávez-Galán, L., Olleros, M. L., Vesin, D., and Garcia, I. (2015). Much more than M1 and M2 macrophages, there are also CD169+ and TCR+ macrophages. *Front. Immunol.* 6, 263. doi:10.3389/fimmu.2015.00263.

Chen, Y., Pu, Q., Ma, Y., Zhang, H., Ye, T., Zhao, C., et al. (2021). Aging Reprograms the Hematopoietic-Vascular Niche to Impede Regeneration and Promote Fibrosis. *Cell Metab.* 33, 395-410.e4. doi:10.1016/j.cmet.2020.11.019.

Chong, S. G., Sato, S., Kolb, M., and Gauldie, J. (2019). Fibrocytes and fibroblasts—Where are we now. *Int. J. Biochem. Cell Biol.* 116, 105595. doi:10.1016/j.biocel.2019.105595.

Choy, J. T., and Eisenberg, M. L. (2018). Male infertility as a window to health. *Fertil. Steril.* 110, 810–814. doi:10.1016/j.fertnstert.2018.08.015.

Chu, H. X., Arumugam, T. V., Gelderblom, M., Magnus, T., Drummond, G. R., and Sobey, C. G. (2014). Role of CCR2 in inflammatory conditions of the central nervous system. *J. Cereb. Blood Flow Metab.* 34, 1425–1429. doi:10.1038/jcbfm.2014.120.

Clark, R. A. F., An, J. Q., Greiling, D., Khan, A., and Schwarzbauer, J. E. (2003). Fibroblast Migration on Fibronectin Requires Three Distinct Functional Domains. *J. Invest. Dermatol.* 121, 695–705. doi:10.1046/j.1523-1747.2003.12484.x.

Cui, N., Hu, M., and Khalil, R. A. (2017). Biochemical and Biological Attributes of Matrix Metalloproteinases. *Prog. Mol. Biol. Transl. Sci.* 147, 1–73. doi:10.1016/bs.pmbts.2017.02.005.

Davies, L. C., Jenkins, S. J., Allen, J. E., and Taylor, P. R. (2013). Tissue-resident macrophages. *Nat. Immunol.* 14, 986–995. doi:10.1038/ni.2705.

de Kretser, D. M., O'Hehir, R. E., Hardy, C. L., and Hedger, M. P. (2012). The roles of activin A and its binding protein, follistatin, in inflammation and tissue repair. *Mol. Cell. Endocrinol.* 359, 101–106. doi:10.1016/j.mce.2011.10.009.

de Oliveira, R. C., and Wilson, S. E. (2020). Fibrocytes, wound healing, and corneal fibrosis. *Investig. Ophthalmol. Vis. Sci.* 61, 28. doi:10.1167/iovs.61.2.28.

Deshmane, S. L., Kremlev, S., Amini, S., and Sawaya, B. E. (2009). Monocyte chemoattractant protein-1 (MCP-1): An overview. *J. Interf. Cytokine Res.* 29, 313–325. doi:10.1089/jir.2008.0027.

Díez-Torre, A., Silván, U., Moreno, P., Gumucio, J., and Aréchaga, J. (2011). Peritubular myoid cell-derived factors and its potential role in the progression of testicular germ cell tumours. *Int. J. Androl.* 34, e252-264. doi:10.1111/j.1365-2605.2011.01168.x.

Distler, J. H. W., Györfi, A. H., Ramanujam, M., Whitfield, M. L., Königshoff, M., and Lafyatis, R. (2019). Shared and distinct mechanisms of fibrosis. *Nat. Rev. Rheumatol.* 15, 705–730. doi:10.1038/s41584-019-0322-7.

Do, C., Drel, V., Tan, C., Lee, D., and Wagner, B. (2019). Nephrogenic Systemic Fibrosis Is Mediated by Myeloid C-C Chemokine Receptor 2. *J. Invest. Dermatol.* 139, 2134-2143.e2. doi:10.1016/j.jid.2019.03.1145.

Dobashi, M., Fujisawa, M., Naito, I., Yamazaki, T., Okada, H., and Kamidono, S. (2003). Distribution of type IV collagen subtypes in human testes and their association with spermatogenesis. *Fertil. Steril.* 80, 755–760. doi:10.1016/S0015-0282(03)00775-1.

Dobin, A., Davis, C. A., Schlesinger, F., Drenkow, J., Zaleski, C., Jha, S., et al. (2013). STAR: Ultrafast universal RNA-seq aligner. *Bioinformatics* 29, 15–21. doi:10.1093/bioinformatics/bts635.

Dong, Y., Yang, M., Zhang, J., Peng, X., Cheng, J., Cui, T., et al. (2016). Depletion of CD8 + T Cells Exacerbates CD4 + T Cell–Induced Monocyte-to-Fibroblast

Transition in Renal Fibrosis . *J. Immunol.* 196, 1874–1881. doi:10.4049/jimmunol.1501232.

Döring, Y., Pawig, L., Weber, C., and Noels, H. (2014). The CXCL12/CXCR4 chemokine ligand/receptor axis in cardiovascular disease. *Front. Physiol.* 5, 212. doi:10.3389/fphys.2014.00212.

Dupin, I., Allard, B., Ozier, A., Maurat, E., Ousova, O., Delbrel, E., et al. (2016). Blood fibrocytes are recruited during acute exacerbations of chronic obstructive pulmonary disease through a CXCR4-dependent pathway. *J. Allergy Clin. Immunol.* 137, 1036-1042.e7. doi:10.1016/j.jaci.2015.08.043.

Dutta, S., Sandhu, N., Sengupta, P., Alves, M. G., Henkel, R., and Agarwal, A. (2021). Somatic-Immune Cells Crosstalk In-The-Making of Testicular Immune Privilege. *Reprod. Sci.* doi:10.1007/s43032-021-00721-0.

Ehmcke, J., Wistuba, J., and Schlatt, S. (2006). Spermatogonial stem cells: Questions, models and perspectives. *Hum. Reprod. Update* 12, 275–282. doi:10.1093/humupd/dmk001.

Falade, T. E., Olude, M. A., Mustapha, O. A., Mbajiorgu, E. F., Ihunwo, A. O., Olopade, J. O., et al. (2017). Connective tissue, glial and neuronal expressions in testis of the African giant rat (Cricetomys gambianus). *J. Morphol. Sci.* 34, 186–193. doi:10.4322/jms.109117.

Fantuzzi, L., Tagliamonte, M., Gauzzi, M. C., and Lopalco, L. (2019). Dual CCR5/CCR2 targeting: opportunities for the cure of complex disorders. *Cell. Mol. Life Sci.* 76, 4869–4886. doi:10.1007/s00018-019-03255-6.

Fijak, M., Damm, L. J., Wenzel, J. P., Aslani, F., Walecki, M., Wahle, E., et al. (2015). Influence of Testosterone on Inflammatory Response in Testicular Cells and Expression of Transcription Factor Foxp3 in T Cells. *Am. J. Reprod. Immunol.* 74, 12–25. doi:10.1111/aji.12363.

Fijak, M., and Meinhardt, A. (2006). The testis in immune privilege. *Immunol. Rev.* 213, 66–81. doi:10.1111/j.1600-065X.2006.00438.x.

Fijak, M., Pilatz, A., Hedger, M. P., Nicolas, N., Bhushan, S., Michel, V., et al. (2018). Infectious, inflammatory and “autoimmune” male factor infertility: How do rodent models inform clinical practice? *Hum. Reprod. Update* 24, 416–441. doi:10.1093/humupd/dmy009.

Foster, R. A. (2016). Male Genital System. *Jubb, Kennedy Palmer’s Pathol. Domest. Anim. Vol. 3*, 465-510.e1. doi:10.1016/B978-0-7020-5319-1.00016-5.

França, L. R., Hess, R. A., Dufour, J. M., Hofmann, M. C., and Griswold, M. D. (2016). The Sertoli cell: One hundred fifty years of beauty and plasticity. *Andrology* 4, 189–212. doi:10.1111/andr.12165.

Francke, A., Herold, J., Weinert, S., Strasser, R. H., and Braun-Dullaeus, R. C. (2011). Generation of mature murine monocytes from heterogeneous bone marrow and

description of their properties. *J. Histochem. Cytochem.* 59, 813–825. doi:10.1369/0022155411416007.

Frantz, C., Stewart, K. M., and Weaver, V. M. (2010). The extracellular matrix at a glance. *J. Cell Sci.* 123, 4195–4200. doi:10.1242/jcs.023820.

Fraser, E., Denney, L., Antanaviciute, A., Blirando, K., Vuppusetty, C., Zheng, Y., et al. (2021). Multi-Modal Characterization of Monocytes in Idiopathic Pulmonary Fibrosis Reveals a Primed Type I Interferon Immune Phenotype. *Front. Immunol.* 12, 623430. doi:10.3389/fimmu.2021.623430.

Fröjdman, K., Harley, V. R., and Pelliniemi, L. J. (2000). Sox9 protein in rat sertoli cells is age and stage dependent. *Histochem. Cell Biol.* 113, 31–36. doi:10.1007/s004180050004.

García-Gareta, E., Levin, A., and Hook, L. (2019). Engineering the migration and attachment behaviour of primary dermal fibroblasts. *Biotechnol. Bioeng.* 116, 1102–1115. doi:10.1002/bit.26927.

Gentek, R., Molawi, K., and Sieweke, M. H. (2014). Tissue macrophage identity and self-renewal. *Immunol. Rev.* 262, 56–73. doi:10.1111/imr.12224.

Gerdprasert, O., O'Bryan, M. K., Nikolic-Paterson, D. J., Sebire, K., De Kretser, D. M., and Hedger, M. P. (2002). Expression of monocyte chemoattractant protein-1 and macrophage colony-stimulating factor in normal and inflamed rat testis. *Mol. Hum. Reprod.* 8, 518–524. doi:10.1093/molehr/8.6.518.

Giannandrea, M., and Parks, W. C. (2014). Diverse functions of matrix metalloproteinases during fibrosis. *DMM Dis. Model. Mech.* 7, 193–203. doi:10.1242/dmm.012062.

Gieseck III, R. L., Wilson, M. S., and Wynn, T. A. (2018). Type 2 immunity in tissue repair and fibrosis. *Nat. Rev. Immunol.* 18, 62–76. doi:10.1038/nri.2017.90.

Griffiths, K., Habiel, D. M., Jaffar, J., Binder, U., Darby, W. G., Hosking, C. G., et al. (2018). Anti-fibrotic Effects of CXCR4-Targeting i-body AD-114 in Preclinical Models of Pulmonary Fibrosis. *Sci. Rep.* 8, 3212. doi:10.1038/s41598-018-20811-5.

Gschwandtner, M., Derler, R., and Midwood, K. S. (2019). More Than Just Attractive: How CCL2 Influences Myeloid Cell Behavior Beyond Chemotaxis. *Front. Immunol.* 10, 2759. doi:10.3389/fimmu.2019.02759.

Guazzone, V. A., Jacobo, P., Theas, M. S., and Lustig, L. (2009). Cytokines and chemokines in testicular inflammation: A brief review. *Microsc. Res. Tech.* 72, 620–628. doi:10.1002/jemt.20704.

Guazzone, V. A., Rival, C., Denduchis, B., and Lustig, L. (2003). Monocyte chemoattractant protein-1 (MCP-1/CCL2) in experimental autoimmune orchitis. *J. Reprod. Immunol.* 60, 143–157. doi:10.1016/j.jri.2003.08.001.

Gurczynski, S. J., Procario, M. C., O'Dwyer, D. N., Wilke, C. A., and Moore, B. B. (2016). Loss of CCR2 signaling alters leukocyte recruitment and exacerbates γ-

herpesvirus-induced pneumonitis and fibrosis following bone marrow transplantation. *Am. J. Physiol. - Lung Cell. Mol. Physiol.* 311, L611–L627. doi:10.1152/ajplung.00193.2016.

Hachiya, K., Masuya, M., Kuroda, N., Yoneda, M., Tsuboi, J., Nagaharu, K., et al. (2021). Irbesartan, an angiotensin II type 1 receptor blocker, inhibits colitis-associated tumourigenesis by blocking the MCP-1/CCR2 pathway. *Sci. Rep.* 11, 19943. doi:10.1038/s41598-021-99412-8.

Haidl, G., Haidl, F., Allam, J. P., and Schuppe, H. C. (2019). Therapeutic options in male genital tract inflammation. *Andrologia* 51, 1–11. doi:10.1111/and.13207.

Hardy, C. L., Rolland, J. M., and Hehir, R. E. O. (2015). The immunoregulatory and fibrotic roles of activin A in allergic asthma. *Clin. Exp. Allergy* 45, 1510–1522. doi:10.1111/cea.12561.

Haub, J., Roehrig, N., Uhrin, P., Schabbauer, G., Eulberg, D., Melchior, F., et al. (2019). Intervention of Inflammatory Monocyte Activity Limits Dermal Fibrosis. *J. Invest. Dermatol.* 139, 2144–2153. doi:10.1016/j.jid.2019.04.006.

Hedger, M. P., and de Kretser, D. M. (2013). The activins and their binding protein, follistatin-Diagnostic and therapeutic targets in inflammatory disease and fibrosis. *Cytokine Growth Factor Rev.* 24, 285–295. doi:10.1016/j.cytogfr.2013.03.003.

Hedger, M. P., and Winnall, W. R. (2012). Regulation of activin and inhibin in the adult testis and the evidence for functional roles in spermatogenesis and immunoregulation. *Mol. Cell. Endocrinol.* 359, 30–42. doi:10.1016/j.mce.2011.09.031.

Hedger, M. P., Winnall, W. R., Phillips, D. J., and Kretser, D. M. De (2011). The regulation and functions of activin and follistatin in inflammation and immunity. *Vitam. Horm.* 85, 255–297. doi:10.1016/B978-0-12-385961-7.00013-5.

Heinrich, A., and DeFalco, T. (2020). Essential roles of interstitial cells in testicular development and function. *Andrology* 8, 903–914. doi:10.1111/andr.12703.

Hemmann, S., Graf, J., Roderfeld, M., and Roeb, E. (2007). Expression of MMPs and TIMPs in liver fibrosis - a systematic review with special emphasis on anti-fibrotic strategies. *J. Hepatol.* 46, 955–975. doi:10.1016/j.jhep.2007.02.003.

Henderson, N. C., Arnold, T. D., Katamura, Y., Giacomini, M. M., Rodriguez, J. D., McCarty, J. H., et al. (2013). Targeting of αv integrin identifies a core molecular pathway that regulates fibrosis in several organs. *Nat. Med.* 19, 1617–1624. doi:10.1038/nm.3282.

Henderson, N. C., Rieder, F., and Wynn, T. A. (2020). Fibrosis: from mechanisms to medicines. *Nature* 587, 555–566. doi:10.1038/s41586-020-2938-9.

Herrera, J., Henke, C. A., and Bitterman, P. B. (2018). Extracellular matrix as a driver of progressive fibrosis. *J. Clin. Invest.* 128, 45–53. doi:10.1172/JCI93557.

Hinz, B., Phan, S. H., Thannickal, V. J., Galli, A., Bochaton-Piallat, M. L., and Gabbiani,

G. (2007). The myofibroblast: One function, multiple origins. *Am. J. Pathol.* 170, 1807–1816. doi:10.2353/ajpath.2007.070112.

Hu, X., Li, N., Tao, K., Fang, X., Liu, J., Wang, Y., et al. (2014). Effects of integrin αvβ3on differentiation and collagen synthesis induced by connective tissue growth factor in human hypertrophic scar fibroblasts. *Int. J. Mol. Med.* 34, 1323–1334. doi:10.3892/ijmm.2014.1912.

Hutson, J. C. (1998). Interactions between testicular macrophages and Leydig cells. *J. Androl.* 19, 394–398.

Iliadou, P. K., Tsametis, C., Kaprara, A., Papadimas, I., and Goulis, D. G. (2015). The sertoli cell: Novel clinical potentiality. *Hormones* 14, 504–514. doi:10.14310/horm.2002.1648.

Jacobo, P., Guazzone, V. A., Jarazo-Dietrich, S., Theas, M. S., and Lustig, L. (2009). Differential changes in CD4+ and CD8+ effector and regulatory T lymphocyte subsets in the testis of rats undergoing autoimmune orchitis. *J. Reprod. Immunol.* 81, 44–54. doi:10.1016/j.jri.2009.04.005.

Jacobo, P., Guazzone, V. A., Pérez, C. V., and Lustig, L. (2015). CD4+ Foxp3+ regulatory T cells in autoimmune orchitis: Phenotypic and functional characterization. *Am. J. Reprod. Immunol.* 73, 109–125. doi:10.1111/aji.12312.

Jacobo, P., Guazzone, V. A., Theas, M. S., and Lustig, L. (2011a). Testicular autoimmunity. *Autoimmun. Rev.* 10, 201–204. doi:10.1016/j.autrev.2010.09.026.

Jacobo, P., Pérez, C. V., Theas, M. S., Guazzone, V. A., and Lustig, L. (2011b). CD4+ and CD8+ T cells producing Th1 and Th17 cytokines are involved in the pathogenesis of autoimmune orchitis. *Reproduction* 141, 249–258. doi:10.1530/REP-10-0362.

Jaffar, J., Griffiths, K., Oveissi, S., Duan, M., Foley, M., Glaspole, I., et al. (2020). CXCR4+cells are increased in lung tissue of patients with idiopathic pulmonary fibrosis. *Respir. Res.* 21, 221. doi:10.1186/s12931-020-01467-0.

Jiang, L., Liu, B., Qi, Y., Zhu, L., Cui, X., and Liu, Z. (2020a). Antagonistic effects of activin A and TNF-α on the activation of L929 fibroblast cells via Smad3-independent signaling. *Sci. Rep.* 10, 20623. doi:10.1038/s41598-020-77783-8.

Jiang, Q., Maresch, C. C., Petry, S. F., Paradowska-Dogan, A., Bhushan, S., Chang, Y., et al. (2020b). Elevated CCL2 causes Leydig cell malfunction in metabolic syndrome. *JCI Insight* 5, e134882. doi:10.1172/jci.insight.134882.

Jones, C. V., and Ricardo, S. D. (2013). Macrophages and CSF-1: Implications for development and beyond. *Organogenesis* 9, 249–260. doi:10.4161/org.25676.

Kardas, G., Daszyńska-Kardas, A., Marynowski, M., Brząkalska, O., Kuna, P., and Panek, M. (2020). Role of Platelet-Derived Growth Factor (PDGF) in Asthma as an Immunoregulatory Factor Mediating Airway Remodeling and Possible Pharmacological Target. *Front. Pharmacol.* 11, 47. doi:10.3389/fphar.2020.00047.

Kauerhof, A. C., Nicolas, N., Bhushan, S., Wahle, E., Loveland, K. A., Fietz, D., et al. (2019). Investigation of activin A in inflammatory responses of the testis and its role in the development of testicular fibrosis. *Hum. Reprod.* 34, 1536–1550. doi:10.1093/humrep/dez109.

Kawaguchi, N., Zhang, T.-T., and Nakanishi, T. (2019). Involvement of CXCR4 in Normal and Abnormal Development. *Cells* 8, 185. doi:10.3390/cells8020185.

Kendall, R. T., and Feghali-Bostwick, C. A. (2014). Fibroblasts in fibrosis: Novel roles and mediators. *Front. Pharmacol.* 5, 123. doi:10.3389/fphar.2014.00123.

Khokha, R., Murthy, A., and Weiss, A. (2013). Metalloproteinases and their natural inhibitors in inflammation and immunity. *Nat. Rev. Immunol.* 13, 649–665. doi:10.1038/nri3499.

Kiagiadaki, F., Kampa, M., Voumvouraki, A., Castanas, E., Kouroumalis, E., and Notas, G. (2018). Activin-A causes Hepatic stellate cell activation via the induction of TNFα and TGFβ in Kupff er cells. *Biochim. Biophys. Acta - Mol. Cell Res.* 1864, 891–899. doi:10.1016/j.bbadis.2017.12.031.

Kiernan, J. (2008). *Histological and histochemical methods: theory and practice*. 4th ed. Bloxham, UK.

Kishore, A., and Petrek, M. (2021). Roles of Macrophage Polarization and Macrophage-Derived miRNAs in Pulmonary Fibrosis. *Front. Immunol.* 12, 678457. doi:10.3389/fimmu.2021.678457.

Kisling, A., Lust, R. M., and Katwa, L. C. (2019). What is the role of peptide fragments of collagen I and IV in health and disease? *Life Sci.* 228, 30–34. doi:10.1016/j.lfs.2019.04.042.

Klinkhammer, B. M., Floege, J., and Boor, P. (2018). PDGF in organ fibrosis. *Mol. Aspects Med.* 62, 44–62. doi:10.1016/j.mam.2017.11.008.

Knight, B. E., Kozlowski, N., Havelin, J., King, T., Crocker, S. J., Young, E. E., et al. (2019). TIMP-1 Attenuates the Development of Inflammatory Pain Through MMP-Dependent and Receptor-Mediated Cell Signaling Mechanisms. *Front. Mol. Neurosci.* 12, 220. doi:10.3389/fnmol.2019.00220.

Kobayashi, T., Kim, H. J., Liu, X., Sugiura, H., Kohyama, T., Fang, Q., et al. (2014). Matrix metalloproteinase-9 activates TGF-β and stimulates fibroblast contraction of collagen gels. *Am. J. Physiol. - Lung Cell. Mol. Physiol.* 306, 1006–1015. doi:10.1152/ajplung.00015.2014.

Kohno, S., Munoz, J. A., Williams, T. M., Teuscher, C., Bernard, C. C., and Tung, K. S. (1983). Immunopathology of murine experimental allergic orchitis. *J. Immunol.* 130, 2675–2682.

Krenkel, O., Puengel, T., Govaere, O., Abdallah, A. T., Mossanen, J. C., Kohlhepp, M., et al. (2018). Therapeutic inhibition of inflammatory monocyte recruitment reduces steatohepatitis and liver fibrosis. *Hepatology* 67, 1270–1283.

doi:10.1002/hep.29544.

Kuroda, N., Masuya, M., Tawara, I., Tsuboi, J., Yoneda, M., Nishikawa, K., et al. (2019). Infiltrating CCR2+ monocytes and their progenies, fibrocytes, contribute to colon fibrosis by inhibiting collagen degradation through the production of TIMP-1. *Sci. Rep.* 9, 8568. doi:10.1038/s41598-019-45012-6.

Kurzepa, J., M, A., Czechowska, G., Kurzepa, J., Celiński, K., Kazmierak, W., et al. (2014). Role of MMP-2 and MMP-9 and their natural inhibitors in liver fibrosis, chronic pancreatitis and non-specific inflammatory bowel diseases. *Hepatobiliary Pancreat. Dis. Int.* 13, 570–579. doi:10.1016/S1499-3872(14)60261-7.

Leber, T. M., and Balkwill, F. R. (1997). Zymography: a single-step staining method for quantitation of proteolytic activity on substrate gels. *Anal. Biochem.* 249, 24–28. doi:10.1006/abio.1997.2170.

Lebrun, A., Lo Re, S., Chantry, M., Izquierdo Carerra, X., Uwambayinema, F., Ricci, D., et al. (2017). CCR2+ monocytic myeloid-derived suppressor cells (M-MDSCs) inhibit collagen degradation and promote lung fibrosis by producing transforming growth factor-β1. *J. Pathol.* 243, 320–330. doi:10.1002/path.4956.

Lee, J. Y., Yun, M., Paik, J. S., Lee, S. B., and Yang, S. W. (2016). PDGF-BB enhances the proliferation of cells in humanorbital fibroblasts by suppressing PDCD4 expression via up-regulation of microRNA-21. *Investig. Ophthalmol. Vis. Sci.* 57, 908–913. doi:10.1167/iovs.15-18157.

Leeman, M., McKay, J., and Murray, G. (2002). Matrix metalloproteinase 13 activity is associated with poor prognosis in colorectal cancer. *J. Clin. Pathol.* 55, 758–762. doi:10.1136/jcp.55.10.758.

Lei, T., Moos, S., Klug, J., Aslani, F., Bhushan, S., Wahle, E., et al. (2018). Galectin-1 enhances TNFα-induced inflammatory responses in Sertoli cells through activation of MAPK signalling. *Sci. Rep.* 8, 3741. doi:10.1038/s41598-018-22135-w.

Li, W., Fan, J., Chen, M., Guan, S., Sawcer, D., Bokoch, G. M., et al. (2004). Mechanism of Human Dermal Fibroblast Migration Driven by Type I Collagen and Platelet-derived Growth Factor-BB. *Mol. Biol. Cell* 15, 294–309. doi:10.1091/mbc.E03.

Liao, Y., Smyth, G. K., and Shi, W. (2014). FeatureCounts: An efficient general purpose program for assigning sequence reads to genomic features. *Bioinformatics* 30, 923–930. doi:10.1093/bioinformatics/btt656.

Lin, C. H., Shih, C. H., Tseng, C. C., Yu, C. C., Tsai, Y. J., Bien, M. Y., et al. (2014). CXCL12 induces connective tissue growth factor expression in human lung fibroblasts through the Rac1/ERK, JNK, and AP-1 pathways. *PLoS One* 9, e104746. doi:10.1371/journal.pone.0104746.

Livak, K. J., and Schmittgen, T. D. (2001). Analysis of relative gene expression data using real-time quantitative PCR and the 2-ΔΔCT method. *Methods* 25, 402–408. doi:10.1006/meth.2001.1262.

Love, M. I., Huber, W., and Anders, S. (2014). Moderated estimation of fold change and dispersion for RNA-seq data with DESeq2. *Genome Biol.* 15, 550. doi:10.1186/s13059-014-0550-8.

Lu, Y., Liu, S., Zhang, S., Cai, G., Jiang, H., Su, H., et al. (2011). Tissue inhibitor of metalloproteinase-1 promotes NIH3T3 fibroblast proliferation by activating p-Akt and cell cycle progression. *Mol. Cells* 31, 225–230. doi:10.1007/s10059-011-0023-9.

Lustig, L., Guazzone, V. A., Theas, M. S., Pleuger, C., Jacobo, P., Pérez, C. V., et al. (2020). Pathomechanisms of Autoimmune Based Testicular Inflammation. *Front. Immunol.* 11, 583135. doi:10.3389/fimmu.2020.583135.

Mack, M. (2018). Inflammation and fibrosis. *Matrix Biol.* 68–69, 106–121. doi:10.1016/j.matbio.2017.11.010.

Mack, M., and Yanagita, M. (2015). Origin of myofibroblasts and cellular events triggering fibrosis. *Kidney Int.* 87, 297–307. doi:10.1038/ki.2014.287.

Maekawa, M., Kamimura, K., and Nagano, T. (1996). Peritubular myoid cells in the testis : Their structure and function. *Arch. Histol. Cytol.* 59, 1–13. doi:10.1679/aohc.59.1.

Mantovani, A., Sica, A., Sozzani, S., Allavena, P., Vecchi, A., and Locati, M. (2004). The chemokine system in diverse forms of macrophage activation and polarization. *Trends Immunol.* 25, 677–686. doi:10.1016/j.it.2004.09.015.

Margadant, C., and Sonnenberg, A. (2010). Integrin-TGF-B crosstalk in fibrosis, cancer and wound healing. *EMBO Rep.* 11, 97–105. doi:10.1038/embor.2009.276.

Mariani, S., Basciani, S., Arizzi, M., Spera, G., and Gnessi, L. (2002). PDGF and the testis. *Trends Endocrinol. Metab.* 13, 11–17. doi:10.1016/s1043-2760(01)00518-5.

Marini, M., Rosa, I., Guasti, D., Gacci, M., Sgambati, E., Ibba-Manneschi, L., et al. (2018). Reappraising the microscopic anatomy of human testis: identification of telocyte networks in the peritubular and intertubular stromal space. *Sci. Rep.* 8, 14780. doi:10.1038/s41598-018-33126-2.

Marsico, G., Russo, L., Quondamatteo, F., and Pandit, A. (2018). Glycosylation and Integrin Regulation in Cancer. *Trends in Cancer* 4, 537–552. doi:10.1016/j.trecan.2018.05.009.

Mayerhofer, A. (2013). Human testicular peritubular cells: More than meets the eye. *Reproduction* 145, R107–R116. doi:10.1530/REP-12-0497.

Mehrad, B., Burdick, M. D., and Strieter, R. M. (2009). Fibrocyte CXCR4 regulation as a therapeutic target in pulmonary fibrosis. *Int. J. Biochem. Cell Biol.* 41, 1708–1718. doi:10.1016/j.biocel.2009.02.020.

Meinhardt, A., Dejucq-Rainsford, N., and Bhushan, S. (2022). Testicular macrophages: development and function in health and disease. *Trends Immunol.* 43, 51–62. doi:10.1016/j.it.2021.11.003.

Meinhardt, A., and Hedger, M. P. (2011). Immunological, paracrine and endocrine aspects of testicular immune privilege. *Mol. Cell. Endocrinol.* 335, 60–68. doi:10.1016/j.mce.2010.03.022.

Meinhardt, A., Wang, M., Schulz, C., and Bhushan, S. (2018). Microenvironmental signals govern the cellular identity of testicular macrophages. *J. Leukoc. Biol.* 104, 757–766. doi:10.1002/JLB.3MR0318-086RR.

Meng, J., Greenlee, A. R., Taub, C. J., and Braun, R. E. (2011). Sertoli cell-specific deletion of the androgen receptor compromises testicular immune privilege in mice. *Biol. Reprod.* 85, 254–260. doi:10.1095/biolreprod.110.090621.

Meroni, S. B., Galardo, M. N., Rindone, G., Gorga, A., Riera, M. F., and Cigorraga, S. B. (2019). Molecular mechanisms and signaling pathways involved in Sertoli cell proliferation. *Front. Endocrinol. (Lausanne).* 10, 224. doi:10.3389/fendo.2019.00224.

Missirlis, D., Haraszti, T., Kessler, H., and Spatz, J. P. (2017). Fibronectin promotes directional persistence in fibroblast migration through interactions with both its cell-binding and heparin-binding domains. *Sci. Rep.* 7, 3711. doi:10.1038/s41598-017-03701-0.

Morianos, I., Papadopoulou, G., Semitekolou, M., and Xanthou, G. (2019). Activin-A in the regulation of immunity in health and disease. *J. Autoimmun.* 104, 102314. doi:10.1016/j.jaut.2019.102314.

Mossadegh-Keller, N., Gentek, R., Gimenez, G., Bigot, S., Mailfert, S., and Sieweke, M. H. (2017). Developmental origin and maintenance of distinct testicular macrophage populations. *J. Exp. Med.* 214, 2829–2841. doi:10.1084/jem.20170829.

Nagase, H., Visse, R., and Murphy, G. (2006). Structure and function of matrix metalloproteinases and TIMPs. *Cardiovasc. Res.* 69, 562–573. doi:10.1016/j.cardiores.2005.12.002.

Nicolas, N., Michel, V., Bhushan, S., Wahle, E., Hayward, S., Ludlow, H., et al. (2017a). Testicular activin and follistatin levels are elevated during the course of experimental autoimmune epididymo-orchitis in mice. *Sci. Rep.* 7, 42391. doi:10.1038/srep42391.

Nicolas, N., Muir, J. A., Hayward, S., Chen, J. L., Stanton, P. G., Gregorevic, P., et al. (2017b). Induction of experimental autoimmune orchitis in mice: responses to elevated circulating levels of the activin-binding protein, follistatin. *Reproduction* 154, 293–305. doi:10.1530/REP-17-0010.

Niedermeier, M., Reich, B., Gomez, M. R., Denzel, A., Schmidbauer, K., Göbel, N., et al. (2009). CD4+ T cells control the differentiation of Gr1+ monocytes into fibrocytes. *Proc. Natl. Acad. Sci. U. S. A.* 106, 17892–17897. doi:10.1073/pnas.0906070106.

O'Connor, T., Borsig, L., and Heikenwalder, M. (2015). CCL2-CCR2 signaling in disease pathogenesis. *Endocrine, Metab. Immune Disord. - Drug Targets* 15, 105–118. doi:10.2174/1871530315666150316120920.

Ogawa, K., Funaba, M., Mathews, L. S., and Mizutani, T. (2000). Activin A Stimulates Type IV Collagenase (Matrix Metalloproteinase-2) Production in Mouse Peritoneal Macrophages. *J. Immunol.* 165, 2997–3003. doi:10.4049/jimmunol.165.6.2997.

Ohga, E., Matsuse, T., Teramoto, S., Katayama, H., Nagase, T., Fukuchi, Y., et al. (1996). Effects of Activin A on Proliferation and Differentiation of Human Lung Fibroblasts. *Biochem. Biophys. Res. Commun.* 228, 391–396. doi:10.1006/bbrc.1996.1672.

Okuma, T., Terasaki, Y., Kaikita, K., Kobayashi, H., Kuziel, W. A., Kawasuji, M., et al. (2004). C-C chemokine receptor 2 (CCR2) deficiency improves bleomycin-induced pulmonary fibrosis by attenuation of both macrophage infiltration and production of macrophage-derived matrix metalloproteinases. *J. Pathol.* 204, 594–604. doi:10.1002/path.1667.

Onozuka, I., Kakinuma, S., Kamiya, A., Miyoshi, M., Sakamoto, N., Kiyohashi, K., et al. (2011). Biochemical and Biophysical Research Communications Cholestatic liver fibrosis and toxin-induced fibrosis are exacerbated in matrix metalloproteinase-2 deficient mice. *Biochem. Biophys. Res. Commun.* 406, 134–140. doi:10.1016/j.bbrc.2011.02.012.

Opdenakker, G., Van den Steen, P. E., and Van Damme, J. (2001). Gelatinase B : a tuner and amplifier of immune functions. *Trends Immunol.* 22, 571–579. doi:10.1016/s1471-4906(01)02023-3.

Palacios, B. S., Estrada-Capetillo, L., Izquierdo, E., Criado, G., Nieto, C., Municio, C., et al. (2015). Macrophages from the synovium of active rheumatoid arthritis exhibit an activin a-dependent pro-inflammatory profile. *J. Pathol.* 235, 515–526. doi:10.1002/path.4466.

Park, E. J., Myint, P. K., Ito, A., Appiah, M. G., Darkwah, S., Kawamoto, E., et al. (2020). Integrin-Ligand Interactions in Inflammation, Cancer, and Metabolic Disease: Insights Into the Multifaceted Roles of an Emerging Ligand Irisin. *Front. Cell Dev. Biol.* 8, 588066. doi:10.3389/fcell.2020.588066.

Parsons, C. J., Bradford, B. U., Pan, C. Q., Cheung, E., Schauer, M., Knorr, A., et al. (2004). Antifibrotic effects of a tissue inhibitor of metalloproteinase-1 antibody on established liver fibrosis in rats. *Hepatology* 40, 1106–1115. doi:10.1002/hep.20425.

Patten, J., and Wang, K. (2021). Fibronectin in development and wound healing. *Adv. Drug Deliv. Rev.* 170, 353–368. doi:10.1016/j.addr.2020.09.005.

Pérez, C. V., Sobarzo, C. M., Jacobo, P. V., Pellizzari, E. H., Cigorraga, S. B., Denduchis, B., et al. (2012). Loss of occludin expression and impairment of blood-testis barrier permeability in rats with autoimmune orchitis: effect of interleukin 6 on Sertoli cell tight junctions. *Biol. Reprod.* 87, 122. doi:10.1095/biolreprod.112.101709.

Perrucci, G. L., Barbagallo, V. A., Corlianò, M., Tosi, D., Santoro, R., Nigro, P., et al.

(2018). Integrin αvβ5 in vitro inhibition limits pro-fibrotic response in cardiac fibroblasts of spontaneously hypertensive rats. *J. Transl. Med.* 16, 352. doi:10.1186/s12967-018-1730-1.

Phillips, R. J., Burdick, M. D., Hong, K., Lutz, M. A., Murray, L. A., Xue, Y. Y., et al. (2004). Circulating fibrocytes traffic to the lungs in response to CXCL12 and mediate fibrosis. *J. Clin. Invest.* 114, 438–446. doi:10.1172/jci20997.

Pitetti, J. L., Calvel, P., Zimmermann, C., Conne, B., Papaioannou, M. D., Aubry, F., et al. (2013). An essential role for insulin and IGF1 receptors in regulating sertoli cell proliferation, testis size, and FSH action in mice. *Mol. Endocrinol.* 27, 814–827. doi:10.1210/me.2012-1258.

Quah, B. J. C., and Parish, C. R. (2010). The use of carboxyfluorescein diacetate succinimidyl ester (CFSE) to monitor lymphocyte proliferation. *J. Vis. Exp.*, 2259. doi:10.3791/2259.

Quan, T. E., Cowper, S. E., and Bucala, R. (2006). The role of circulating fibrocytes in fibrosis. *Curr. Rheumatol. Rep.* 8, 145–150. doi:10.1007/s11926-006-0055-x.

Radbill, B. D., Gupta, R., Ramirez, M. C. M., DiFeo, A., Martignetti, J. A., Alvarez, C. E., et al. (2011). Loss of Matrix Metalloproteinase-2 Amplifies Murine Toxin-Induced Liver Fibrosis by Upregulating Collagen I Expression. *Dig. Dis. Sci.* 56, 406–416. doi:10.1007/s10620-010-1296-0.

Raghu, H., Lepus, C. M., Wang, Q., Wong, H. H., Lingampalli, N., Oliviero, F., et al. (2017). CCL2/CCR2, but not CCL5/CCR5, mediates monocyte recruitment, inflammation and cartilage destruction in osteoarthritis. *Ann. Rheum. Dis.* 76, 914–922. doi:10.1136/annrheumdis-2016-210426.

Reich, B., Schmidbauer, K., Rodriguez Gomez, M., Johannes Hermann, F., Göbel, N., Brühl, H., et al. (2013). Fibrocytes develop outside the kidney but contribute to renal fibrosis in a mouse model. *Kidney Int.* 84, 78–89. doi:10.1038/ki.2013.84.

Reilkoff, R. A., Bucala, R., and Herzog, E. L. (2011). Fibrocytes: Emerging effector cells in chronic inflammation. *Nat. Rev. Immunol.* 11, 427–435. doi:10.1038/nri2990.

Ridiandries, A., Tan, J. T. M., and Bursill, C. A. (2018). The role of chemokines in wound healing. *Int. J. Mol. Sci.* 19, 3217. doi:10.3390/ijms19103217.

Risinger, G. M., Hunt, T. S., Updike, D. L., Bullen, E. C., and Howard, E. W. (2006). Matrix Metalloproteinase-2 Expression by Vascular Smooth Muscle Cells Is Mediated by Both Stimulatory and Inhibitory Signals in Response to Growth Factors. *J. Biol. Chem.* 281, 25915–25925. doi:10.1074/jbc.M513513200.

Rival, C., Guazzone, V. A., von Wulffen, W., Hackstein, H., Schneider, E., Lustig, L., et al. (2007). Expression of co-stimulatory molecules, chemokine receptors and proinflammatory cytokines in dendritic cells from normal and chronically inflamed rat testis. *Mol. Hum. Reprod.* 13, 853–861. doi:10.1093/molehr/gam067.

Rival, C., Theas, M., Suescun, M., Jacobo, P., Guazzone, V., van Rooijen, N., et al.

(2008). Functional and phenotypic characteristics of testicular macrophages in experimental autoimmune orchitis. *J. Pathol.* 215, 108–117. doi:10.1002/path.

Robert, S., Gicquel, T., Victoni, T., Valença, S., Barreto, E., Bailly-Maître, B., et al. (2016). Involvement of matrix metalloproteinases (MMPs) and inflammasome pathway in molecular mechanisms of fibrosis. *Biosci. Rep.* 36, e00360. doi:10.1042/BSR20160107.

Romano, F., Tripiciano, A., Muciaccia, B., De Cesaris, P., Ziparo, E., Palombi, F., et al. (2005). The contractile phenotype of peritubular smooth muscle cells is locally controlled: Possible implications in male fertility. *Contraception* 72, 294–297. doi:10.1016/j.contraception.2005.03.009.

Ruytinx, P., Proost, P., Van Damme, J., and Struyf, S. (2018). Chemokine-induced macrophage polarization in inflammatory conditions. *Front. Immunol.* 9, 1930. doi:10.3389/fimmu.2018.01930.

Sahin, H., and Wasmuth, H. E. (2013). Chemokines in tissue fibrosis. *Biochim. Biophys. Acta - Mol. Basis Dis.* 1832, 1041–1048. doi:10.1016/j.bbadis.2012.11.004.

Sakai, N., Wada, T., Yokoyama, H., Lipp, M., Ueha, S., Matsushima, K., et al. (2006). Secondary lymphoid tissue chemokine (SLC/CCL21)/CCR7 signaling regulates fibrocytes in renal fibrosis. *Proc. Natl. Acad. Sci. U. S. A.* 103, 14098–14103. doi:10.1073/pnas.0511200103.

Santamaria, L., Martinez-Onsurbe, P., Paniagua, R., and Nistal, M. (1990). Laminin, type IV collagen, and fibronectin in normal and cryptorchid human testes. An immunohistochemical study. *Int. J. Androl.* 13, 135–146. doi:10.1111/j.1365-2605.1990.tb00970.x.

Schnittert, J., Bansal, R., Storm, G., and Prakash, J. (2018). Integrins in wound healing, fibrosis and tumor stroma: High potential targets for therapeutics and drug delivery. *Adv. Drug Deliv. Rev.* 129, 37–53. doi:10.1016/j.addr.2018.01.020.

Schram, K., Ganguly, R., No, E. K., Fang, X., Thong, F. S. L., and Sweeney, G. (2011). Regulation of MT1-MMP and MMP-2 by leptin in cardiac fibroblasts involves Rho/ROCK-dependent actin cytoskeletal reorganization and leads to enhanced cell migration. *Endocrinology* 152, 2037–2047. doi:10.1210/en.2010-1166.

Schuppe, H. C., Neumann, N., Scheffzyk, A., Schock-Skasa, G., Hofmann, N., and Schill, W. (2001). Inflammatory reactions in testicular biopsies of infertile men. *Andrologia* 33, 327–328.

Sengupta, N., and MacDonald, T. T. (2007). The role of matrix metalloproteinases in stromal/epithelial interactions in the gut. *Physiology* 22, 401–409. doi:10.1152/physiol.00027.2007.

Shen, J. Z., Morgan, J., Tesch, G. H., Fuller, P. J., and Young, M. J. (2014). CCL2-dependent macrophage recruitment is critical for mineralocorticoid receptor-mediated cardiac fibrosis, inflammation, and blood pressure responses in male mice. *Endocrinology* 155, 1057–1066. doi:10.1210/en.2013-1772.

Sierra-Filardi, E., Nieto, C., Domínguez-Soto, Á., Barroso, R., Sánchez-Mateos, P., Puig-Kroger, A., et al. (2014). CCL2 Shapes Macrophage Polarization by GM-CSF and M-CSF: Identification of CCL2/CCR2-Dependent Gene Expression Profile. *J. Immunol.* 192, 3858–3867. doi:10.4049/jimmunol.1302821.

Sierra-Filardi, E., Puig-Kröger, A., Blanco, F. J., Nieto, C., Bragado, R., Palomero, M. I., et al. (2011). Activin A skews macrophage polarization by promoting a proinflammatory phenotype and inhibiting the acquisition of anti-inflammatory macrophage markers. *Blood* 117, 5092–5101. doi:10.1182/blood-2010-09-306993.

Song, J., Wu, C., Korpos, E., Zhang, X., Agrawal, S. M., Wang, Y., et al. (2015). Focal MMP-2 and MMP-9 Activity at the Blood-Brain Barrier Promotes Chemokine-Induced Leukocyte Migration. *Cell Rep.* 10, 1040–1054. doi:10.1016/j.celrep.2015.01.037.

Stukenborg, J. B., Kjartansdóttir, K. R., Reda, A., Colon, E., Albersmeier, J. P., and Söder, O. (2014). Male germ cell development in humans. *Horm. Res. Paediatr.* 81, 2–12. doi:10.1159/000355599.

Szarek, M., Bergmann, M., Konrad, L., Schuppe, H., Kliesch, S., Hedger, M. P., et al. (2019). Activin A target genes are differentially expressed between normal and neoplastic adult human testes : clues to gonocyte fate choice. *Andrology* 7, 31–41. doi:10.1111/andr.12553.

Tang, P. M. K., Zhang, Y. Y., Xiao, J., Tang, P. C. T., Chung, J. Y. F., Li, J., et al. (2020). Neural transcription factor Pou4f1 promotes renal fibrosis via macrophage–myofibroblast transition. *Proc. Natl. Acad. Sci. U. S. A.* 117, 20741–20752. doi:10.1073/pnas.1917663117.

Taylor, S., Wakem, M., Dijkman, G., Alsarraj, M., and Nguyen, M. (2010). A practical approach to RT-qPCR-Publishing data that conform to the MIQE guidelines. *Methods* 50, S1–S5. doi:10.1016/j.ymeth.2010.01.005.

Theocharis, A. D., Skandalis, S. S., Gialeli, C., and Karamanos, N. K. (2016). Extracellular matrix structure. *Adv. Drug Deliv. Rev.* 97, 4–27. doi:10.1016/j.addr.2015.11.001.

Toth, M., and Fridman, R. (2012). Assessment of Gelatinases (MMP-2 and MMP-9) by Gelatin Zymography. *Methods Mol. Med.* 878, 121–135. doi:10.1385/1-59259-136-1:163.

Trojian, T., Lishnak, T., and Heiman, D. (2009). Epididymitis and orchitis：An Overview. *Am. Fam. Phys.* 79, 583–587. doi:10.1002/9781119021506.ch17.

UniProt Consortium (2014). Activities at the Universal Protein Resource (UniProt). *Nucleic Acids Res.* 42, 191–198. doi:10.1093/nar/gkt1140.

Vale, W., Rivier, J., Vaughan, J., McClintock, R., Corrigan, A., Woo, W., et al. (1986). Purification and characterization of an FSH releasing protein from porcine ovarian follicular fluid. *Nature* 321, 776–779. doi:10.1038/321776a0.

Vierhout, M., Ayoub, A., Naiel, S., Yazdanshenas, P., Revill, S. D., Reihani, A., et al. (2021). Monocyte and macrophage derived myofibroblasts: Is it fate? A review of the current evidence. *Wound Repair Regen.* 29, 548–562. doi:10.1111/wrr.12946.

Wada, T., Sakai, N., Matsushima, K., and Kaneko, S. (2007). Fibrocytes: A new insight into kidney fibrosis. *Kidney Int.* 72, 269–273. doi:10.1038/sj.ki.5002325.

Wang, M., Fijak, M., Hossain, H., Markmann, M., Nüsing, R. M., Lochnit, G., et al. (2017). Characterization of the Micro-Environment of the Testis that Shapes the Phenotype and Function of Testicular Macrophages. *J. Immunol.* 198, 4327–4340. doi:10.4049/jimmunol.1700162.

Wang, X., Zhou, Y., Tan, R., Xiong, M., He, W., Fang, L., et al. (2010). Mice lacking the matrix metalloproteinase-9 gene reduce renal interstitial fibrosis in obstructive nephropathy. *Am. J. Physiol. Physiol.* 299, 973–982. doi:10.1152/ajprenal.00216.2010.

Weischenfeldt, J., and Porse, B. (2008). Bone marrow-derived macrophages (BMM): Isolation and applications. *Cold Spring Harb. Protoc.* 2008, pdb.prot5080. doi:10.1101/pdb.prot5080.

Weiskirchen, R., Weiskirchen, S., and Tacke, F. (2019). Organ and tissue fibrosis: Molecular signals, cellular mechanisms and translational implications. *Mol. Aspects Med.* 65, 2–15. doi:10.1016/j.mam.2018.06.003.

Weng, Y., Lou, J., Liu, X., Lin, S., Xu, C., Du, C., et al. (2019). Effects of high glucose on proliferation and function of circulating fibrocytes: Involvement of CXCR4/SDF-1 axis. *Int. J. Mol. Med.* 44, 927–938. doi:10.3892/ijmm.2019.4260.

Wietecha, M. S., Pensalfini, M., Cangkrama, M., Müller, B., Jin, J., Brinckmann, J., et al. (2020). Activin-mediated alterations of the fibroblast transcriptome and matrisome control the biomechanical properties of skin wounds. *Nat. Commun.* 11, 2604. doi:10.1038/s41467-020-16409-z.

Wijayarathna, R., and de Kretser, D. M. (2016). Activins in reproductive biology and beyond. *Hum. Reprod. Update* 22, 342–357. doi:10.1093/humupd/dmv058.

Wijayarathna, R., and Hedger, M. P. (2019). Activins, follistatin and immunoregulation in the epididymis. *Andrology* 7, 703–711. doi:10.1111/andr.12682.

Wijayarathna, R., Sarraj, M. A., Genovese, R., Girling, J. E., Michel, V., Ludlow, H., et al. (2017). Activin and follistatin interactions in the male reproductive tract : activin expression and morphological abnormalities in mice lacking follistatin 288. *Andrology* 5, 578–588. doi:10.1111/andr.12337.

Wilkening, A., Krappe, J., Mühe, A. M., Lindenmeyer, M. T., Eltrich, N., Luckow, B., et al. (2020). C-C chemokine receptor type 2 mediates glomerular injury and interstitial fibrosis in focal segmental glomerulosclerosis. *Nephrol. Dial. Transplant.* 35, 227–239. doi:10.1093/ndt/gfy380.

Wipff, P. J., and Hinz, B. (2008). Integrins and the activation of latent transforming

growth factor β1 - An intimate relationship. *Eur. J. Cell Biol.* 87, 601–615. doi:10.1016/j.ejcb.2008.01.012.

Wynn, T. A., and Ramalingam, T. R. (2012). Mechanisms of fibrosis: Therapeutic translation for fibrotic disease. *Nat. Med.* 18, 1028–1040. doi:10.1038/nm.2807.

Wynn, T. A., and Vannella, K. M. (2016). Macrophages in Tissue Repair, Regeneration, and Fibrosis. *Immunity* 44, 450–462. doi:10.1016/j.immuni.2016.02.015.

Xia, Y., Entman, M. L., and Wang, Y. (2013). CCR2 Regulates the Uptake of Bone Marrow-Derived Fibroblasts in Renal Fibrosis. *PLoS One* 8, e77493. doi:10.1371/journal.pone.0077493.

Xie, L., and Zhao, L. (2017). Role of CXCL12/CXCR4-Mediated Circulating Fibrocytes in Pulmonary Fibrosis. *J. Biomed.* 2, 134–139. doi:10.7150/jbm.18949.

Xu, J., Mora, A., Shim, H., Stecenko, A., Brigham, K. L., and Rojas, M. (2007). Role of the SDF-1/CXCR4 axis in the pathogenesis of lung injury and fibrosis. *Am. J. Respir. Cell Mol. Biol.* 37, 291–299. doi:10.1165/rcmb.2006-0187OC.

Xu, L., Sharkey, D., and Cantley, L. G. (2019). Tubular GM-CSF promotes late MCP-1/CCR2-mediated fibrosis and inflammation after ischemia/reperfusion injury. *J. Am. Soc. Nephrol.* 30, 1825–1840. doi:10.1681/ASN.2019010068.

Yamashita, S., Maeshima, A., Kojima, I., and Nojima, Y. (2004). Activin A Is a Potent Activator of Renal Interstitial Fibroblasts. *J. Am. Soc. Nephrol.* 15, 91–101. doi:10.1097/01.ASN.0000103225.68136.E6.

Yang, J., Lin, S. C., Chen, G., He, L., Hu, Z., Chan, L., et al. (2013). Adiponectin promotes monocyte-to-fibroblast transition in renal fibrosis. *J. Am. Soc. Nephrol.* 24, 1644–1659. doi:10.1681/ASN.2013030217.

Yang, S., Lin, C., Yang, P., Chao, S., and Ye, Y. (2009). Increased Expression of Gelatinase (MMP-2 and MMP-9) in Pterygia and Pterygium Fibroblasts with Disease Progression and Activation of Protein Kinase C. *Invest. Ophthalmol. Vis. Sci.* 50, 4588–4596. doi:10.1167/iovs.08-3147.

Yosef, G., Arkadash, V., and Papo, N. (2018). Targeting the MMP-14/MMP-2/integrin v3 axis with multispecific N-TIMP2– based antagonists for cancer therapy. *J. Biol. Chem.* 293, 13310–13326. doi:10.1074/jbc.RA118.004406.

Yoshimura, T. (2018). The chemokine MCP-1 (CCL2) in the host interaction with cancer: A foe or ally? *Cell. Mol. Immunol.* 15, 335–345. doi:10.1038/cmi.2017.135.

Yu, Q., and Stamenkovic, I. (2000). Cell surface-localized matrix metalloproteinase-9 proteolytically activates TGF-β and promotes tumor invasion and angiogenesis. *Genes Dev.* 14, 163–176.

Yu, S., Han, B., Xing, X., Li, Y., Zhao, D., Liu, M., et al. (2021). A Protein from Dioscorea polystachya (Chinese Yam) Improves Hydrocortisone-Induced Testicular Dysfunction by Alleviating Leydig Cell Injury via Upregulation of the Nrf2 Pathway. *Oxid. Med. Cell. Longev.* 2021, 3575016. doi:10.1155/2021/3575016.

Yuan, A., Lee, Y., Choi, U., Moeckel, G., and Karihaloo, A. (2015). Chemokine receptor Cxcr4 contributes to kidney fibrosis via multiple effectors. *Am. J. Physiol. - Ren. Physiol.* 308, F459–F472. doi:10.1152/ajprenal.00146.2014.

Yuan, C., Ni, L., and Wu, X. (2021). Activin A activation drives renal fibrosis through the STAT3 signaling pathway. *Int. J. Biochem. Cell Biol.* 134, 105950. doi:10.1016/j.biocel.2021.105950.

Yue, B. (2014). Biology of the extracellular matrix: An overview. *J. Glaucoma* 23, S20–S23. doi:10.1097/IJG.0000000000000108.

Zhang, P., Wu, C., Huang, X. H., Shen, C. L., Li, L., Zhang, W., et al. (2017a). Aspirin suppresses TNF-α-induced MMP-9 expression via NF-κB and MAPK signaling pathways in RAW264.7 cells. *Exp. Ther. Med.* 14, 5597–5604. doi:10.3892/etm.2017.5252.

Zhang, W. H., Li, X. L., Guo, Y., and Zhang, Y. (2017b). Proliferation and osteogenic activity of fibroblasts induced with fibronectin. *Brazilian J. Med. Biol. Res.* 50, 2–7. doi:10.1590/1414-431x20176272.

Zhao, S., Zhu, W., Xue, S., and Han, D. (2014). Testicular defense systems: Immune privilege and innate immunity. *Cell. Mol. Immunol.* 11, 428–437. doi:10.1038/cmi.2014.38.

Zheng, Y., Feng, Y., Wang, Y., Kong, L., Zhou, M., Wu, M., et al. (2021). Islet transplantation ameliorates diabetes-induced testicular interstitial fibrosis and is associated with inhibition of TGF- β1 / Smad2 pathway in a rat model of type 1 diabetes. *Mol. Med. Rep.* 23, 376. doi:10.3892/mmr.2021.12015.

Zhou, R., Wu, J., Liu, B., Jiang, Y., Chen, W., Li, J., et al. (2019). The roles and mechanisms of Leydig cells and myoid cells in regulating spermatogenesis. *Cell. Mol. Life Sci.* 76, 2681–2695. doi:10.1007/s00018-019-03101-9.

Zhou, X., Yan, T., Huang, C., Xu, Z., Wang, L., Jiang, E., et al. (2018). Melanoma cell-secreted exosomal miR-155-5p induce proangiogenic switch of cancer-associated fibroblasts via SOCS1/JAK2/STAT3 signaling pathway. *J. Exp. Clin. Cancer Res.* 37, 242. doi:10.1186/s13046-018-0911-3.

Zirkin, B. R., and Papadopoulos, V. (2018). Leydig cells: formation, function, and regulation. *Biol. Reprod.* 99, 101–111. doi:10.1093/biolre/ioy059.

9. PUBLICATIONS

Original article

- Peng W, Kepsch A, Kracht TO, Hasan H, Wijayarathna R, Wahle E, et al. Activin A and CCR2 regulate macrophage function in testicular fibrosis caused by experimental autoimmune orchitis. Cell Mol Life Sci. 2022 Nov 24;79(12):602. doi: 10.1007/s00018-022-04632-4.

Conference abstracts

- 14th Giessen Graduate Centre for the Life Sciences (GGL) Conference on Life Science (29 – 30 September 2021) Giessen, Germany. Loss of CCR2 inhibits testicular fibrosis caused by experimental autoimmune orchitis. Oral presentation.
- 21st European Testis Workshop - ETW 2021 (30 May – 03 June 2021) Virtual Edition. Loss of CCR2 inhibits testicular fibrosis caused by EAO: possible role for activin A in fibrosis development. Oral presentation.
- 12th International, 11th European and 32nd German Congress of Andrology (05 – 09 December 2020) Virtual Edition. Loss of CCR2 inhibits the development of testicular fibrosis – a possible role for activin A. Oral presentation.
- 1st Giessen Graduate Centre for the Life Sciences (GGL) Digital Conference on Life Science (29 – 30 September 2020) Giessen, Germany. Loss of CCR2 inhibits the development of testicular fibrosis - possible implications for activin A. Oral presentation.
- 6th International Molecular Andrology Workshop (24 – 26 September 2019) Giessen, Germany. Investigation of mechanisms involved in the development of the fibrotic response during testicular inflammation. Poster presentation.
- 12th Giessen Graduate Centre for the Life Sciences (GGL) Conference on Life Science (04 – 05 September 2019) Giessen, Germany. Investigation of mechanisms involved in the development of the fibrotic response during testicular inflammation. Poster presentation.

10. ACKNOWLEDGEMENTS

The experimental work of this dissertation was performed at the Department of Anatomy and Cell Biology at Justus Liebig University of Giessen, Germany, under the supervision of Prof. Dr. Andreas Meinhardt and Dr. Monika Fijak.

First of all, I would like to thank my supervisors Prof. Dr. Andreas Meinhardt and Dr. Monika Fijak who gave me this precious opportunity to study and work in their team, and supported my project in the past three years. Many thanks to Prof. Dr. Andreas Meinhardt for his enthusiasm and guidance. In particular, I want to express my deepest gratitude to Dr. Monika Fijak. Thank you so much for your kind and warm help both in research and daily life. Thanks for your financial support when I lacked a scholarship. In addition, I appreciate your effort and the time you dedicated to revise this thesis. Your scientific input, knowledge and experience in reproductive biology, your rigorous attitude towards research as well as the encouragement you have provided to me have all helped push me to become a better researcher in the field of andrology.

I would like to thank Prof. Dr. Mark P. Hedger, Dr. Sudhanshu Bhushan and Prof. Dr. Kate L. Loveland for their valuable suggestions during the project discussion and writing.

I would like also to thank my colleagues Hiba Hasan, Eva Wahle, Dr. Yalong Yang, Dingding Ai, Dr. Christiane Pleuger, Suada Fröhlich, Dr. Jörg Klug, Dr. Aileen Harrer, Vishnu Kumar, Dr. A. Christine Kauerhof, Artem Kepsch, Jakob A. Obermaier, etc., for their warm-hearted help and for their patience when I faced difficulties in my experimental work and when I needed assistance in German language-based paperwork. I am also grateful to Pia Jürgens and Eva Wewel for their assistance when it came to accommodation arrangement, PhD registration, conference funding and dissertation defense.

Additionally, I would like to express my appreciation to Prof. Dr. Malgorzata Wygrecka and her team members for teaching me the gelatin-zymography technique.

The successful implementation of this project could not have been achieved without the support of the IRTG “Molecular pathogenesis on male reproductive disorders” funded by the Deutsche Forschungsgemeinschaft and Monash University. The financial support of

China Scholarship Council and Von Behring-Röntgen-Stiftung to me is also gratefully appreciated.

The GGL program offered many seminars, practical courses and communication skills to me, and taught me professional skills that are instrumental not only for my current PhD study but also for my future career. Thanks to the GGL program as well as to Prof. Dr. Daniela Fietz for putting a lot of effort and time in organization and management.

Moreover, I would like to appreciate my friends (Joyce, Xiaoping, Muyao, Tongtong, Yao, Yuxi, Yinfu, etc.) for being with me in the past three years. Life here would be boring without you.

Finally, I want to express my thanks to my family for their endless love, and silent dedication and support.

11. CURRICULUM VITAE

12. EHRENWÖRTLICHE ERKLÄRUNG

Ich erkläre: Ich habe die vorgelegte Dissertation selbständig und ohne unerlaubte fremde Hilfe und nur mit den Hilfen angefertigt, die ich in der Dissertation angegeben habe. Alle Textstellen, die wörtlich oder sinngemäß aus veröffentlichten oder nicht veröffentlichten Schriften entnommen sind, und alle Angaben, die auf mündlichen Auskünften beruhen, sind als solche kenntlich gemacht. Bei den von mir durchgeführten und in der Dissertation erwähnten Untersuchungen habe ich die Grundsätze guter wissenschaftlicher Praxis, wie sie in der „Satzung der Justus-Liebig-Universität Giessen zur Sicherung guter wissenschaftlicher Praxis“ niedergelegt sind, eingehalten.

I declare that I have completed this dissertation single-handedly without the unauthorized help of a second party and only with the assistance acknowledged therein. I have appropriately acknowledged and referenced all text passages that are derived from or are based on the content of published or unpublished work of others, and all information that relates to verbal communication. I have abided by the principles of good scientific conduct laid down in the charter of the Justus Liebig University of Giessen in carrying out the investigations described in the dissertation.

Giessen, den

_____

Wei Peng